Gravity-sensing processes and gravity-dependent gene expression in plants

studied under altered gravity conditions

Dissertation
zur Erlangung des Doktorgrades (Dr. rer. nat.)
der Mathematisch-Naturwissenschaftlichen Fakultät
der Rheinischen Friedrich-Wilhelms-Universität Bonn

vorgelegt von
Nicole Vagt
aus Bornheim

Bonn 2010

Angefertigt mit Genehmigung der Mathematisch-Naturwissenschaftlichen Fakultät
der Rheinischen Friedrich-Wilhelms-Universität Bonn

1. Referent: Priv.-Doz. Dr. Markus Braun
2. Referentin: Prof. Dr. Dorothea Bartels

Tag der Promotion: 13.09.2010

Erscheinungsjahr: 2010

TABLE OF CONTENTS

ABBREVIATIONS

ATH1	Arabidopsis thaliana genome array
BaSO4	barium sulfate
°C	degree celsius
CO_2	carbon dioxide
d	day
°	degree
DLR	Deutsches Zentrum für Luft- und Raumfahrt (German Aerospace Center)
ESA	European Space Agency
FC	fold change
g	gravity ($1g = 9.81\ ms^{-2}$)
h	hour
IML-2	second International Microgravity Laboratory mission
K	represents 1000
m	meter
µ	micro
µ*g*	microgravity
µL	microliter
mm	millimeter
mL	milliliter
min	minute
mol	Mol
NCBI	National Center for Biotechnology Information
#	number
OD	optical density
o/n	over night
O_2	oxygen
%	percent
PVC	polyvinyl chloride
p/n	part number
RIN	RNA integrity number
RefSeq	Reference Sequence database
RT	room temperature
rpm	rounds per minute
s	second
SE	standard error
SSC	Swedish Space Cooperation
TAIR	The Arabidopsis Information Resource
TEXUS	Technological Experiments Under Reduced Gravity
TIGR	The Institute for Genomic Research
UniGene	NCBI transcriptome database

LIST OF FIGURES

LIST OF TABLES

1. INTRODUCTION

1.1 Gravitropism-related processes in plants

Plants need to orientate their organs in the most beneficial way with respect to changing environmental conditions in habitats below and above the surface of the Earth. In order to produce energy-rich metabolites, shoots grow upwards toward the light, while roots grow downwards into the soil to supply the plant with nutrients and water as well as to anchor the plant body. In contrast to fluctuating environmental conditions due to seasonal or photoperiodic changes, gravity is the only constant factor providing plants with reliable information for the spatial orientation of their organs. Therefore, plants have evolved a highly sophisticated gravisensing system whose basic characteristics have persisted throughout plant evolution.

Plants perceive gravity by specialized cells, referred to as statocytes, in which starch-filled amyloplasts (statoliths) are free to sediment in the direction of gravity and, thereby, function as susceptors of the gravistimulus (starch-statoliths theory, Němec, 1900; Haberlandt, 1900). The gravity-induced sedimentation of statoliths leads to graviperception, the transduction of the physical stimulus into a physiological signal. Investigations on starch-less mutants of *Arabidopsis thaliana* and *Nicotiana tabacum* showed that these mutants were still gravitropic but their gravisensitivity was strongly reduced, thus, confirming the crucial role of statoliths as primary susceptors of gravistimuli in plants (Kiss et al., 1996; MacCleery and Kiss, 1999; Weise and Kiss, 1999). Furthermore, high-magnetic field studies supported the starch-statoliths theory of gravisensing in plant cells, since gravitropic curvature responses of plant organs were induced solely by the magnetophoretic displacement of statoliths in the statocytes of nominal vertically oriented roots and shoots (Kuznetsov and Hasenstein, 1996, 1997; Kuznetsov et al., 1999; Weise et al., 2000). These experiments provide strong evidence that the displacement of statoliths is the decisive initial step of gravisensing in plant cells.

During the last decades, numerous experimental approaches, based on cellular and molecular assays, were conducted to increase our knowledge about the processes during plant gravisensing and gravitropic response. Beside physiological studies at normal 1*g* conditions (e.g. various inhibitor-treatment analyses), instruments modifying acceleration conditions on ground by centrifugation or clinorotation became a powerful tool to investigate gravisensing processes in plants. The response of plants to hyper-*g* during centrifugation (e.g. Sievers and Heyder-Caspers, 1983; Wendt et al., 1987; Braun et al., 2002) and to 'simulated weightlessness' by applying a multilateral 1*g* stimulus during clinorotation (e.g. Sacks, 1887; Sievers and Hejnowicz, 1992; Cai et al., 1997) have been analyzed by physiological and biochemical studies. In recent years, a sensitive analysis method on

genomic level, the microarray technology that had already been successfully established in other gene-expression studies in plants (e.g. Girke et al., 2000; Hanano and Davis, 2007; Kilian et al., 2007; Goda et al., 2008), became an important tool for these ground-based studies on the effect of various acceleration conditions (Moseyko et al., 2002; Martzivanou and Hampp, 2003; Kimbrough et al., 2004; Salmi and Roux, 2008). Oligonucleotide probe microarrays facilitate precise evaluation of gene expression changes for hundreds to thousands of genes in parallel. In contrast to most of the physiological and biochemical studies, which are generally focused on one or a few targets of interest, the array technology provides a research tool to study effects on the whole genome-expression pattern.

1.1.1 The unicellular models Chara rhizoid and Chara protonema for research on gravisensing in plant cells

In contrast to the gravisensing statocytes of higher plants, which are located in compact tissues, the gravitropically growing transparent rhizoids and protonemata of the characean green algae are easily accessible for numerous experimental approaches. In addition, all steps of gravisensing including susception, perception, signal transduction and the gravitropic response are limited to one single cell. These beneficial features of rhizoids and protonemata have allowed for intensive investigations of the cellular and molecular mechanisms underlying the gravisensing mechanisms (for review, see Braun and Wasteneys, 2000; Braun and Limbach, 2005). In particular, experiments that have been performed in microgravity (µ*g*) or on clinostats and centrifuges on ground, have decisively contributed to our current understanding of gravity-suscpetion and -perception processes in characean rhizoids and protonemata (Buchen et al., 1993; Buchen et al., 1997; Cai et al., 1997; Hoson et al., 1997; Braun et al., 2002).

Rhizoids and protonemata, both tube-like cells with a diameter of up to 30 µm, exhibit a very similar polar organization of their cytoplasm. However, they show opposite gravitropic growth orientation, i.e. rhizoids grow downwards (positive gravitropism) in order to anchor the algal thallus in the sediment, whereas protonemata grow upwards (negative gravitropism) by reason of regenerative function. Both cell types originate from nodal cells of the algal thallus. Protonemata are produced in the absence of blue light, e.g. when the thallus was buried by sediment. As soon as protonemata have reached light, tip growth terminates and cell divisions are inititated in order to regenerate the thallus.

The polar organization of the cytoplasm in rhizoids and protonemata is based upon the highly dynamic arrangement of actin microfilaments. Microtubules are also involved in the organization of the subapical and basal region, but they are absent from the apical tip region and are not involved in the primary steps of gravisuception and -perception. A multitude of actin-binding proteins manage the distinct arrangement of the actin cytoskeleton in the different zones of

rhizoids and protonemata. In the basal zone two populations of actin bundles with opposite polarities underlie the cytoplasmic streaming, which surrounds the large vacuole of the cell. The subapical region is characterized by a dense meshwork of mainly axially oriented, fine actin microfilament bundles (Braun et al., 2004). In the apical region, actin microfilaments and actin-associated proteins organize the so-called Spitzenkörper consisting of a dense aggregate of endoplasmic-reticulum (ER) membranes and secretory vesicles. The position of the Spitzenkörper defines the center of growth and, thus, the plasma membrane area with the maximal exocytosis rate of vesicles (Hejnowicz et al., 1977; Sievers et al., 1979; Braun, 1996; Limbach et al., 2008). Inhibitor treatment experiments with actin disrupting drugs and calcium (Ca^{2+}) ionophores have demonstrated that the structural integrity of the Spitzenkörper and the function of the center of growth are dependent on a specific subset of actin-associated proteins (Braun and Richter, 1999; Braun, 2001). A gradient of cytoplasmic free Ca^{2+} with the highest concentration at the outmost tip regulates the activity of spectrin-like proteins and the distribution of secretory vesicles (Braun and Richter, 1999; Braun et al., 2004).

The actomyosin system of rhizoids and protonemta precisely controls the positioning and the sedimentation of statoliths, small vacuoles containing barium-sulfate crystals (Schröter et al., 1975). Actomyosin forces prevent statoliths from settling into the cell tip by acting net-basipetally in tip-downward growing rhizoids. In tip-upward growing protonemata, the actomyosin system acts net-acropetally in order to prevent statoliths from sedimenting toward the cell base (Hodick et al., 1998; Braun et al., 2002; Braun, 2002). In downward growing rhizoids and in upward growing protonemata under normal 1g conditions (g = 9.81 ms^{-2}), statoliths are kept in a dynamically stable position of balance in an area a few µm from the cell tip by actomyosin forces compensating the oppositely acting gravity force (Braun et al., 2002). Inhibitor studies with Cytochalasin D have shown that disrupting the actin cytoskeleton in rhizoids and protonemata leads to termination of tip growth and causes the sedimentation of statoliths in the direction of gravity. After removing the drug, statoliths are retransported to the original position and tip growth continues (Braun et al., 2004).

In contrast to the highly regulated statolith positioning in both axial directions of the rhizoid, the control by the actomyosin system is less pronounced in lateral direction. The rather weakly regulated statolith position in lateral direction of the rhizoid is the prerequisite for a fast and sensitive gravisensing mechanism. In rhizoids that are stimulated by 90°, the sedimenting statoliths mainly follow the gravity vector and settle onto the physically lower cell flank where gravipercepti-on takes place and the gravitropic response is initiated. In rhizoids reoriented by angles different from 90°, statoliths no longer simply sediment along the gravity vector, but are actively guided by actomyosin forces against the gravity force onto the beltlike gravisensitive

plasma-membrane area (10-35 µm from the tip) – the only membrane area where gravireceptors are located (Braun, 2002). Pushing statoliths onto other plasma-membrane regions by centrifugation or laser-tweezer micromanipulations does not initiate a curvature response of the rhizoid. However, the displaced statoliths are retransported to the gravisensitive subapical membrane area, where graviperception occurs (Leitz et al., 1995; Braun, 2002). In contrast to rhizoids, the gravisensitive plasma-membrane site in protonemata is located at 5-10 µm basal to the tip (Braun, 2002). During reorientation of protonemata, net-acropetally actomyosin forces guide sedimenting statoliths to the graviperception site initiating gravitropic response (Hodick et al., 1998).

Fluorescence imaging of Ca^{2+} and of dihydropyridine, an L-type Ca^{2+} channel blocker, in rhizoids and protonemata indicated that the gradient of cytplasmic free Ca^{2+} in the cell tip is altered by gravireceptor activation. During the readjustment of the nominal growth direction in protonemta, a drastic shift of the tip-high calcium gradient toward the upper flank is observed. This asymmetric Ca^{2+} gradient results most likely from the statolith-induced differential activation or local inhibition of Ca^{2+} channels in the protonema tip. The Spitzenkörper and, therewith, the growth center, is most likely displaced by Ca^{2+}-dependent actomyosin-generated movements toward the upper cell flank and the new outgrowth occurs at that site ('bending by bulging'; Braun and Richter, 1999; Braun, 2001). In contrast to protonemata, the growth center remains symmetrically positioned in the center of the tip during the gravitropic response of rhizoids (Braun, 2001). The sedimentation of statoliths onto the gravisensitive site results in the local inhibition of Ca^{2+} influx leading to differential growth of the opposite cell flanks in rhizoids ('bending by bowing'; Braun and Richter, 1999).

Although the molecular nature of the gravireceptors in plants is still unknown, the mechanism of gravireceptor activation has recently been functionally characterized in the rhizoid of the green alga Chara (Limbach et al., 2005). Earlier experiments have shown that statoliths have to be fully sedimented onto the gravisensitive area of the plasma membrane. The sedimentation process of statoliths itself does not induce a curvature response (Braun, 2002). Parabolic flight experiments aboard the Airbus A300 Zero-G were conducted to reveal the activation mechanism of the gravireceptors in rhizoids. It was found that the sedimented statoliths in gravistimulated rhizoids remained settled onto the plasma membrane during the different acceleration levels of the parabolic flight profile (1*g*, hypergravity and microgravity) and did not loose contact with the gravireceptors (Limbach et al., 2005). Flight samples experienced all 31 periods of microgravity during the 2-h flight. In-flight control samples were centrifuged at 1*g* during the microgravity phases. Surprisingly, the final curvature angles of flight samples were not different from in-flight controls. This provided clear evidence that graviperception was not interrupted

when statoliths became weightless during microgravity. Weightless statoliths were able to activate the gravireceptors and, thus, pressure exerted by the weight of statoliths is not required for gravireceptor activation and graviperception to occur in characean rhizoids (Limbach et al., 2005). This finding was supported by ground-control experiments, which demonstrated that an increase of pressure of statoliths exerted on gravireceptors by the application of hyper-*g* accelerations did not result in enhanced gravitropic responses. On the other hand, disruption of the contact between statoliths and gravireceptor molecules by inverting roots in further ground-control experiments led to significantly smaller curvature responses. Even short-term removal of statoliths from the gravisensitive plasma membrane for only 10 s was found to significantly impair gravitropic curvature. Considering the results of the flight and ground-control experiments the gravireceptor in characean rhizoids must be referred to as a receptor, which is activated by direct interactions with components of the statolith surface (Limbach et al., 2005).

1.1.2 Arabidopsis as a muticellular plant model system for research on gravitropism-related signaling pathways

The pioneering studies on graviresponsive characean rhizoids and protonemata have resulted in a considerable progress in the understanding of the primary mechanisms of gravitropic sensing and signaling in relatively simple lower plant cell types. Gravisensing processes in the statocytes of higher plants are less well understood and results of experiments were often contradictory. Models of graviperception in higher plant statocytes postulated that sedimentation of statoliths generates tension or shearing forces, which are transferred via actin-dependent mechanisms to putative mechanosensitive receptors in the cortical ER membrane or the plasma membrane (Sievers et al., 1991; Yoder et al., 2001; Zheng and Staehelin, 2001; Boonsirichai et al., 2002, Sievers et al., 2002; Blancaflor and Masson, 2003; Perbal and Driss-Ecole, 2003). However, until today the nature of the gravireceptors in higher plants is unknown and studies have so far not given proof of mechanosensitive receptors involved in plant gravitropism.

As already mentioned above, in contrast to the relatively big and transparent single-celled rhizoids and protonemata, the major problem for addressing questions about gravitropic mechanisms in higher plants is the complexity of the gravisensing tissues and the transmission and integration of the gravity-induced signals from a multitude of cells. Therefore, experimental investigations, e.g. microscopic or molecular applications on gravity-susception and –perception mechanisms in higher plants are quite difficult. However, previous findings have identified second messengers that are most likely involved in the early processes of gravisignal transduction including cytoplasmic free Ca^{2+} (Lu and Feldman, 1997; Plieth and Trewavas, 2002; Belyavskaya, 2004), cytosolic protons (pH) (Scott and Allen, 1999; Fasano et al., 2001), and inositol-1,4,5-triphosphate (IP3) (Perera et al., 2001, 2006). According to the Cholodny-Went theory,

the physiological signal generated by graviperception is transmitted from the sensing statocytes to the responding cells by means of the directional transport of the growth hormone auxin (Cholodny, 1928; Went, 1933). A lateral gradient of auxin in the gravistimulated organ results in the differential growth of the opposite flanks of the organ. The establishment of the auxin gradient during gravitropic reorientation has been intensively investigated. Auxin influx carriers and efflux carriers, PIN-formed (PIN) proteins, were identified as key components of the auxin transport mechanism (Friml, 2002, 2003; Ottenschläger, 2003; Blilou et al., 2005). Results of previous experiments have also implicated a role for the hormones cytokinin (Aloni et al., 2004), ethylene (Lee et al., 1990; Madlung et al., 1999; Buer et al., 2006), brassinosteroids (Kim et al., 2000; Li et al., 2005) and gibberellic acid (Brock and Kaufmann, 1988) in the regulation of growth during gravitropic responses.

In recent years, several studies reported on gravity-related alterations in protein expression involved in stress responses, primary metabolism, general signaling, protein translation and ion homeostasis (Wang et al., 2006; Barjaktarović et al., 2007, 2008, 2009). Treatment-related changes were detected in Arabidopsis cell cultures exposed to hypergravity or 'simulated' microgravity conditions (clinorotation or random-positioning machine). Within 10 min, first changes in expression patterns of phosphorylated proteins were detected (Barjaktarović et al., 2009). In addition to analyses on protein-regulation level, in the last years, the analyses via oligonucleotide-microarray technology has become a sensitive tool for investigating changes in gene-expression patterns in response to altered gravitational conditions in ground and flight experiments. It was unclear, for a long time, whether the regulation of gravity-related genes is also involved in the plant response to altered *g* conditions. However, recent studies on Arabidopsis demonstrated that altered *g* forces affect plants, causing changes in metabolic processes, signaling pathways, cellular organization and stress-related responses, which are regulated by gene expression (Moseyko et al., 2002; Martzivanou and Hampp, 2003; Martzivanou et al., 2006; Kimbrough et al., 2004). Findings indicated that both, complex interacting and independent regulatory pathways, are affected by different *g* conditions (Centis-Aubay et al., 2003). The genomic studies reported on a high sensitivity for gravity-related gene responses to only transient stimuli, e.g. the transient reorientation by rotating the plant (360°) within 10 s (Moseyko et al., 2002). Furthermore, it was shown that the significant up- or rather down-regulation of gravitropism-related genes was detected even 2 min after stimulation (Moseyko et al., 2002).

1.2 Objectives of the study

In this study, experiments were conducted under altered gravitational conditions provided by sounding rocket and parabolic plane flights in order to unravel the fundamental mechanisms, which underlie the sensitivity and the effectivity during gravisusception and -perception in plants.

1.2.1 Threshold acceleration level required for lateral statolith displacement in Chara rhizoids

In downward growing rhizoids, the equilibrium position of the statoliths results from the actomyosin forces acting against the gravity force. Sounding-rocket and clinostat experiments demonstrated that, when the influence of gravity was abolished, the basipetal acting actomyosin forces caused the displacement of statoliths against the former direction of gravity (Buchen et al, 1993; Cai et al., 1997; Braun et al., 2002). Earlier studies conducted on sounding rocket MAXUS-3 and MAXUS-5 missions have already shown that the acceleration level required for statoliths to overcome the cytoskeletal positioning forces and to induce lateral statolith displacement, i.e. sedimention, is $\leq 0.14g$ in Chara rhizoids (Limbach et al., 2005). In the present study, a microgravity experiment during the MAXUS-8 campaign in spring 2010 aimed at narrowing down this approximation of acceleration value. The results allowed for calculating of the energetic concept underlying the gravity-susception and -perception mechanisms in such a precise way, as it had never been possible before for any plant- or animal-model system.

1.2.2 Statolith-mediated graviperception in Arabidopsis root statocytes

Encouraged by the findings on the gravireceptor-activation mechanism in Chara rhizoids, in this study, higher plants were investigated in a similar way under microgravity conditions provided by parabolic plane flights aboard the Airbus A300 Zero-G. Comparison of the growth curvatures of characean rhizoids, which experienced 31 microgravity phases during 2-h flights and of those, which were centrifuged at $1g$ to avoid the microgravity phases (in-flight controls), revealed no significant differences. Therefore, abolishing the weight of sedimented statoliths during the microgravity phases did not interrupt the activation of gravireceptors in Chara rhizoids (Limbach et al., 2005). In the present study, it was tested for the first time if the statoliths in higher plant root statocytes also stay in contact with the gravireceptors and are not displaced during the μg phases of parabolic plane flights, as it was shown for characean rhizoids (Limbach et al., 2005). It has already been shown that the final curvature angles of primary Arabidopsis roots, which experienced all conditions of a parabolic plane flight including the μg phases, were sometimes slightly higher but never smaller than those of the in-flight controls, which did not experience microgravity (Greuel, 2007; Hauslage, 2008). Therefore, showing that the sedimented statoliths in the horizontally positioned Arabidopsis seedlings during flight are not displaced

from the lower cell flank but stay in contact with the gravireceptors during flight, would support the idea that graviperception in higher plant statocytes relies on graviperception by contact-interactions between sedimented statoliths and receptor molecules. For this purpose, the primary roots of Arabidopsis seedlings were fixed with potassium permanganate ($KMnO_4$) in the different phases of parabolic plane flights. Semithin sections of the plant samples allowed for analyses of the statoliths' position.

1.2.3 Gravity-dependent gene expression in plants

After the successful functional characterization of the gravireceptor activation in characean rhizoids and in higher plant statocytes, the consequent next step comprises the investigation of the molecular basis of gravity sensing in plants. To provide a basis for the identification and detailed molecular characterization of key components involved in graviperception, e.g. the gravireceptors or crucial membrane components on the statoliths' surface, the general effect on the protein- and gene-expression pattern during plant reorientation under different gravitational conditions has to be evaluated. In this respect, the third part of the present study is focused on the regulation of gene-expression during gravity-related responses in Arabidopsis seedlings. As already mentioned above, genome analyses on the effect of altered gravitational conditions in plants have already been conducted (Moseyko et al., 2002; Martzivanou and Hampp, 2003; Kimbrough et al., 2004; Paul et al., 2005). However, none of these studies comprised experiments during parabolic plane flights providing fast and successive changes of different acceleration conditions (1*g*, hyper- and microgravity). For the first time, this study aimed at investigating the changes in gene expression patterns in response to the different gravitational conditions of parabolic plane flights using the aircraft A300 Zero-G (10^{th} DLR (Deutsches Zentrum für Luft- und Raumfahrt) campaign). In parallel, a comprehensive experiment series on ground was performed, in order to evaluate the effects of plant stimulation by reorientation under 1*g* and 2*g* conditions. In contrast to the previous studies using oligonucleotide probe arrays with maximum 8,300 transcripts, in the present study, an Arabidopsis-DNA microarray covering the entire Arabidopsis genome (43,803 transcripts) was applied, ensuring a whole-genome analysis.

2. MATERIALS AND METHODS

2.1 Plant Material

2.1.1 Chara rhizoids

Thallus of *Chara globularis* Thuill. was collected from a pond in the Botanical Garden of the University of Bonn, Germany. For the production of rhizoids, thalli were cut into segments comprising two nodes and one internodial cell. The side branches of the lower node were cut off to induce rhizoid development. Thallus segments were embedded in a thin layer of agar (1.2% in distilled water) in TEXUS (Technological Experiments Under Reduced Gravity) cuvettes (Fig. 1, constructed by Astrium Space Transportation, Bremen, Germany and first described by Volkmann et al., 1991) in 1.2 % agar in distilled water at RT and under constant illumination at 200 µmol m^{-2} s^{-1} for 3-4 d.

2.1.2 Arabidopsis

Arabidopsis thaliana ecotype Wassilewskija and ecotype Columbia were cultivated in a cultivation room at alternating illumination with 16 h of light and 8 h of darkness. Mature seeds were harvested and stored at 4°C.

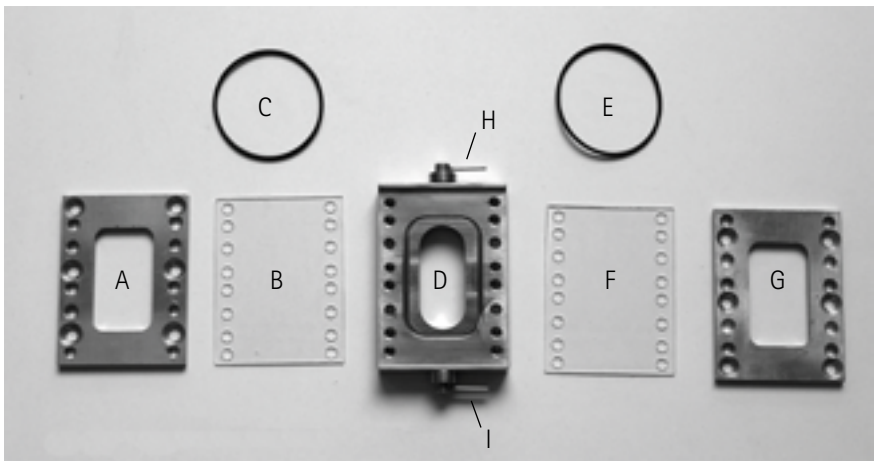

Fig. 1. Components of a TEXUS cuvette. The core frame (D) and a Makrolon® window (B, F) on either side are sealed with o-rings (C, E). Two aluminium frames (A, G) on either side protect the cuvette against pressure disturbances. The components are srewed together on either side. (The in- and outlet ports (H, I) are attached to the core frame only for the experiments with Arabidopsis. These ports are sealed for the MAXUS experiment.)

2.1.2.1 Arabidopsis root seedlings for fixation by $KMnO_4$

Seeds of *Arabidopsis thaliana* ecotype Wassilewskija were sterilized with 75% EtOH for 3 min and 1% NaOCl for 10 min. Sterilized seeds were washed 4 times with distilled water. Arabidopsis seedlings were cultivated on filter paper in TEXUS cuvettes (Fig. 2). The cuvettes comprised a core frame (V2A steel), two Makrolon® window and two aluminium frames on either side. The core frame and the two Makrolon® windows were sealed with o-rings. Between the core frame and one Makrolon® window the filter paper with the Arabidopsis seeds (15-20 seeds per filter paper) was embedded (Fig. 2). Inlet and outlet ports on each side of the cuvette facilitated the injection of liquids and the ventilation. Distilled water (0.5 mL) was injected into the

Fig. 2. Arabidopsis seeds on wet filter paper in a TEXUS cuvette.

cuvettes. After a cold stratification at 4°C in darkness for 2 d, germination was induced and seedlings were cultivated at 24°C under constant illumination (Radium Bonalux super, NL24W/11-860 Spectralux daylight). The cuvettes were daily vented with 10 mL O_2. Three-days old seedlings were used for the experiments.

2.1.2.2 Arabidopsis seedlings for dry-ice fixation

Seeds of *Arabidopsis thaliana* ecotype Columbia were sterilized with 75% EtOH for 3 min and 5% NaOCl for 15 min. Sterilized seeds were washed 4 times with distilled water. Arabidopsis seedlings were cultivated on filter paper in 60-mm Petri dishes. The filter paper was saturated with 1% bacto-agar in medium containing micronutrients (modified after Legué, 1997). Petri dishes were sealed with Parafilm® to avoid contamination. After a cold stratification at 4°C in darkness for 2 d germination was induced in an incubator at 24°C under constant illumination (Radium Bonalux super, NL24W/11-860 Spectralux daylight). In the sterile environment of the incubator a small hole in the Petri dishes ensured air exchange during cultivation. Four days old seedlings were used for the experiments (Fig. 3). Approximately 12 h before start of the experiments, seedlings were habituated to darkness, since all flight and ground experiments were performed in darkness.

Fig. 3. Arabidopsis seedlings for dry-ice fixation. Plants are cultivated on filter paper in 60-mm Petri dishes.

2.2 MAXUS-8 sounding rocket flight experiment

MAXUS is an enlarged version of TEXUS. Both, MAXUS and TEXUS missions, are part of the European sounding rocket program that provides a platform for scientific experiments under microgravity conditions. The MAXUS program is a joint venture between SSC (Swedish Space Cooperation) and Astrium Space Transportation funded by ESA (European Space Agency). The parabolic flight of MAXUS rockets provides scientists a reliable access to high quality microgravity (µ*g*) conditions of up to $10^{-4}g$ for 12-14 min. The experiment modules can be accessed until about one hour before lift-off. In-flight data recording via telemetry is possible. Telecommand and video transmission provides controlling and monitoring of the experiment during the 12 to 14 min of µ*g*. Biological samples are recovered directly after landing and brought back to the laboratories at Esrange (near Kiruna, Sweden) usually within 1-2 h after launch.

Previous experiments have demonstrated that parabolic flights of sounding rockets are consummately suited to study the actomyosin mediated statolith sedimentation in Chara rhizoids (Volkmann et al., 1991; Buchen et al., 1997; Braun et al., 2002). The MAXUS-8 experiment was conducted in order to determine the cytoskeletal forces underlying the gravisensing mechanisms of characean rhizoids.

2.2.1 Sample preparation

Internodal segments of Chara thalli were prepared in the laboratory at Esrange and Chara rhizoids were cultivated in TEXUS cuvettes (see 2.1.1). The cuvettes comprised a core frame (V2A steel), which was covered by two Makrolon® windows on either side. The core frame and the Makrolon® windows were sealed with o-rings. Two aluminium frames on either side protected the cuvette against the vacuum in the orbit. Three hours before lift-off, 3 TEXUS cuvettes with rhizoids showing good growth rates (~100-200 µm h^{-1}) and well positioned statoliths were selected and mounted on late-access units (see Fig. 4, C), which were mounted in the payload module about 2 h before lift-off.

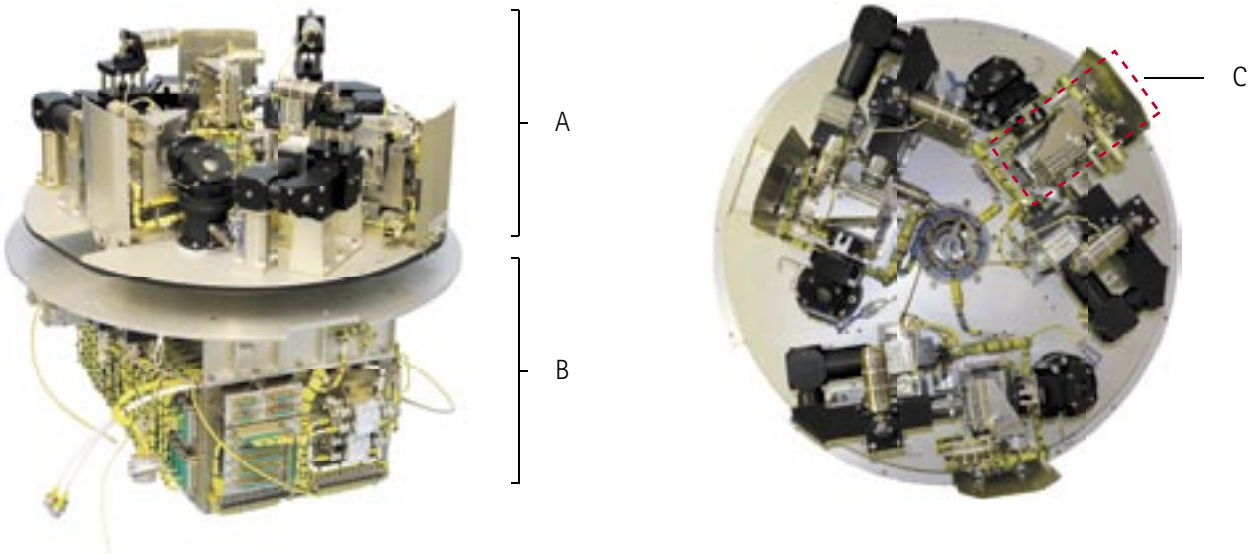

Fig. 4. Chara module TEM 06-RO1M of MAXUS-8. The module (side view on the left and top view on the right) consists of a motor and telemetry unit (B) and a rotatable platform (A), on which 3 microscopic units are attached. The flight cuvettes with rhizoids are mounted on late-access units (C), which are mounted in the module approximately 2 h before lift-off.

2.2.2 Chara module TEM 06-5RO1M

A precursor version of the payload module TEM 06-RO1M (Fig. 4), constructed by Astrium Space Transportation (Bremen, Germany), had already been successfully flown on MAXUS-3 and MAXUS-5. The precursor module was slightly modified for the MAXUS-8 experiment. The Chara module consisted of a stationary lower motor and telemetry unit and an upper rotatable platform, on which 3 horizontal microscopic units were installed (Zeiss, Oberkochem, Germany). Each microscopic unit comprised a 20x objective lens and a 2.5x optovar system resulting in a total magnification of 50x. Observing and recording was performed with the black/white CCD camera XC-ST50 (Sony, Cologne, Germany). Three flight cuvettes with rhizoids were mounted in late-access units (Fig. 4), which were inserted into the module approximately 120 min before lift-off. The three cuvettes were located on three different radii of the rotatable platform. The position of the cuvettes with regard and the focus was adjusted by telecommand. The rhizoid samples in the cuvettes were observed via in-vivo video microscopy during the sounding rocket flight. Temperature was kept at 22°C ± 1 °C.

2.2.3 Experiment procedure

The ESA MAXUS-8 sounding rocket was launched from the SSC's launch facility Esrange Space Center outside Kiruna in Northern Sweden in March 26th, 2010. MAXUS-8 reached an apogee of 700 km and provided µ*g* conditions of $10^{-4}g$ for 836 s. Rotation of the platform of the experiment module TEM 06-5RO1M was started 75 s after lift-off, at the beginning of microgravity, and continued until re-entry of the payload (836 s after lift-off). Dependent on the different distances of the three cuvettes from the center of the platform, the rhizoids experienced lateral accelerations of 0.060*g*, 0.080*g* or 0.100*g* (Fig. 4). Via telecommand access on the rotation of the platform, at 400 s after lift-off, lateral accelerations were decreased to 0.055*g*, 0.073*g* and 0.092*g*. At 550 s after lift-off, lateral accelerations were further decreased to 0.050*g*, 0.067*g* and 0.083*g* and at 720 s after lift-off they were upregulated again (0.055*g*, 0.073*g* and 0.092*g*) until re-entry. During flight, the rhizoids were observed and checked for lateral displacement of the statolith complex.

2.2.4 Data analysis

The video-microscopic images were analyzed to identify and track the movements and, in particular, any lateral displacements of statoliths during the lateral centrifugation under the microgravity conditions of the MAXUS-8 sounding rocket flight. The original video format VOB of the video microscopy recording was converted to WMV1 codec (*Aura Video Converter 1.21, http://download.cnet.com/Aura-Video-Converter/3000-2194_4-10966793.html*). Single video images were extracted with *Ulead VideoStudio 6* (Bitmap format) and processed with *Adobe® Photoshop®* (JPEG format). Tracking of the statoliths and the statolith complex was performed with ImageJ (http://rsbweb.nih.gov/ij/download.html). Because the images during the first 110 s after lift-off were out of focus (re-focusing was performed), tracking analysis of the statoliths was done from +110 s until +800 s after lift-off.

2.3 Parabolic plane-flight experiments

Parabolic plane-flight experiments were performed during the 10th DLR parabolic plane-flight campaign at Cologne airport, Germany, in September 2007 (2.3.2), and during the 13th DLR parabolic plane flight campaign at Bordeaux Airport, France, in February 2009 (2.3.1).

Parabolic plane flights with the Novespace Airbus A300 Zero-G provide alternating levels of 1*g*, microgravity and hypergravity conditions. Therefore, parabolic plane-flight experiments are well suited to study the effect of different acceleration levels on gravitropism-related processes, in particular, on gravity sensing mechanisms in biological organisms. At the beginning of each parabola, the aircraft is pulled up with full engine power from the horizontal flight to an ascending angle of 47°. The aircraft is subjected to approximately

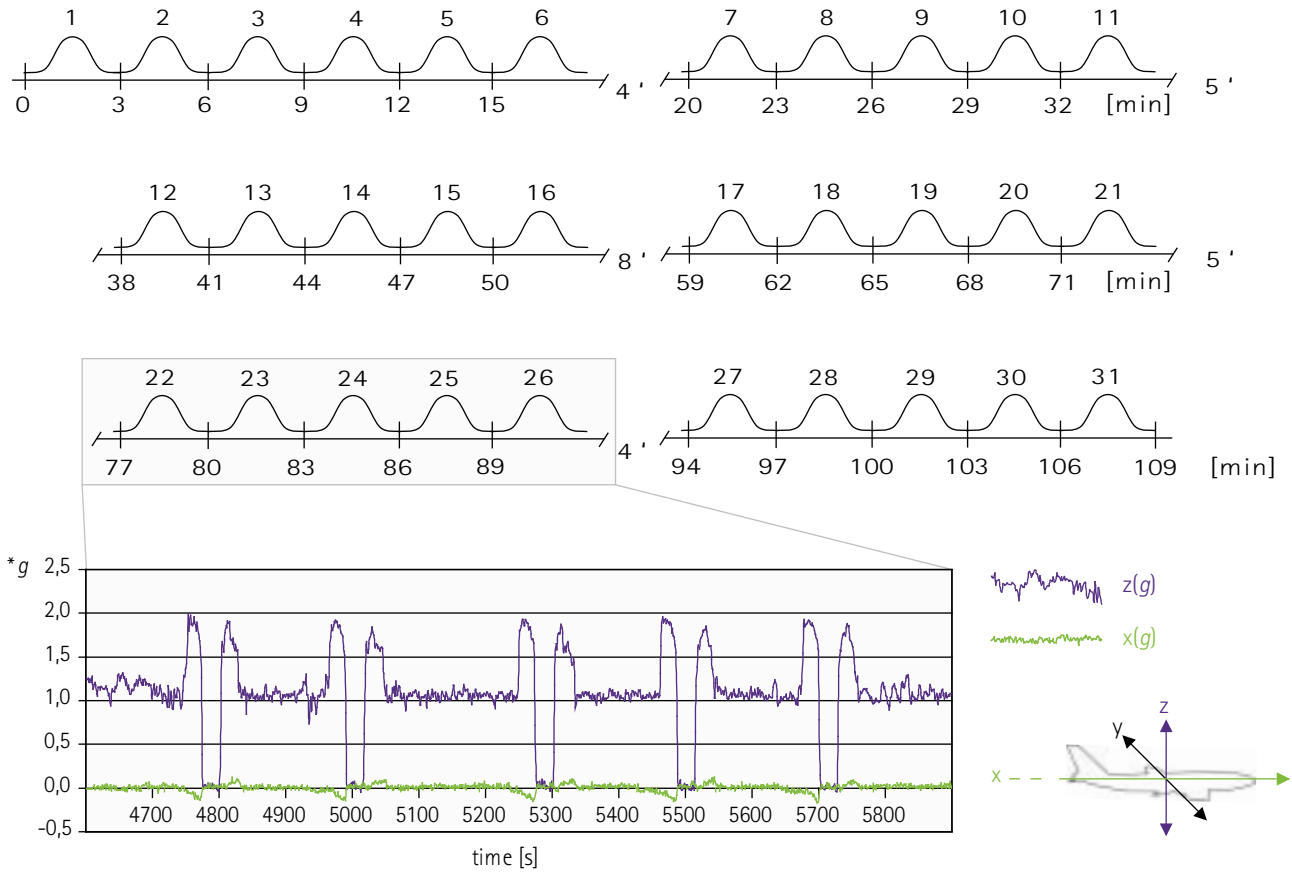

Fig. 5. Scheme showing the parabolic flight profile of the aircraft A300 Zero-G on one flight day with the alternating acceleration levels of 1*g*, hypergravity and microgravity. Within approximate 109 min 31 parabolas are flown at intervals of about 3 min. After a first test parabola, 6 sets of 5 parabolas are interrupted by breaks of four, five and eight minutes with 1*g* conditions. The real acceleration values in the direction of the z and x axis of the aircraft are shown for the parabolas number 22 to 26.

twice of normal Earth gravity (1*g* = 9.81 ms^{-2}). After 20 s of hypergravity, the aircraft engines are throttled down to a minimum thrust ('injection'). During this phase of the parabolic flight curve, all forces acting on the aircraft compensate each other and the aircraft freely falls in the gravitational field of the Earth. The aircraft is exposed to microgravity (< 10^{-2}*g*) for 22 s per parabola until at a descending angle of 42° the engines are reset to full power again. The aircraft is pulled out of the parabola in a second 2*g* phase of 20 s followed by normal horizontal flight phase (Fig. 5). The flight profile consists of 31 parabolas, which were flown within approximately 2 h on each of the three flight days per campaign (Fig. 5), thus, total microgravity time per flight is approximately 12 min or 10 % of the entire flight time. The 10th DLR parabolic flight campaign provided another two flight days with 11 parabolas, which were flown within approximately 50 min (8% total µ*g*).

Definition of orientation for the Arabidopsis seedlings in parabolic flight and ground experiments

In the recent study during all in-flight and on-ground experiments (2.3.1 and 2.3.2) the position of the Arabidopsis samples was defined relative to the vector of the applied acceleration, i.e. 1*g* Earth gravity, hyper- and microgravity, respectively. Therefore, a vertically (0°) positioned plant grew parallel to the direction of the applied gravity vector while a horizontally (90°) positioned seedling was orientated perpendicular to the direction of the gravity vector.

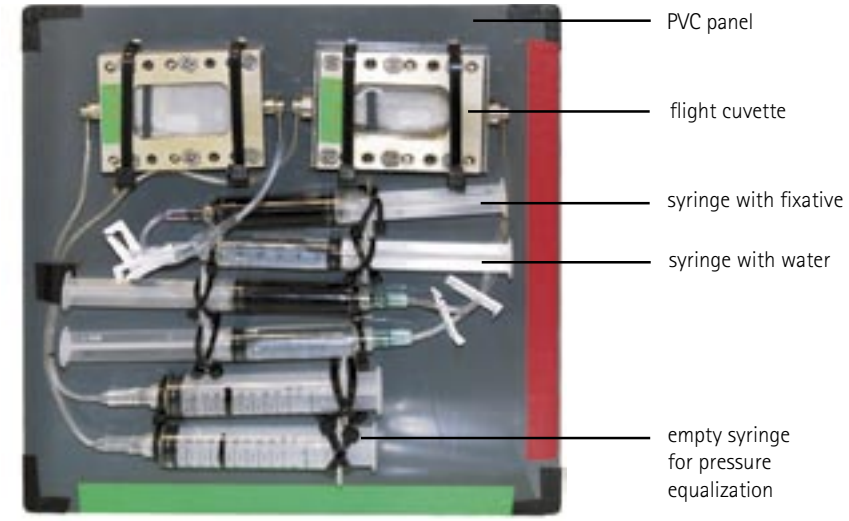

Fig. 6. Flight hardware Charabolix-8. Two flight cuvettes with Arabidopsis seedlings are attached to a PVC panel. Each flight cuvette is connected with three syringes: one containing the fixative ($KMnO_4$), one with water to wash after fixation and one empty syringe for pressure equalization.

2.3.1 Analysis of the position of sedimented statoliths during parabolic plane flight

In previous parabolic plane-flight experiments, it was demonstrated that in Chara rhizoids and in higher plant root statocytes, weightless statoliths, which do not exert pressure on membrane-bound gravireceptor molecules are still able to activate the gravireceptors (Limbach et al., 2005; Greuel, 2007). This notion has been made under the assumption that, during the microgravity phases of the parabolic plane flight, statoliths remain in contact with the gravireceptors and are not removed from the gravisensitive membrane. In order to investigate if this is also true for higher plant statocytes, the current experiment focused on the microscopic analysis of the position of sedimented statoliths in the root statocytes of Arabidopsis seedlings during the parabolic plane flights of the 13th DLR campaign.

2.3.1.1 Sample preparation

Approximately two to three hours before flight 18 cuvettes with Arabidopsis seedlings showing good growth rates (~120-180 µm h^{-1}) and a good alignment with respect to the gravity vector were mounted in the fixation units. A small PVC (polyvinyl chloride) bar was pinched between the filter paper and the Makrolon® window of the cuvettes to prevent a direct flow-through of the fixation solution and to facilitate a good distribution of the solution on the samples.

2.3.1.2 Flight hardware Charabolix-8

Eight PVC panels, each equipped with two flight cuvettes, were flown on every flight day. The cuvettes were fixed on the panels with cable straps. The inlet port of the flight cuvettes was connected via a LS-2 connecting tube with two 5 mL Omnifix® Luer Lock syringes (B. Braun Melsungen AG, Melsungen, Germany), one filled with 5 mL $KMnO_4$ fixation solution (3% in tap water) and one filled with 5 mL

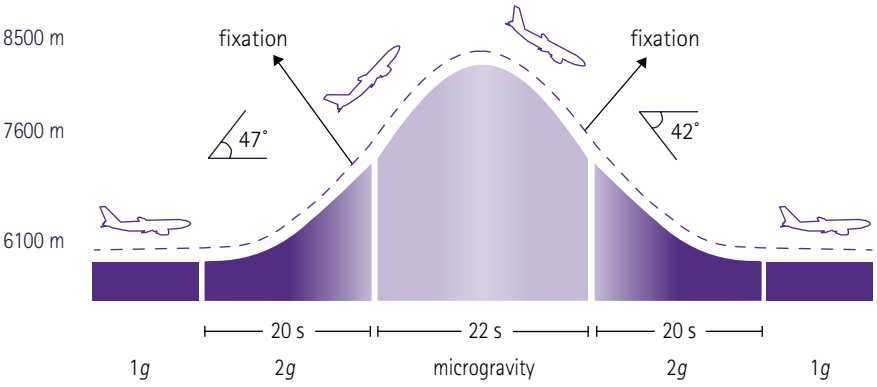

Fig. 7. Flight profile of one parabola with the Airbus A300 Zero-G. The 22 s of µ*g* is accompanied by two phases of hyper-*g* during ascend and descend lasting approximately 20 s. Sample fixation is performed at the beginning and at the end of the µ*g*-phase.

tap water. Connecting tubes were locked with clamps until fixation and elution, respectively. The exit port of the flight cuvettes was connected via Original Perfusor® connecting tube (type MR) with one empty 10 mL Omnifix® Luer Lock syringe (B. Braun Melsungen AG, Melsungen, Germany). The syringes were also fixed with cable straps on the panel (Fig. 6). The whole panel including two fixation units was sealed in a transparent Ziploc® bag (Toppits®) providing a second containment. The panels were arranged in an aluminium box mounted on the experiment rack Charabolix-8 (hardware of Charabolix described in detail by Hauslage, 2008). The temperature in the experiment box was kept at 23-25°C.

2.3.1.3 In-flight procedure

To determine the effect of microgravity on the positioning of sedimented statoliths in the root statocytes of horizontally positioned Arabdiopsis roots, the seedlings were fixed with $KMnO_4$ shortly before the beginning and shortly before the end of the µ*g*-phase (Fig. 7). Fixation was performed during the first and the 16th parabola on all three flight days. The seedlings were horizontally stimulated 20 min prior to the fixation. Thereby, sedimentation of the statoliths in the root statocytes was assured. For fixation, 5 mL $KMnO_4$ (3% in tap water) were injected into the cuvettes. The $KMnO_4$ solution was extracted of the cuvettes after 30 s. Immediately, 5 mL tap water were injected to wash out residual $KMnO_4$.

Video recording of the fixation procedure was done for one fixation unit on each flight day to control the optimal distribution of the fixation solution on the plant seedlings. On each flight day, the fixation of control samples was done 5 min before the first parabola. These control samples were also horizontally pre-stimulated 20 min before fixation, and were directly compared with fixed seedlings at the beginning and at the end of the µ*g* phases.

2.3.1.4 Post-flight procedure

Immediately after flight, the root tips of the fixed Arabidopsis seedlings were cut off in a 45° angle with a razor blade. The 45° cut indicated the orientation of the root relative to the gravity vector during parabolic flight (Fig. 9). The root tips were transferred to tap water and stored at 4°C for 4 to 6 d until they were further processed and

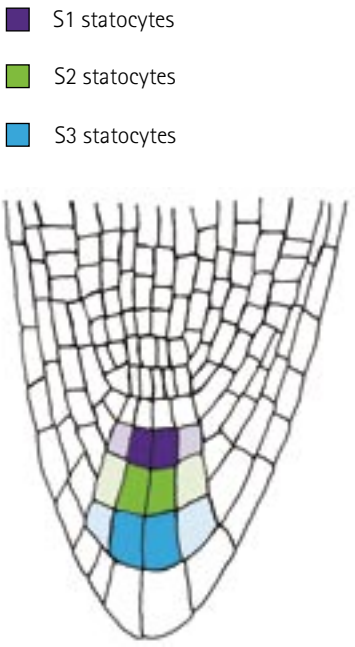

Fig. 8. Arabidopsis root scheme showing the location of S1, S2 and S3 statocytes.

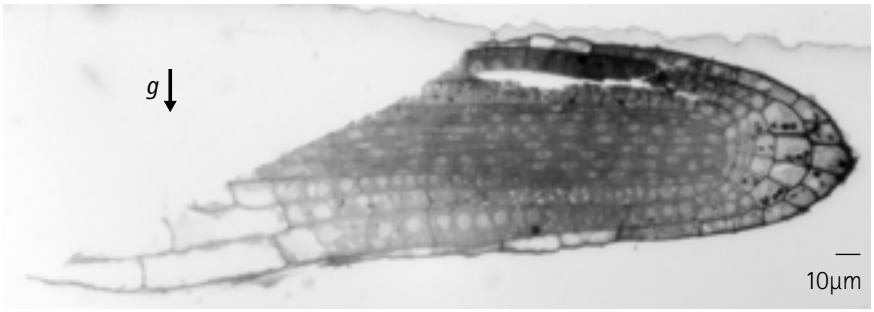

Fig. 9. Processing of the fixed Arabidopsis root seedlings. The root tips of the fixed root seedlings are cut off in a 45° angle to indicate the orientation of the root relative to the gravity vector during parabolic flight.

prepared for performing semithin sections via a microtome (Ultramikrotom OM U3, Reichert Jung, Vienna, Austria). Details of the dehydration, infiltration, embedding and polymerization procedure are summarized in Table I (p 17). During the embedding procedure the root tips were arranged with a needle in the ERL block (Spurr Low Viscosity Embedding Media, Polysciences Europe GmbH, Eppelheim, Germany), such that the longitudinal root axis was positioned parallel to the subsequent microtome section. The embedded samples were trimmed with a razer blade and a mill (TM 60, Reichert Jung, Vienna, Austria). Median semithin sections (0.5 µm) were stained with Methylene Blue/Azure II for 10 s on a heater.

2.3.1.5 Data analysis

Stained semithin sections were examined with the inverse microscope Axiovert 135 (Carl Zeiss Jena GmbH, Jena, Germany). Pictures of the sections were taken using the AxioCam HRC (Carl Zeiss AxioVision software). With the software Segment (developed for MATLAB, The MathWorksTM) the position of the statoliths was determined. The analysis exclusively considered fully sedimented stato-

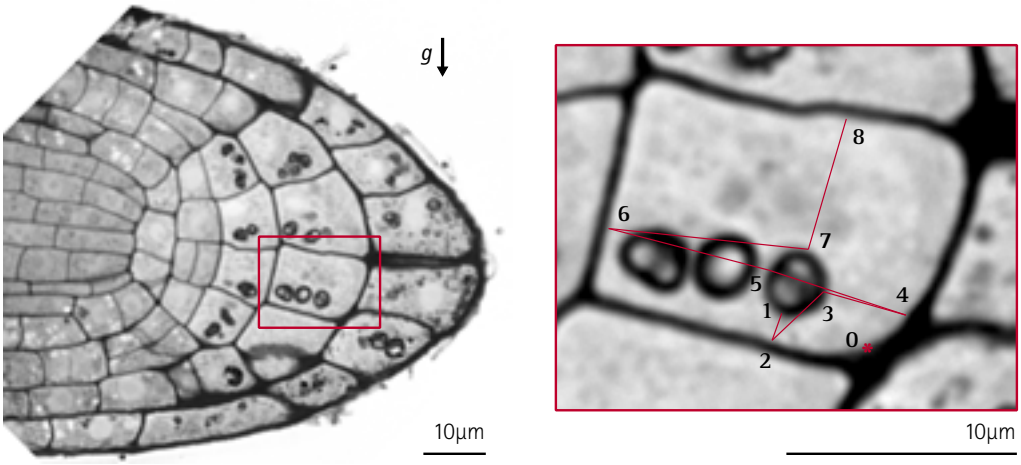

Fig. 10. Determination of the statoliths' position. With the software Segment (MATLAB, The MathWorksTM) the position of a statolith is defined by the distances between the statolith's outer membrane and the lateral and axial cell flanks (1-8) as well as by the coordinates relative to the reference point (0 *) set on the physical lower cell flank in the outmost apical corner of the cell.

Table I. Processing of the Arabidopsis root seedlings after fixation with $KMnO_4$. The protocol comprises dehydration, infiltration, embedding and polymerization of the seedling samples. (o/n = over night)

processing	incubation	incubation time
dehydration	15% acetone in H_2O	15 min
	30% acetone in H_2O	15 min
	50% acetone in H_2O	30 min
	75% acetone in H_2O	45 min
	90% acetone in H_2O	45 min
	100% acetone	45 min
	100% acetone	30 min
	100% acetone	1.5 h
infiltration	acetone:ERL 3:1	o/n
	acetone:ERL 1:1	1 h
	acetone:ERL 1:3	1 h
	ERL, pure	o/n
	ERL, pure	4-5 h
embedding	ERL, pure	
polymerization	70°C	7 h

liths on the physical lower cell flank, i.e. statoliths whose sedimentation was not inhibited by other statoliths. The distances between the outer membrane of the statoliths and the lateral and axial cell wall flanks of the statocytes (the plasma membrane was not visible in the semithin sections) were analyzed. Furthermore, the position of each statolith was described by coordinates relative to a reference point, which was set on the physical lower cell wall flank in the outmost apical corner of the cell (Fig. 10). The pixel values were converted to µm and statistical analyses of the data were performed with Microsoft Excel®. The position of the statoliths in the S2 and S3 statocytes were analyzed (Fig. 8).

2.3.1.6 Ground experiments

In control experiments on ground (1*g*) Arabidopsis roots were horizontally stimulated for 20 min, subsequently inverted from 90° to 270° for 10 s, 60 s and 120 s and then the seedlings were immediately fixed with $KMnO_4$ (2% in tap water). In order to determine the sedimentation velocity of the statoliths within a certain period of inversion time, the mean distances between the statoliths and the lateral cell flank of the statocytes were measured in the inverted roots and in the non-inverted controls. The analysis exclusively considered statoliths whose sedimentation was not inhibited by other statoliths (see also 2.3.1.5).

2.3.2 Gravity-dependent gene expression in plants

2.3.2.1 Sample preparation

Two to three hours before flight, 35-40 Petri dishes with Arabidopsis seeldings showing good growth rates (~120-180 µm h-1) and a good alignment with respect to the gravity vector were selected. On each of the first three flight days (each with 31 parabolas) 20 Petri dishes with samples were mounted in a fixation chamber (flight samples) and 15 Petri dishes with samples were mounted in the on-board 1g-reference centrifuge (in-flight control samples). Flight and in-flight control samples showed a vertical orientation and were not stimulated by 90°. On the fourth and fifth flight day (each with 12 parabolas) in one fixation chamber, plant seedlings were mounted in a vertical orientation (20 Petri dishes) and in, one fixation chamber, plants were mounted in a horizontal orientation (20 Petri dishes).

2.3.2.2 Flight hardware Carbocryonix

The experiment hardware Carbocryonix, described in detail by Horn (2007) and Hauslage (2008), was mounted on a custom-made aluminium rack and included two steel cylinders as fixation chambers, each with a volume of 3.6 liter and each connected with a 10kg CO_2 (carbon dioxide) gas bottle (Fig. 11). The hardware allows the shock-freezing of biological samples on ground as well as in parabolic plane-flight experiments. A custom-made sample holder for 60 mm Petri dishes allows mounting of Arabidopsis seedlings in vertical as well as in horizontal orientation in the fixation chambers (Fig. 12). For fixation, gaseous CO_2 is conducted into the fixation chambers. The CO_2 gas abruptly expands in the chambers. Due to the released pressure and the spontaneous cooling, CO_2 dry ice with a temperature of -79.5 °C is produced. Within seconds the samples and all biological processes, respectively, are fixed for subsequent processing and genome or proteome analyses. Temperatures inside the fixation chambers are monitored via a temperature measurement system. Temperatures of approximate -60 °C are consistently hold for more than one hour after fixation (Fig. 13).

2.3.2.3 In-flight procedure

In the present experiment it was tested whether acceleration levels differing from normal Earth gravity (1*g*) have an effect on gene expression level in Arabidopsis seedlings. Therefore, plants were exposed to the hyper- and microgravity conditions of a parabolic plane flight with the Airbus A300 Zero-G. On three flight days vertically oriented flight samples, which experienced all the different acceleration levels of 31 parabolas, were shock-frozen by producing dry-ice after the last parabola. Vertically oriented in-flight control samples, which experienced the same conditions as the flight samples including the hypergravity phases except that they were accelerated with 1*g* in an on-board centrifuge when the flight samples experienced the µ*g* phases, were fixed by dry-ice production after the last parabola as well. By using swing-out chambers in the on-board centrifuge it was

Fig. 11. The experiment rack Carbocryonix allows for shock-freeze fixation of the Arabidopsis seedlings during parabolic flight. The rack comprises two fixation chambers (A), each one connected with a 10kg CO_2 gas bottle (B). Temperature inside the fixation chambers is controlled (C) during shock-freezing procedure by dry-ice production. (Hardware described in detail by Horn, 2007 and Hauslage, 2008.)

ensured that all accelerations acted in the same direction. On two additional flight days comprising 12 parabolas, vertically oriented as well as flight samples stimulated by 90° were simultaneously shock-frozen after the last parabola. Fixed samples were immediately recovered after landing and transferred to the lab for further processing.

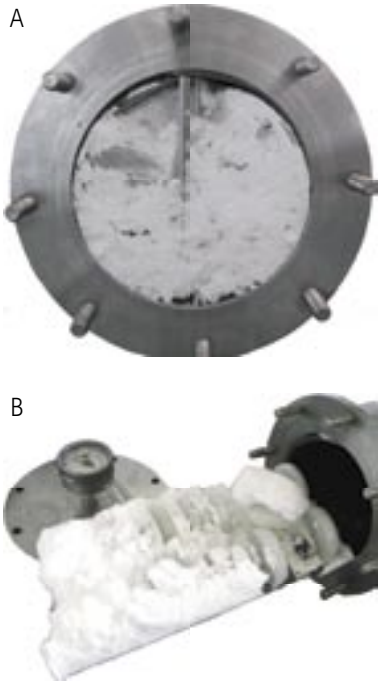

Fig. 12. After CO_2 is conducted into the fixation chambers, the Petri dishes with the Arabidopsis seedlings are completely covered by dry ice. Front view of one fixation chamber (A) and Petri dishes with plants mounted in a holder (B).

2.3.2.4 Post-flight procedure

Total RNA of the shock-frozen seedlings (approx. 300 seedlings per experiment) was isolated via guanidinium thiocyanate-phenol-chloroform extraction (modified after Chomczynski and Sacchi, 1987):

RNA extraction via TRIzol® reagent

- homogenize 100 mg of the sample in 1 mL TRIzol®
- centrifuge for 10 min at 12,000 g at 4-8 °C
- transfer supernatant into 200 µL chloroform
- incubate for 2-3 min at RT
- centrifuge for 15 min at 12,000 g at 4-8 °C
- transfer upper aqueous phase into 0.5 mL icecold isopropanol
- incubate for 10 min at RT
- centrifuge for 10 min at 12,000 *g* at 4-8 °C
- discard the supernatant
- wash the RNA pellet with 75 % ethanol
- mix by vortexing
- centrifuge for 5 min at 7,500 g at 4-8 °C
- air-dry the pellet on ice
- resuspend the pellet in 100 µL H2O

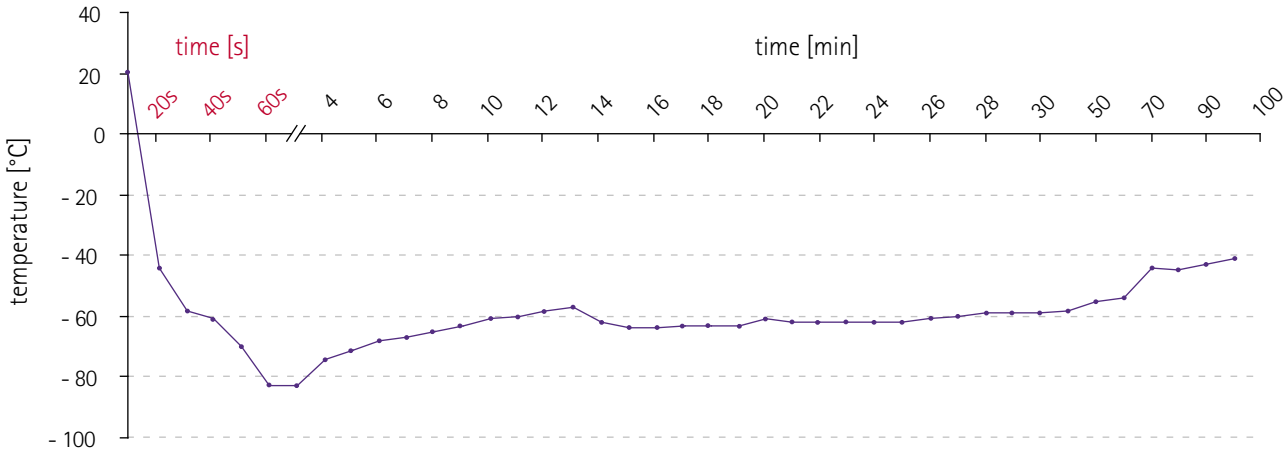

Fig. 13. Temperature recording during the shock-freezing procedure by dry-ice production demonstrates that the temperature inside the fixation chambers abruptly decreases from RT to -80°C. Within seconds the Arabidopsis seedlings and all biological processes, respectively, are fixed. Temperatures of less than -60 °C are hold for more than one hour after fixation.

The extracted RNA was subsequently treated with DNAse and purified according to the protocol of the RNeasy® Mini Kit (p/n 79254, p/n 74104, Qiagen, Hilden, Germany):

DNAse treatment and RNA purification
- mix the following in a microcentrifuge tube:
  ≤ 87.5 µL RNA solution
  10 µL buffer RDD
  2.5 µL DNase I stock solution
  make the volume up to 100 µL with H20
- incubate for 10 min at 20-25°C
- clean up RNA according to the RNA Cleanup protocol of the RNeasy® Mini Kit
- solve the purified RNA in 30 µL H20

Quantity and quality of the purified RNA was determined via photometric analyses (UltrospecTM 3100 pro, Amersham Biosciences Europe GmbH, Germany) and gel electrophoresis. Information about the RNA sample integrity was extracted from a bioanalyzer electrophoretic trace (Agilent 2100 Bioanalyzer, p/n G2938A, Agilent Technologies, Germany). Table II (p 21) summarizes the criteria, which had to be satisfied by the RNA samples for further processing.

2.3.2.5 Agilent one-color microarray technology

To detect transcriptional changes in flight and ground samples, which were exposed to different gravity conditions, Agilent's *Arabidopsis thaliana* 60-mer oligonucleotide microarrays were processed (Agilent Technologies, Germany). The 4x 44K slide format, covering the entire Arabidopsis genome, was selected (www.agilent.com/chem/dna). Each slide provided four identical microarrays with 43,803 *Arabidopsis thaliana* probes represented (content sourced from RefSeq, UniGene, TAIR, TIGR and ATH1).

Table II: Optimal values for RNA concentration, OD ratio, rRNA ratio and RNA integrity number, which had to be satisfied by the RNA samples for further processing.

RNA concentration [ng/µL]	**OD260/OD280** (indication of protein contamination)	**OD260/OD230** (indication of phenol, isothiocyanate, polysaccharides)	**rRNA ratio** (28s/18s) Bioanalyzer	**RIN** (RNA integrity number)
> 200	> 2.0	> 1.8	> 1.2	> 7.0

Each sample was hybridized on a seperate microarray. In contrast to the two-color ratio-based approach, where all gene expression ratios are generated from two samples compared on the same microarray, the one-color intensity-based microarray solution provided the ability to compare the measured gene expression output of one sample directly across the other samples.

Sample preparation and microarray processing

Sample labeling and microarray processing was performed as detailed in the Agilent "One-Color Microarray-Based Gene Expression Analysis (Quick Amp Labeling)" protocol (p/n G4140-90040, version 5.7, March 2008). The labeling reactions were performed using the Agilent Quick Amp Labeling Kit One-Color (p/n 5190-0442) in the presence of cyanine 3-CTP dye. For microarray hybridization the cyanine 3-labeled cRNA samples were hybridized on the Agilent *Arabidopsis thaliana* 4x 44K microarrays using the Agilent Gene Expression Hybrization Kit (p/n 5188-5242). Together with the samples the in vitro synthesized spike-in transcripts of the Agilent One-Color RNA Spike-In Kit (p/n 5188-5282) were hybridized onto the microarrays for the purpose of quality checks. The spike-in transcripts show a minimal self- or cross-hybridization and hybridize only onto the complementary control probes on the microarrays. The expected versus the observed log ratios enabled the monitoring of the microarray workflow for sensitivity and accuracy.
The hybridized microarrays were washed in Agilent Gene Expression Wash Buffer 1 (p/n 5188-5325) for one minute at RT and subsequently in Agilent Gene Expression Wash Buffer 2 (p/n 5188-5326) for one minute at 37 °C. The processed microarrays were scanned with the Agilent DNA microarray scanner (p/n G2565BA), and extracted with Agilent Feature Extraction software (version 10.5). The spot intensity data was loaded into the Agilent GeneSpring® GX software (version 10.0) for data analysis.

2.3.2.6 Data analysis

The technical replicates comprised two to five microarrays. Each of the 11 biological experiments consisted of two to six independent biological replicates to achieve good reproducibility of microarray analyses. The Arabidopsis seedlings for all of the 11 biological experiments were cultivated from three different harvests of seeds (see overview

about all experiments in Table III in the appendix). The median intensity value of all samples was taken for further calculation of intensity dependent normalization of spots for each microarray slide (standard normalization: threshold raw signals to 1.0, normalization algorithm percentile shift of 75). The entities were filtered based on their flag values. The acceptable flags for at least one out of the samples were present or marginal. Up-/down-regulated genes were determined by a higher/lower than 2-fold change in their expression ratio (experiment versus control "0° 2h 1*g*") in all microarrays. The normalized values of up-/down-regulated genes were tested for statistical confidence. Student's t-test analyses showed all changes in gene expression to be statistically significant at a *P*-value of 0.05 or less. Self-organizing cluster analyses were performed on the log(2) fold changes of normalized expression values. Classification of genes into functional categories for biological processes, molecular functions or cellular components by gene ontology annotation was performed at The Arabidopsis Information Resource (TAIR, www.arabidopsis.org/tools/bulk/go/index.jsp, status April 2010).

2.3.2.7 Ground experiments

The parabolic plane-flight experiments offer the possibility to study changes in plant gene regulation as a response to the successively changing acceleration stimuli of µ*g*, 1*g* and 2*g* as well as to the other flight conditions, e.g. vibrations. However, to evaluate the effects of different *g*-conditions on gene expression, various ground experiments were performed.

Vertically oriented control seedlings at 1*g*

Vertically oriented plants under normal Earth 1*g* conditions were the corresponding controls for all ground and flight experiments.

Horizontal stimulation at 1*g*

To assess the effect on gene expression during stimulation by 90°, seedlings were horizontally positioned for 2 h (typical gravitropic response).

Inversion experiment at 1*g*

Horizontally stimulated Arabidopsis seedlings were inverted from 90° to 270° 31 times for 10 s within a total gravistimulation time of 2 h, to determine the effect of repeated short-term inversions on gene expression.

Hypergravity experiments at 2*g*

In order to analyze whether hyper-*g* conditions have an effect on gene expression, seedlings were centrifuged parallel to the direction of the resulting acceleration vector for 2 h at 2*g*. Furthermore, for simulating the short-term hyper-*g* phases of the parabolic flight profile, plants were intermittently centrifuged 62 times at 2*g* for 20s within a total experiment time of 2 h. The hyper-*g* experiments were performed with vertically and horizontally oriented Arabidopsis seedlings.

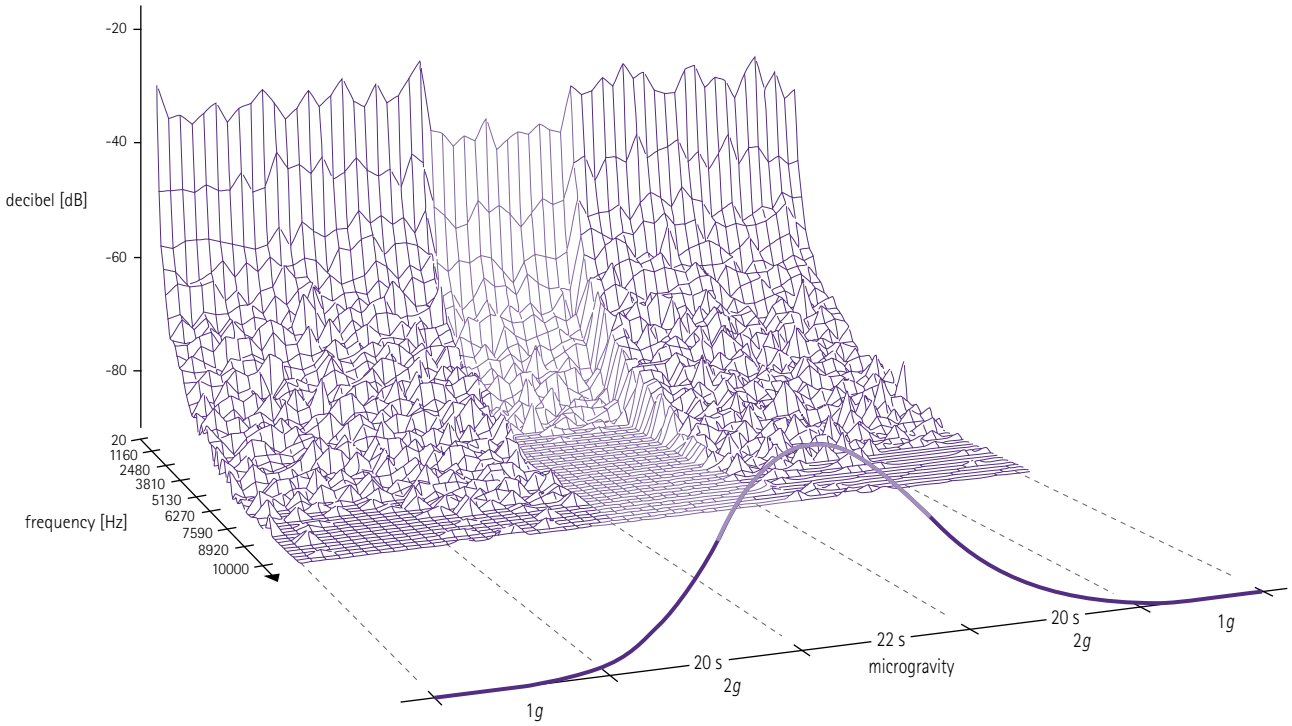

Fig. 14. During vibration experiments on ground, the vibration spectrum of a parabolic flight with the aircraft A300 Zero-G is applied to Arabidopsis seedlings. The vibration pattern and its parabola-phase specific changes for one parabola is illustrated (amplitude in logarithmic scale, frequency in linear scale).

Vibration experiments at 1*g*

During parabolic flights vibrations are generated particularly by the operation of the aircraft engines. Schmidt (2004) demonstrated that the vibrations during a parabolic flight were transmitted to the experiment hardware and to the experiment samples, respectively. In order to evaluate the effect of the vibrations, specific for parabolic plane flights, on the gene expression pattern of Arabidospsis, ground controls were performed. The analysis during parabolic flights in the aircraft A300 Zero-G, conducted by Schmidt (2004), was the basis for the vibration simulation on *Vibraplex*, a newly developed hardware (developed and constructed by Dr. Jens Hauslage, DLR, Germany). The pattern of various vibrations of different frequencies (0.2Hz - 14kHz) and intensities (maximum 56 Wm^{-2}), as specific for a parabolic plane flight, was programmed in terms of an audio sound file (WAV format). The digital file signal was amplified with an audio amplifier and directly transmitted to the vibration platform of the *Vibraplex* unit, on which the vertically oriented Arabidopsis seedlings were attached. The applied signal strength in terms of vibrations was controlled via a piezoelectric crystal, which was installed directly on the vibration platform and, therefore, allowed for oscilloscope monitoring of the signal. During the 2-h ground experiment, the vibration spectrum of a 2-h parabolic flight with 31 parabolas including the parabola-phase specific changes in vibration intensities (Fig. 14) was simulated.

2.4 Chemicals and Reagents

A. dest	aqua destillatum
acetone	Carl Roth GmbH & Co. KG
agar	extra pure, fine powder, Merck KGaA, Darmstadt, Germany
Azure II	Merck KGaA, Darmstadt, Germany
bacto-agar	Sigma Aldrich Chemie GmbH, Steinheim, Germany
EtOH	ethanol, Carl Roth GmbH & Co. KG
Gene Expression Hybridization Kit	p/n 5188-5242, Agilent Technologies, Germany
Gene Expression Wash Buffer 1	p/n 5188-5325, Agilent Technologies, Germany
Gene Expression Wash Buffer 2	p/n 5188-5326, Agilent Technologies, Germany
H_2O	water
$KMnO_4$	potassium permanganate, crystalline, Sigma Aldrich Chemie GmbH, Steinheim, Germany
Methylene Blue	Merck KGaA, Darmstadt, Germany
NaOCl	sodium hypochlorite solution
Quick Amp Labeling Kit, One Color	p/n 5190-0442, Agilent Technologies, Germany
RNA Spike-In Kit, One Color	p/n 5188-5282, Agilent Technologies, Germany
RNeasy® Mini Kit	Qiagen, Hilden, Germany
sodium tetraborate (Borax)	Merck KGaA, Darmstadt, Germany
TRIzol®	Invitrogen GmbH, Karlsruhe, Germany
TWEEN®	TWEEN® 20 pure (polyoxyethylene sorbitan monooleate), Serva Electrophoresis GmbH, Heidelberg Germany

2.5 Solutions and Media

Medium for Arabidopsis cultivation (modified after Legué, 1997)

1M KNO_3
1M $Ca(NO_3)_2$ x4H_2O
1M $(NH_4)2H_2PO_4$
0.5M $MgSO_4$ x7H_2O

micronutrients:
25µM KCl
25µM Fe-Na EDTA
17.5µM H_3BO_3
1µM $MnSO_4$
1µM $ZnSO_4$
0.25µM $CuSO_4$
0.25µM $(NH_4)_6MoO_{24}$

ERL (Spurr Low Viscosity Embedding Media, Catalog No. 17706-1, Polysciences Europe GmbH, Eppelheim, Germany)

soft medium:
4.1g ERL 4221
1.9g Diglycidyl ether of polypropylene glycol (D.E.R. 736)
5.9g Nonenyl succinic anhydride (NSA)
0.1g Dimethylaminoethanol (DMAE)

Methylene Blue/Azure II

Filter 1% Methylene Blue in A. dest and 1% Azure II in sodium tetraborate (Borax). Mix 1:1.
Before use, mix dye solution : A. dest (1:3).

3. RESULTS

3.1 Threshold-acceleration level required for lateral statolith displacement in Chara rhizoids

During the 13-min µ*g*-phase of the MAXUS-8 sounding rocket flight, lateral centrifugal forces were applied to vertically growing characean rhizoids. Three different cells, each of them subjected to a different acceleration profile (Fig. 15), were observed by video microscopic recording. The accelerations 0.100*g*, 0.080*g* and 0.060*g* in the µ*g*-phase from +75 s to +400 s were subsequently stepwise decreased in the course of the flight (Fig. 15). Analyses of single images, that were extracted from the video microscopic recording, showed that the statolith complex in all three rhizoids was symmetrically distributed across the cell diameter before lift off (Fig. 15, t = -180 s). Centrifugal displacement of statoliths caused by the 0.100*g* and the 0.080*g* acceleration in microgravity was first detectable at +360 s (Fig. 15, A and B). During continued but stepwise decreasing of the lateral acceleration from 0.100*g* to 0.083*g* and from 0.080*g* to 0.067*g*, statoliths were further displaced toward the centrifugal plasma membrane (Fig. 15; A, t = +600 s; B, t = +720 s). Toward the end of the microgravity phase, individual statoliths sedimented onto the centrifugal cell flank (Fig. 15; A, t = +800 s; B, t = +800 s). Analyses of the mean lateral displacement ± SE (standard error) for individual statoliths in lateral direction (n = 5), demonstrated that the lateral accelerations 0.08*g* and higher were sufficient for significant lateral displacement of the statoliths (Fig. 16, A.3 and B.3). The lateral accelerations 0.073*g*, 0.067*g* and 0.060*g* induced a distinct but not significant tendency of a lateral shift of the statoliths (Fig. 16, B.3 and C.3). In addition to the lateral statolith displacement, induced by the centrifugal forces, the basipetal actomyosin-dependent transport of the statoliths was observed in all rhizoids. Toward the end of the µ*g*-phase at t = +800 s, the basipetal edge of the statolith complex was at 38 - 43 µm from the outmost tip of the rhizoid (Fig. 16, A.1 - C.1, dark gray shapes).

Fig. 15. Distribution of statoliths in characean rhizoids before lift off (-180 s) of the MAXUS-8 sounding rocket and during lateral centrifugation in microgravity (indicated in seconds after lift off). The rhizoids exhibited a symmetrical distribution of statoliths across the cell diameter before lift off. From +75 s to + 400 s during microgravity, the lateral accelerations 0.100*g* (A), 0.080*g* (B) and 0.060*g* (C) were applied to the rhizoids by centrifugation. In the residual microgravity phase of the flight the lateral acceleration stimulus was stepwise changed. Centrifugal displacement of the statoliths caused by the 0.100*g* and the 0.080*g* acceleration in microgravity was first detectable at +360 s (A, B). Decreasing of the acceleration to 0.092*g* and 0.083*g* (A) and 0.073*g* and 0.067*g* (B), respectively, caused further displacement of the statoliths and individual statoliths settled onto the centrifugal cell flank toward the end of the microgravity phase (+800 s, A and B). However, in the rhizoid, which experienced accelerations between 0.055*g* and 0.006*g*, no significant lateral statolith displacement was observed (C). The arrows indicate the direction of gravitational and centrifugal forces. The diameter of each rhizoid was 25 µm.

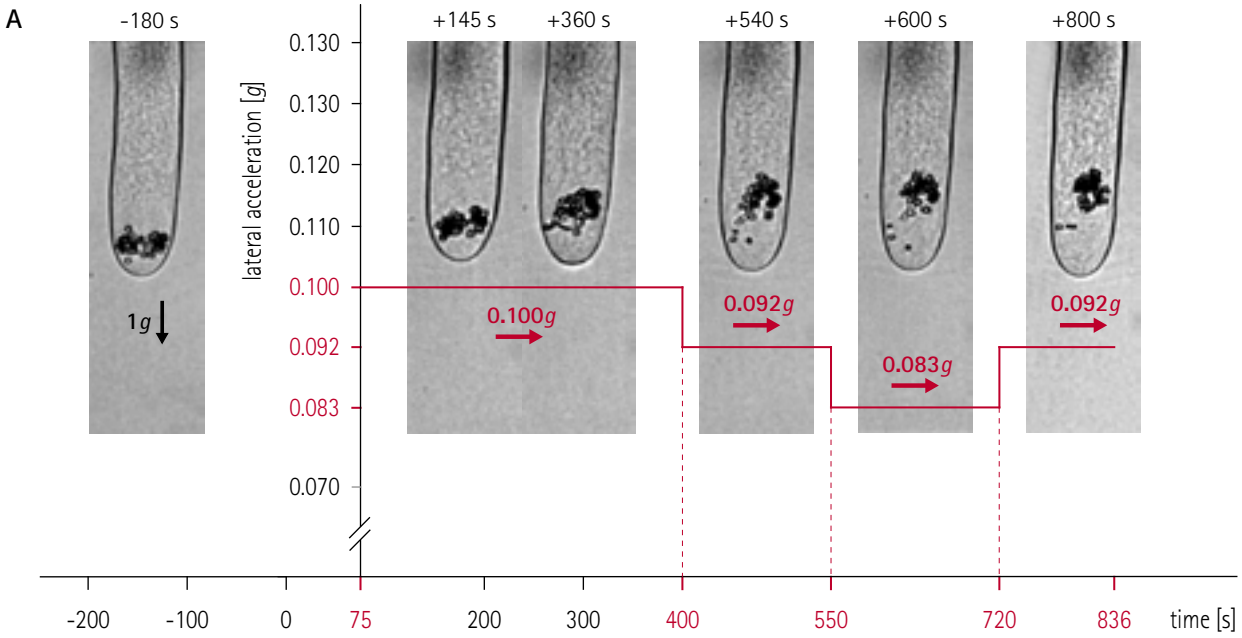
A
-180 s
+145 s
+360 s
+540 s
+600 s
+800 s
lateral acceleration [g]
0.130
0.130
0.120
0.110
0.100
0.092
0.083
0.070
1g
0.100g
0.092g
0.083g
0.092g
-200
-100
0
75
200
300
400
550
720
836
time [s]

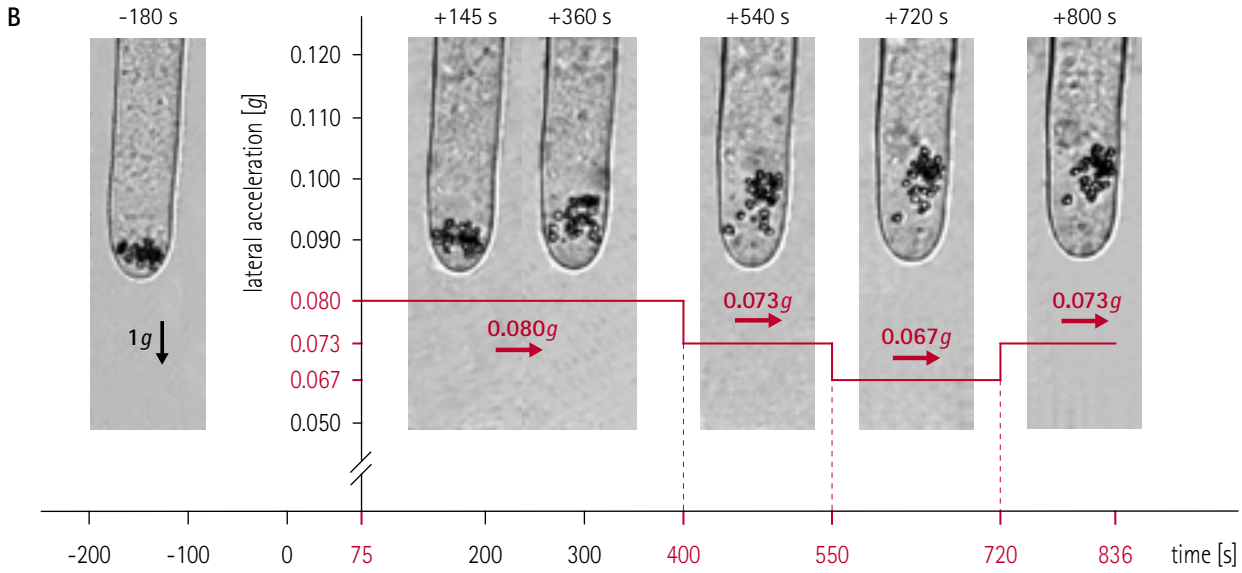
B
-180 s
+145 s
+360 s
+540 s
+720 s
+800 s
lateral acceleration [g]
0.120
0.110
0.100
0.090
0.080
0.073
0.067
0.050
1g
0.080g
0.073g
0.067g
0.073g
-200
-100
0
75
200
300
400
550
720
836
time [s]

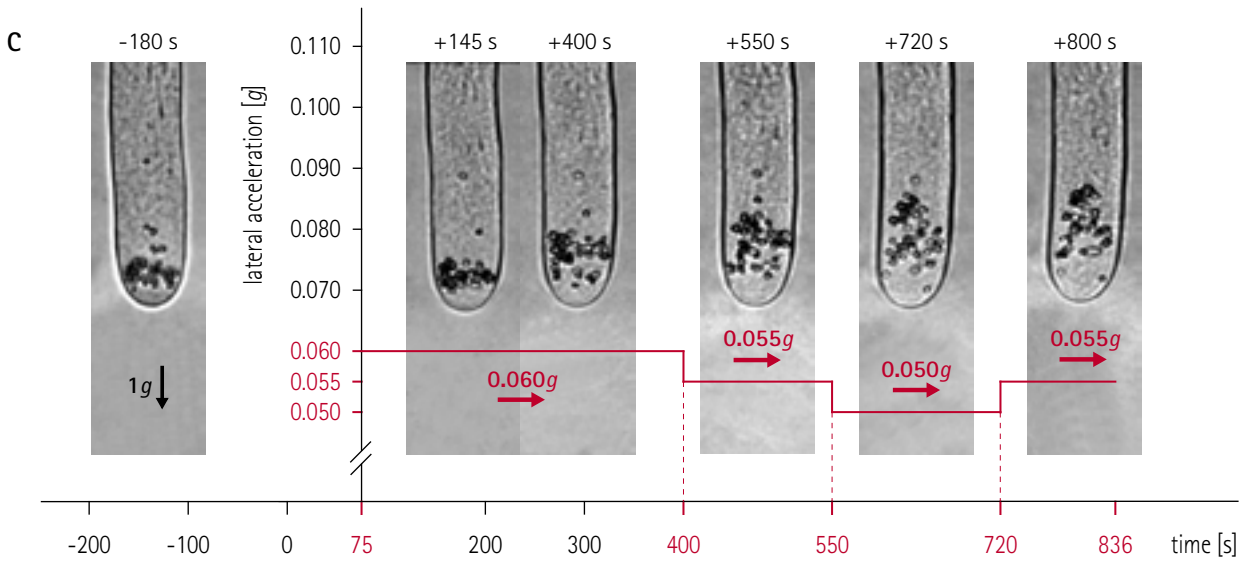
C
-180 s
+145 s
+400 s
+550 s
+720 s
+800 s
lateral acceleration [g]
0.110
0.100
0.090
0.080
0.070
0.060
0.055
0.050
1g
0.060g
0.055g
0.050g
0.055g
-200
-100
0
75
200
300
400
550
720
836
time [s]

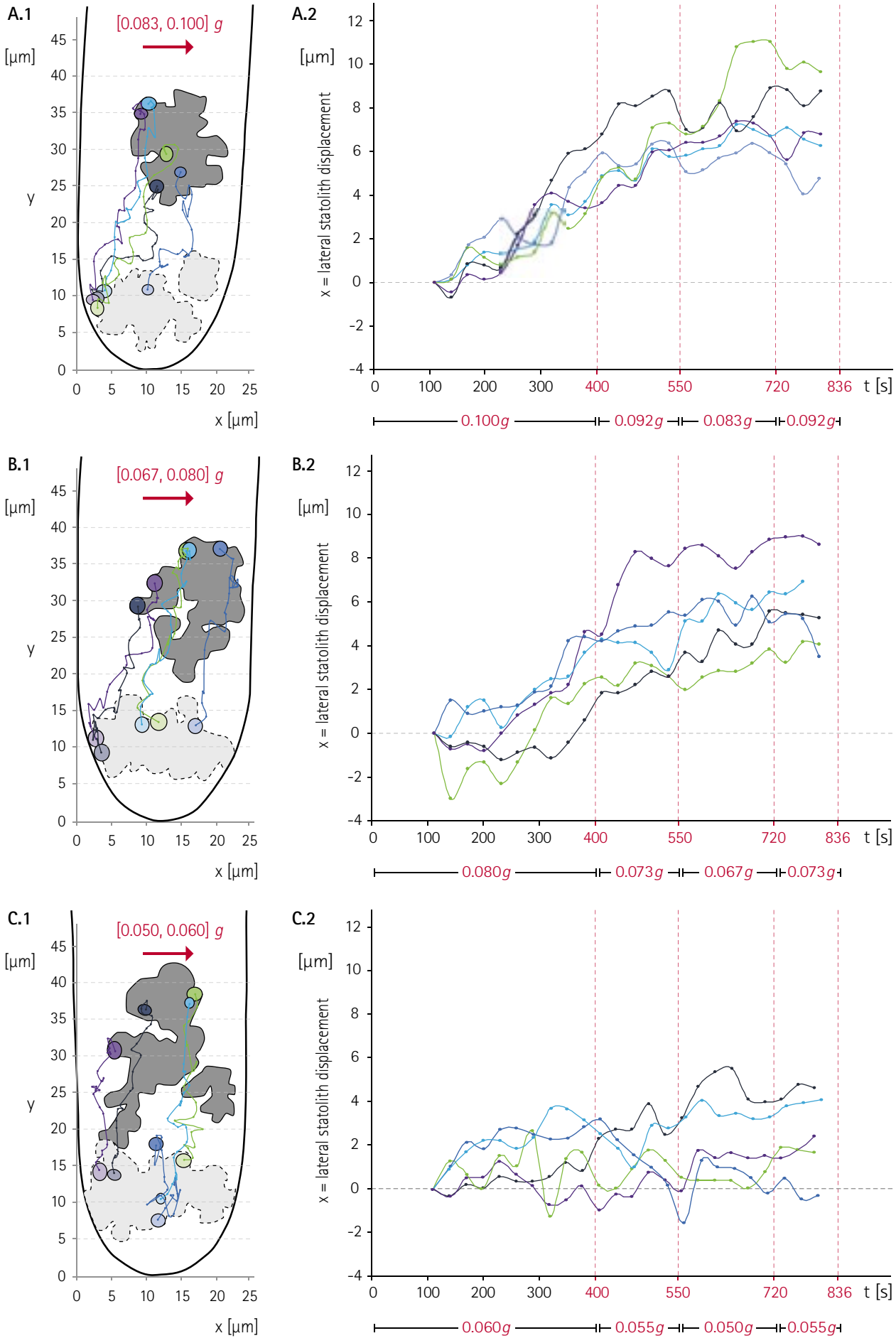
A.1
[0.083, 0.100] g
[µm]
y
x [µm]
A.2
[µm]
x = lateral statolith displacement
t [s]
0.100g
0.092g
0.083g
0.092g
B.1
[0.067, 0.080] g
[µm]
y
x [µm]
B.2
[µm]
x = lateral statolith displacement
t [s]
0.080g
0.073g
0.067g
0.073g
C.1
[0.050, 0.060] g
[µm]
y
x [µm]
C.2
[µm]
x = lateral statolith displacement
t [s]
0.060g
0.055g
0.050g
0.055g

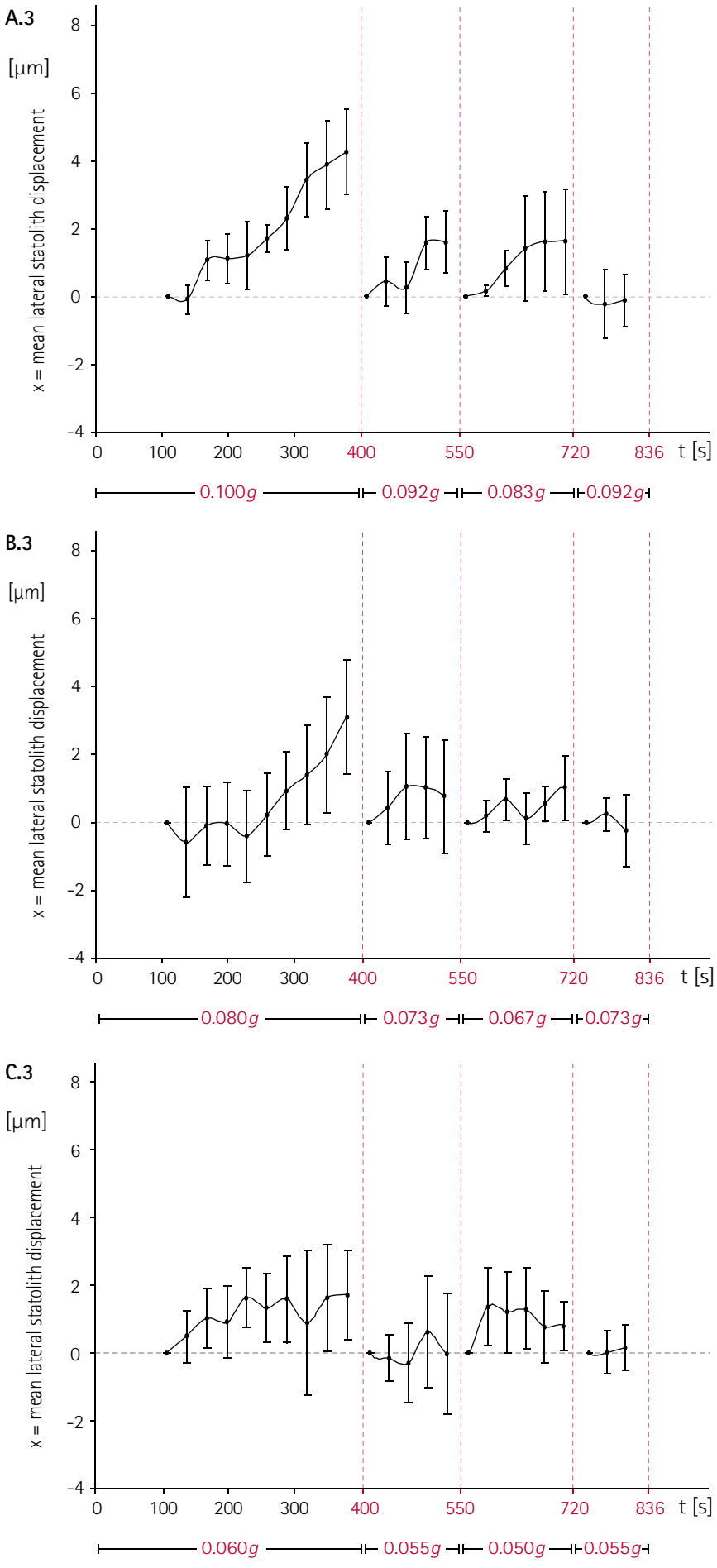

Fig. 16 (pp 29 – 30). Displacement of the statolith complex and of single statoliths by lateral centrifugation during 13 min of microgravity. Rhizoids that were laterally centrifuged with lowest 0.050*g* to 0.060*g* and highest 0.083*g* to 0.100*g* showed the displacement of the statolith complex and of individual statoliths during microgravity from +110 s after lift-off (light gray shape) to +800 s after lift-off (dark gray shape) (A.1 - C.1) . For all rhizoids the position of each of five individual statoliths was set to zero at +110 s for analyzing their lateral displacement over time (A.2 - C.2). The analyses of the mean lateral displacement for the statoliths ± SE in lateral direction (illustrated for each of the experimental phases with different accelerations) demonstrated that centrifugation with minimum 0.080*g* induced a significant displacement of statoliths (A.3 - C.3). A distinct albeit not significant tendency of lateral statolith displacement was observed at the 0.060*g* centrifugation during the first 400s of microgravity (C.3).

3.2 Statolith-mediated graviperception in Arabidopsis root statocytes

In order to deliver proof that in the 20-s µ*g*-phases of the parabolic plane flight sedimented statoliths are not displaced from the gravireceptor site in higher plant root statocytes, during parabolic flights with the Airbus A300 Zero-G horizontally positioned Arabidopsis root seedlings were fixed at the beginning and at the end of the µ*g*-phases. Fixation of the seedlings with $KMnO_4$ was performed during the first and the 16th parabola on three flight days. The fixed Arabidopsis root seedlings, which were cut off in a 45° angle to indicate the orientation of the root relative to the gravity vector during flight (see 2.3.1.4 in Materials and Methods), were cut into semithin sections and the position of the statoliths was determined relative to the physical lower cell flank (see 2.3.1.5 in Materials and Methods).
Video recording of the fixation procedure on each flight day confirmed the optimal distribution of the fixation solution on the plant seedlings. The microscopic analyses revealed no significantly different values for the position of the statoliths at the beginning and at the end of the µ*g*-phases (Fig. 18). The mean distances between the sedimented statoliths and the physical lower cell flank of the root statocytes were between 0.62 µm at the beginning of the µg-phase and 0.57 µm at the end of the µg-phase (Fig. 18, A), corresponding to a non-significant difference of 8% (Fig. 18, B). However, in root seedlings, which were prestimulated on ground at 90° and subsequently inverted to 270° for the duration of 10 s, the mean distances between the sedimented statoliths and the lateral cell flank of the statocytes were significantly enhanced by 80% (from 0.46 µm to 0.83 µm, Fig. 17) compared to non-inverted controls. Longer inversion times of 60 s and 120 s further increased distances (Fig. 17).

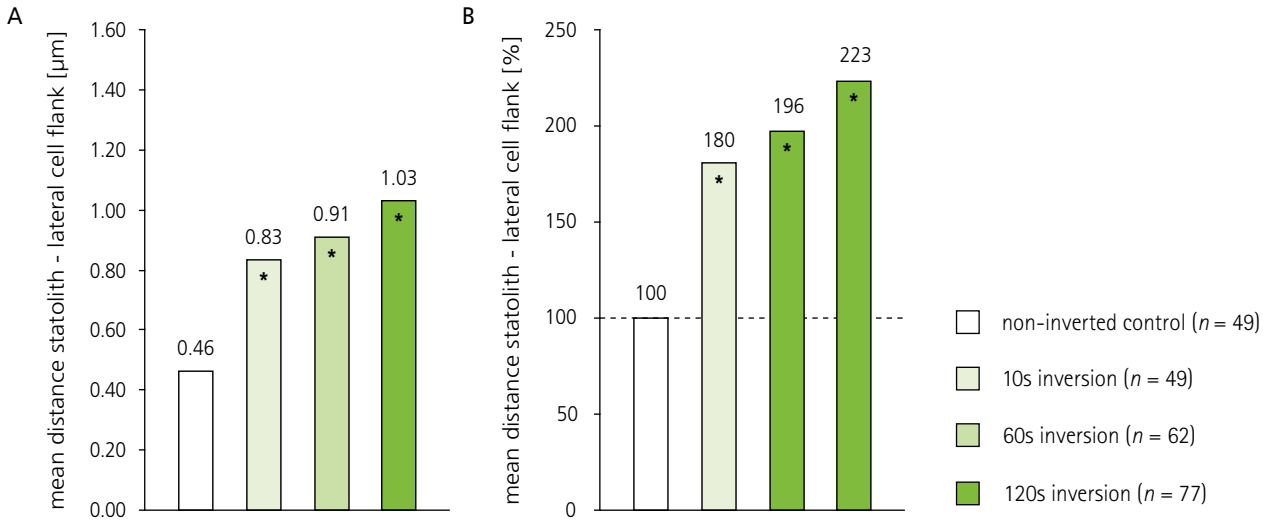

Fig. 17. The mean distances between sedimented statoliths and the lower cell flank of Arabidopsis root statocytes were significantly enhanced in all inversion experiments. In plant seedlings, which were prestimulated on ground for 20 min at 90° and subsequently inverted to 270° for the duration of 10 s, the mean distances between the sedimented statoliths and the lateral cell flank of the root statocytes were signficantly enhanced from 0.46 µm to 0.83 µm (A), i.e. by 80% (B) compared to non-inverted controls that were set to 100% (Student's t test, $P \leq 0.01$; indicated by an asterisk). Distances were further increased by longer inversion durations (60s and 120s).

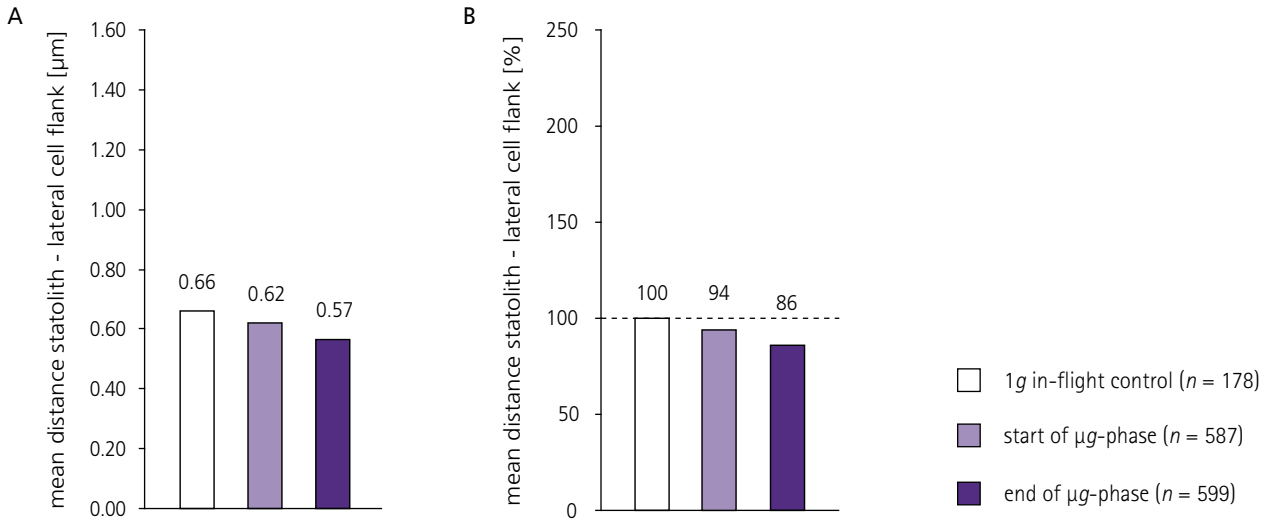

Fig. 18. During the µ*g*-phases of the parabolic flight, in horizontally positioned Arabidopsis seedlings, the position of sedimented statoliths in the root statocytes was not significantly altered. The mean distances between the sedimented statoliths and the physical lower cell flank were not significantly different at 1*g* during flight (in-flight control before first parabola), at the beginning and at the end of the µ*g*-phases (mean data for parabola 1 and 16).

3.3 Gravity-dependent gene expression in plants

The parabolic flight profile with its alternating phases of 1*g*, 2*g* and µ*g* as well as various experimental conditions on ground were used to determine the influence of altered *g*-conditions on the gene expression pattern of plants. One of the main objectives was to identify sets of genes whose expression is explicitly regulated in repsonse to specific *g* conditions and to detect similarities and differences in the plants response to normal Earth gravity, hyper- and microgravity conditions.

Unless otherwise noted, in the present study, the significant differential expression of a transcript under the experimental conditions was determined on the level of the at least 2-fold up- or down-regulation of the transcript compared to the expression in the control plants at 1*g* (0° 2h 1*g*) (exceptions to this rule are explicitly described in the figure legends).

An overview of all experiments and their gravitational conditions as well as the normalized intensity values of selected sets of genes are listed in the appendix (Table III). Total microarray data on the differential gene expression in the experiments is listed in the digital appendix on the enclosed compact disk.

3.3.1 The quality of the technical and biological replicates of ground and flight experiments confirms a high reproducibility of the data

The isolated RNA of biological replicates, i.e. samples, which experienced the same experimental conditions, were hybridised on slides of different arrays (technical replicates) (for overview about all biological and technical replicates see Table III in the appendix). The transcript abundances of the biological replicates were nearly identical. Except for single outliers, the replicates did not show significant differences in gene regulation (Fig. 19). In plant seedlings, which were exposed to quite different experimental treatments, however, diverse genes with minimum twice up- or down-regulation were detected (Fig. 19). Selected housekeeping genes were used to ensure the quality of the biological replicates. Under the different experimental conditions, the average expression level of the housekeeping genes was not significantly regulated compared to the control (0° 2h 1*g*). The level of expression for almost all housekeeping transcripts was far below the defined 2-fold change threshold for a significant gene expression change (Fig. 20). These results confirm the reproducibility of the data in the present study.

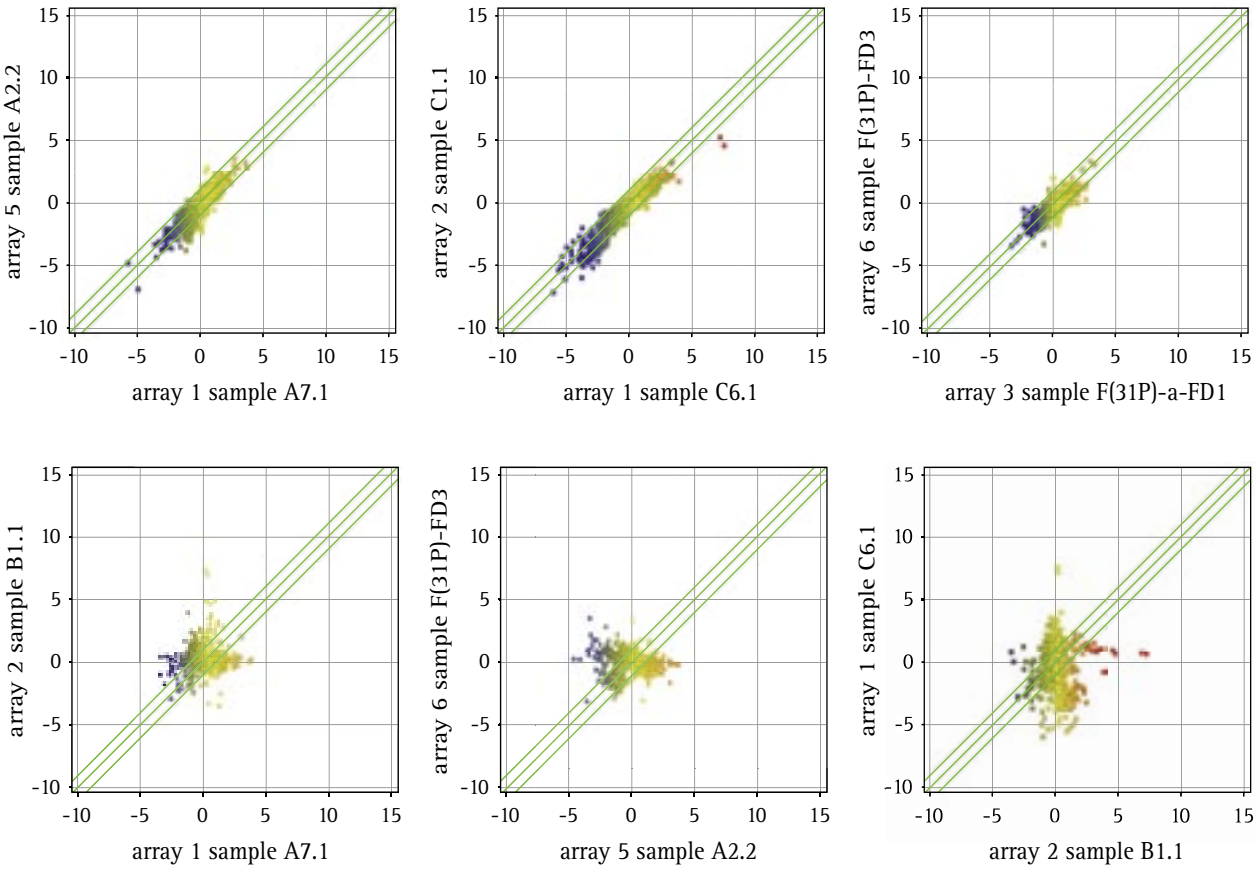

Fig. 19. Examples of scatter-plot graphics for transcript samples of different experiments. The transcript abundances of independently obtained samples were plottet against each other. Each spot represents one transcript. The up- or down-regulation of a transcript is indicated by the position of the corresponding spot relative to the inner green line. The outer green lines signify a change in the expression level of at least 2-fold up- or rather down-regulation. Biological replicates, which were exposed to the same experimental conditions, did not show significant differences in gene regulation and, therefore, confirmed the reproducibility of the data (upper row). In samples, which experienced different experimental treatments, however, the abundances of diverse genes were significantly different (lower row).

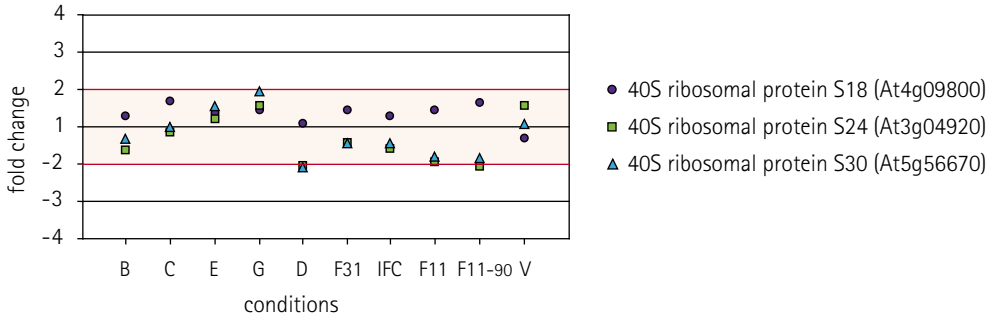

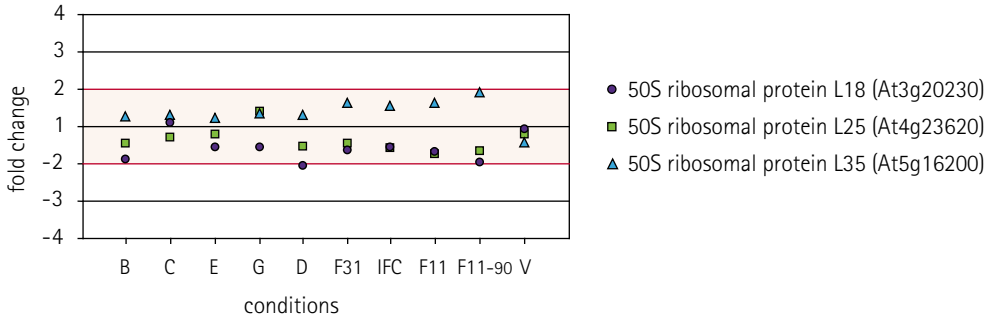

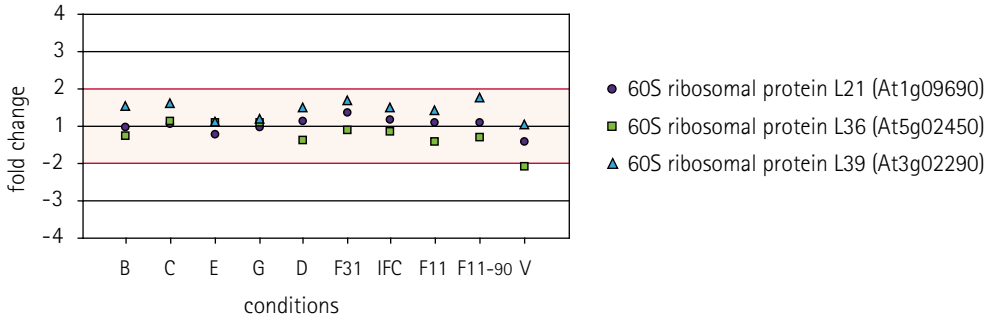

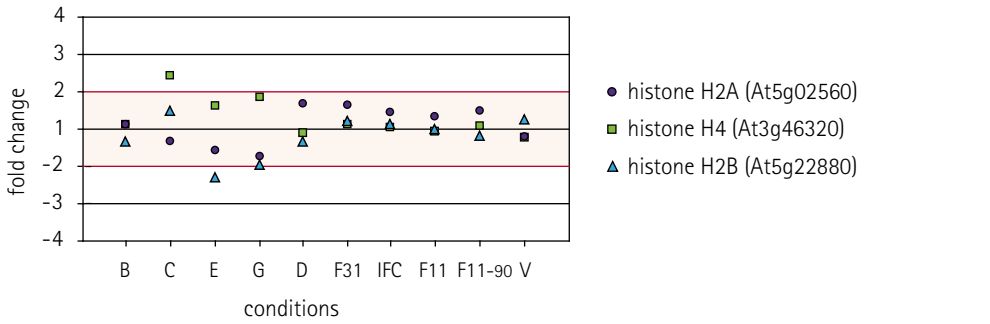

B	90° 2h 1*g*
C	0° 62x 20s 2*g* in 2h 1*g*
E	90° 62x 20s 2*g* in 2h 1*g*
G	90° 2h 2*g*
D	90° 31x 10s inversion in 2h 1*g*
F31	0° 2h flight, 31 parabolas (µ*g*, 1*g*, 2*g*)
ICF	0° 2h in-flight control, 31 parabolas (1*g*, 2*g*)
F11	0° 1h flight, 12 parabolas (µ*g*, 1*g*, 2*g*)
F11-90	90° 1h flight, 12 parabolas (µ*g*, 1*g*, 2*g*)
V	0° 2h vibrations in 2h 1*g*

Fig. 20. Expression of prominent housekeeping genes. Except for two single outliers (histone H4 at condition C and histone H2B at condition E), the gene expression levels of the selected housekeeping genes did not exceed the 2-fold change threshold of siginificant expression change (red lines) at the different conditions of the diverse flight and ground experiments. These results confirm the reproducibility of the data.

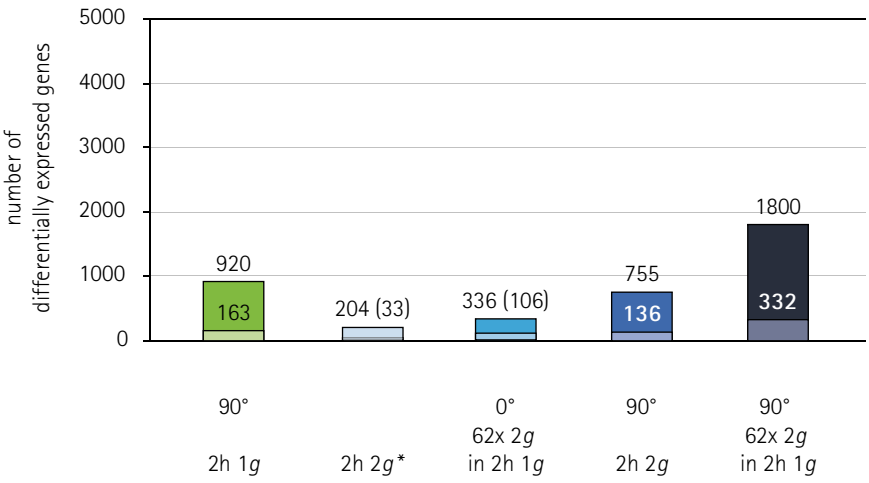

Fig. 21 (pp 37 - 38). Number of differentially expressed genes under the different gravity conditions. Differential expression in all experiments was determined compared to the control (0° 2h 1*g*), except for 2h 2*g** (90° 2h 2*g* versus 90° 2h 1*g*). The upper bars describe the number of at least 2-fold up-/down-regulated genes while the lower bars indicate the number of at least 4-fold higher or lower expressed genes.

3.3.2 The number of significantly up-/down-regulated genes varied depending on the gravity conditions in the ground and parabolic flight experiments

920 genes were differentially expressed during 90°-reorientation at 1*g*

During horizontal stimulation of plant seedlings under 1*g* conditions, 920 genes were at least twice up- or down-regulated compared to the vertically growing controls at 1*g* (Fig. 21). Thus, during the typical gravitropic response, i.e. the plants response to 90° stimulation at 1*g* conditions (in the recent study for 2 h), a set of 920 genes is differentially expressed. More than 17% (163) of these genes were at least 4-fold up- or down-regulated (Fig. 21).

The effect of repeated short-term 2*g* centrifugation on gene expression was stronger than of continuous 2*g* centrifugation

Non-stop centrifugation with 2*g* for 2 h induced the differential expression of 204 genes (33 at FC ≥ 4). Intermittently centrifugation at 2*g* (62x 2*g* for 20s in 2 h) resulted in 336 significantly regulated genes (106 at FC ≥ 4) (Fig. 21). In horizontally stimulated plant seedlings under the same hyper-*g* conditions the expression level of 755 genes at continuous centrifugation and 1800 genes at intermittently centrifugation was 2-fold changed (136 and 332 at FC ≥ 4). Therefore, with regard to the number of significantly up- or down-regulated genes, the effect of periodically applied hyper-*g* centrifugation was three to five times higher than at continuous 2*g* conditions.

Within the ground experiments, repetitive inversion led to the highest impact on gene expression level

The repetitive inversion of horizontally stimulated plant seedlings from the 90° position to the 270° position for 10 s within a total gravistimulation time of 2 h strongly affected the gene-expression pattern of Arabidopsis. Inversion samples versus controls resulted in 3130 genes, which were minimimun twice up- or down-regulated (937 at FC ≥ 4) (Fig. 21). Vibration of the seedlings according to a simulation

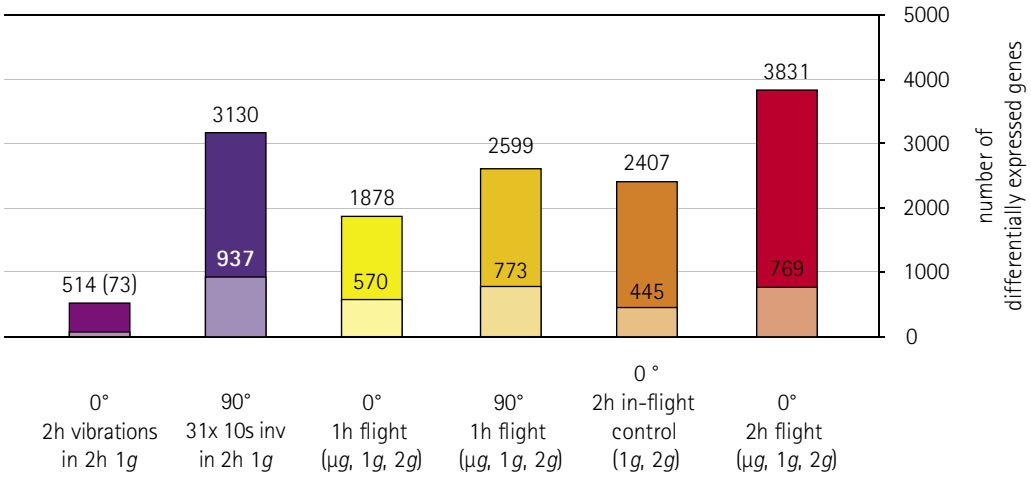

of the flight-vibration profile induced the significant up- and down-regulation of less genes (514 at FC ≥ 2 and 73 at FC ≥ 4) (Fig. 21).

The effect of parabolic flight conditions on gene expression was dependent on the duration of flight and the plant orientation during flight

Parabolic flight conditions had a strong impact on the transcriptome pattern of Arabidopsis compared to the ground experiment conditions. In the flight experiments 1878-3831 genes were at least 2-fold higher or lower regulated than in the corresponding ground control (0° 2h 1*g*). Between 18% and 30% of these affected genes showed a 4-fold and higher change in their expression rate (Fig. 21). The number of significantly up-/down-regulated genes increased in the seedlings exposed to a 2-h flight compared to those which exprienced a 1-h flight. The 1-h flight comprising 11 parabolas induced a significant change in expression for 1878 genes, whereas in the 2-h flight comprising 31 parabolas approximately twice this amount of genes (3831) was affected (Fig. 21). Therefore, in terms of the number of differentially expressed genes, the extend of influence on gene regulation is dependent on the duration of the flight and the number of parabolas, respectively. In in-flight controls (2-h flight), which experienced all flight conditions but not the µ*g* phases as they were accelerated with 1*g* during microgravity, less genes were differentially expressed. A total of 2407 genes, 1424 less than in the 2-h flight samples, was involved in the plants response to the 1*g* and 2*g* flight conditions (in-flight control) (Fig. 21). During flight, an additional stimulation of the plants by 90° resulted in an increase from 1878 differentially expressed genes (570 at FC ≥ 4) in the vertically positioned plants to 2599 (773 at FC ≥ 4) in the horizontally positioned plants (1-h flight).

Classification of the differentially expressed genes in ground and flight experiments into functional categories by annotation for biological processes

The functional categorization of the differentially expressed genes in ground and flight experiments was performed on the basis of the gene

Fig. 22. Classification of the differentially expressed genes into functional categories by annotation for biological processes (based on the gene ontology at TAIR). The number of at least twice up-/down-regulated genes for the categories is shown for ground and flight experiments. Multiple attribution of genes to different categories possible.

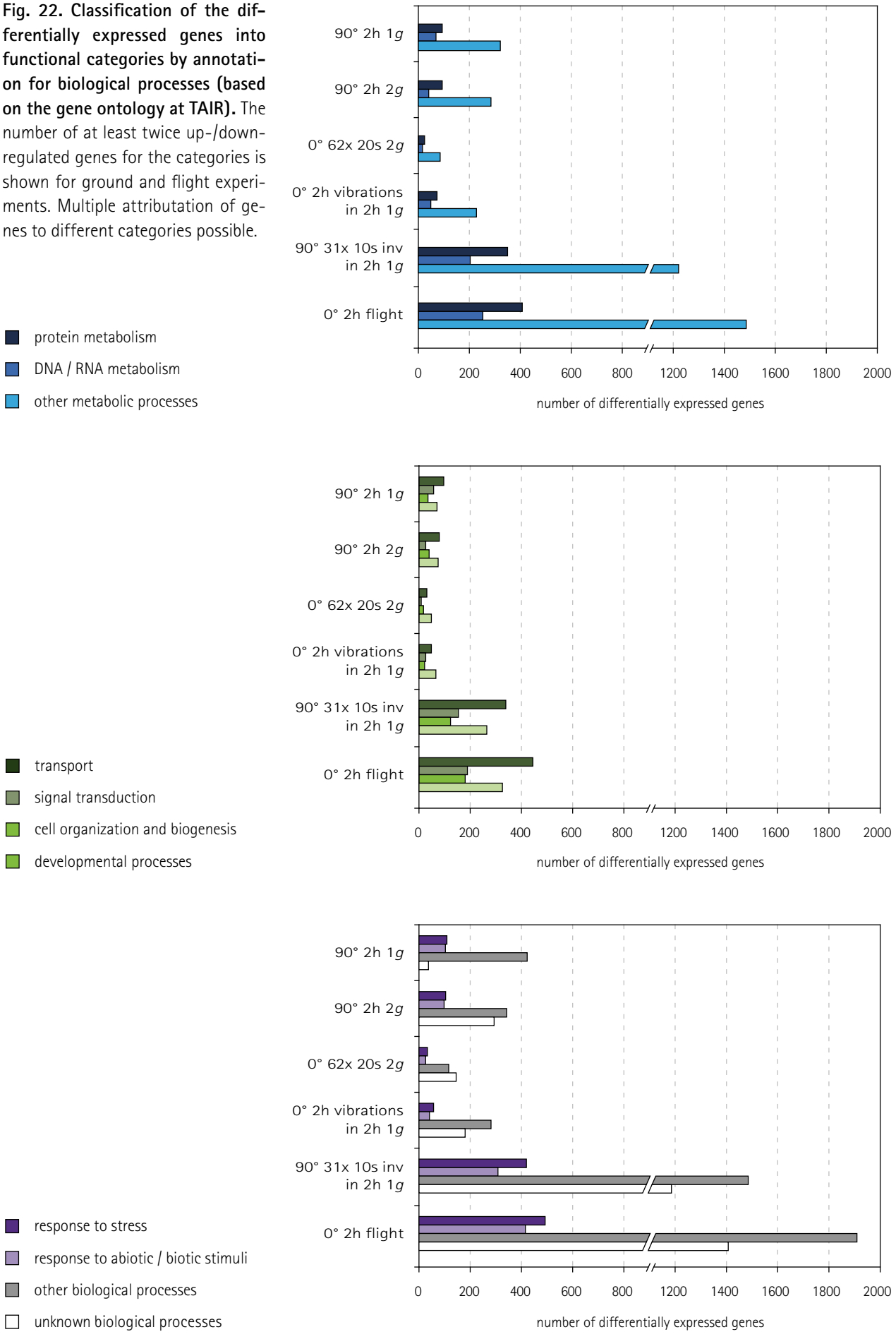

ontology at The Arabidopsis Information Resource (TAIR; status April 2010). The high numbers of differentially expressed genes in inversion and flight experiments (0° 2h flight) are substantially attributed to increases of metabolic processes, transport activities, responses to stress and abiotic/biotic stimuli (Fig. 22). For the ground experiments providing different gravity conditions (90° 2h 1*g*, 90° 2h 2*g*, 0° 62x 20s 2*g*, 0° 2h vibrations), the classification of the significantly up-/down-regulated genes is similar. Because of insufficient annotation details, the TAIR gene ontology of several hundreds of genes, especially for the inversion and flight experiments, did not provide any functional category.

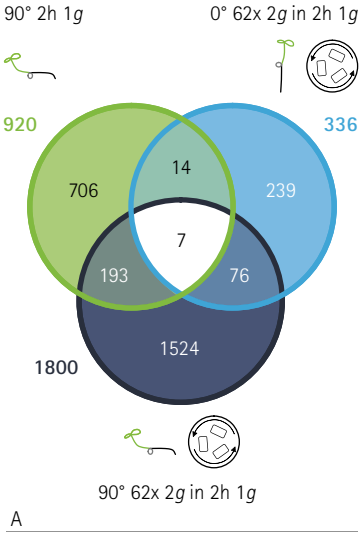

3.3.3 Genes involved in the response to 90° reorientation at 1*g* were not significantly affected by 2*g* but by the conditions of parabolic plane flights

Under hyper-*g* conditions other genes were differentially expressed than during response to horizontal stimulation at 1*g*

At both, 2 h of nonstop 2*g*-centrifugation and repetitive short-time centrifugation with 2*g* (62x 20s 2g in 2 h 1g), other genes were differentially expressed than during the gravitropic plant response at 1*g* (90° 2h 1*g*). Only 21 genes were shared between the experiment groups '0° 62x 2*g* in 2h 1*g*' and '90° 2h 1*g*' (Fig. 23, A). Only 25 genes were common components of the gene regulation processes in the experimental groups '2h 2*g*' (* 90° 2h 2g versus 90° 2h 1g) and '90° 2h 1*g*' (Fig. 23, B). However, as part of the specific response to the 90°-stimulus in horizontally positioned plants, 88 genes were regulated under both, 1*g* and 2*g* conditions (Fig. 23, C).

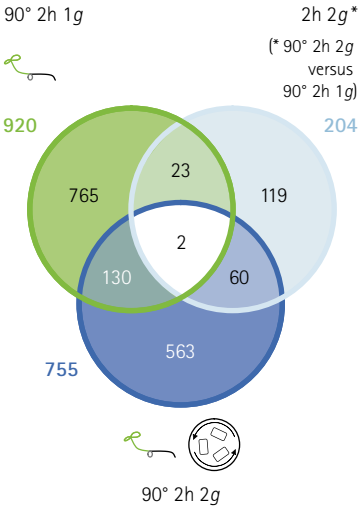

108 genes were particularaly regulated due to the repeated short-term 2*g* stimuli in ground and flight experiments

On ground, the successive short-term centrifugation simulating the hyper-*g* phases of the parabolic flight profile (62x 20s 2*g*) resulted in 336 differentially expressed genes. Approximately one-third of these genes (108) were also affected by the 2*g* conditions of parabolic plane flight (Fig. 23, D). When plants were horizontally positioned during centrifugation in the ground experiment, the number of genes differentially expressed at both, repeated 2*g* centrifugation and flight conditions, increased to 389 (Fig. 23, E).

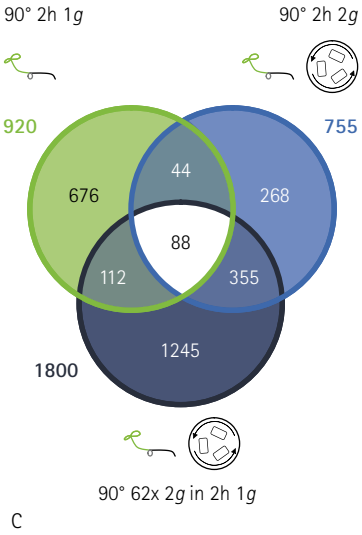

Fig. 23 (pp 40 – 42). Venn diagrams in the side columns visualize specificities and interferences of the plant-gene responses to different *g*-conditions (created with Agilent GeneSpring® GX). Each of the three circles of a venn diagram represents one set of differentially expressed genes under a specific experiment condition. The total number of at least twice up-/down-regulated genes (3.3.2) compared to the control (0° 2h 1*g*) is displayed next to the corresponding circle. The intersections of two circles illustrate the genes shared between two experimental groups, while the intersections of three circles comprise the genes differentially expressed under all of the three experimental conditions.

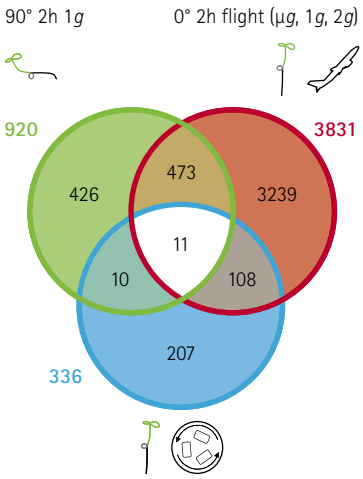
90° 2h 1g
0° 2h flight (µg, 1g, 2g)
920
3831
426
473
3239
11
10
108
207
336
0° 62x 2g in 2h 1g

D

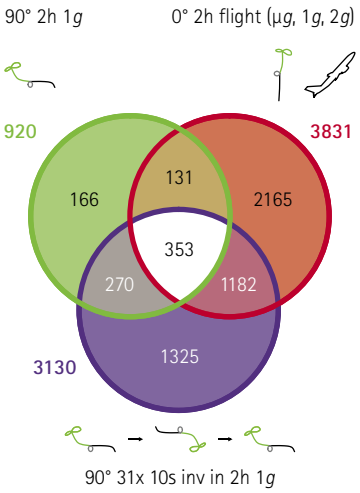
90° 2h 1g
0° 2h flight (µg, 1g, 2g)
920
3831
166
131
2165
353
270
1182
3130
1325
90° 31x 10s inv in 2h 1g

G

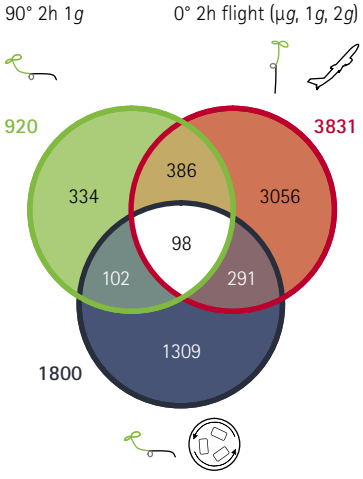
90° 2h 1g
0° 2h flight (µg, 1g, 2g)
920
3831
334
386
3056
98
102
291
1800
1309
90° 62x 2g in 2h 1g

E

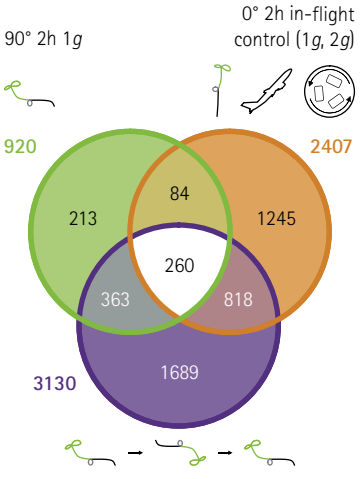
90° 2h 1g
0° 2h in-flight control (1g, 2g)
920
2407
213
84
1245
260
363
818
3130
1689
90° 31x 10s inv in 2h 1g

H

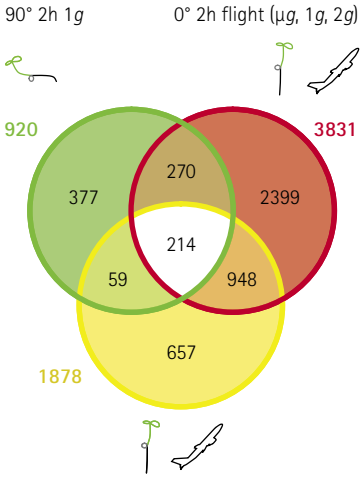
90° 2h 1g
0° 2h flight (µg, 1g, 2g)
920
3831
377
270
2399
214
59
948
1878
657
0° 1h flight (µg, 1g, 2g)

F

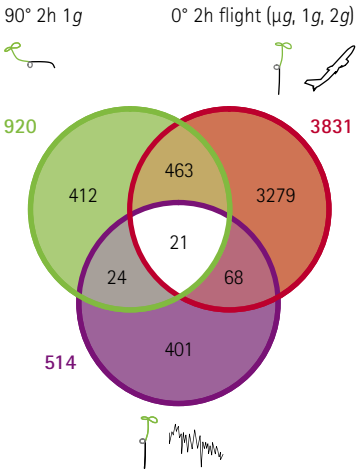
90° 2h 1g
0° 2h flight (µg, 1g, 2g)
920
3831
412
463
3279
21
24
68
514
401
0° 2h vibrations in 2h 1g

I

Gravitropism-related genes, which were involved in the plant response to horizontal stimulation, were differentially expressed in vertical growing plants during flight

Several hundreds of the 920 genes, managing the plants response to the horizontal stimulation under 1*g* conditions, were significantly up-/down-regulated in vertically positioned plants during flight. In a 1-h flight, comprising 11 parabolas, more than one-quarter of the 920 genes (273) were affected, while in a 2-h flight, comprising 31 parabolas, more than half of the 920 genes (484) were involved (Fig. 23, F).

The expression of several hundred genes was significantly altered under all of the three experiment conditions, i.e. 'horizontal stimulation at 1*g*', 'repeated inversion at 1*g*' and 'flight'

The number of transcripts altered in their expression due to repeated short-term inversion (90° 31x 10s in 2h 1*g*) was 3130 and, thus, more than three times higher than in the non-inverted horizontally stimulated control. 623 genes were differentially expressed under both experimental conditions, in the inverted and in the non-inverted samples (Fig. 23, G). 1078 genes, which were regulated due to the multiple inversions, were also significantly up- or down-regulated in the vertically positioned in-flight controls that experienced all conditions of the 2-h flight except for the µ*g*-phases (Fig. 23, H). In the flight samples, which were exposed to all acceleration changes including microgravity, 1535 of the genes, which were regulated due to the multiple inversions, were differentially expressed (Fig. 23, G). However, the number of differentially expressed genes in both, the vibration and flight experiments, was less. The expression of 89 genes was significantly altered in the 2-h flight and due to the simulated flight-vibration profile in the 2-h ground experiment. The intersection of the experiment groups '0° 2h vibrations in 2h 1*g*' and '90° 2h 1*g*' comprised 45 genes (Fig. 23, I).

The repeated short-term µ*g* phases during parabolic plane flight had an additional effect on gene regulation processes

Independent of the flight duration (1 h versus 2 h) and the orientation of the plant samples (vertical versus horizontal), in all flight experiments, a set of several hundreds of genes was affected by flight conditions (792, Fig. 23, L). Venn diagram L in figure 23 shows that one-third (1162) of the differentially expressed 3831 genes in a 2-h flight was also significantly altered in its expression in the 1-h flight experiment. In both experiment groups of the horizontally stimulated and the vertically positioned flight samples (1 h), a set of 1623 genes was differentially regulated because of the flight conditions (Fig. 23, J). More than 80% of the significantly up-/down-regulated 2407 genes in the in-flight controls (1*g*, 2*g*) was also affected in the corresponding flight samples (1*g*, 2*g*, µ*g*). However, in the flight samples which were exposed to all acceleration changes including microgravity, additional 1837 transcripts were changed in their expression compared to control (0° 2h 1*g*) (Fig. 23, K).

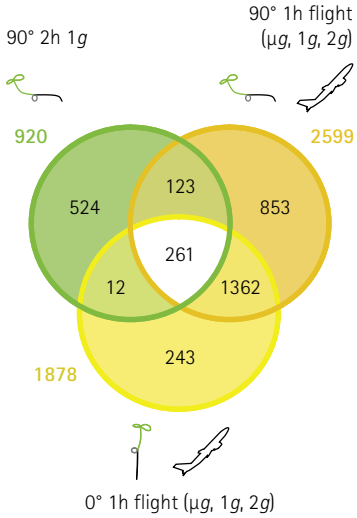

J

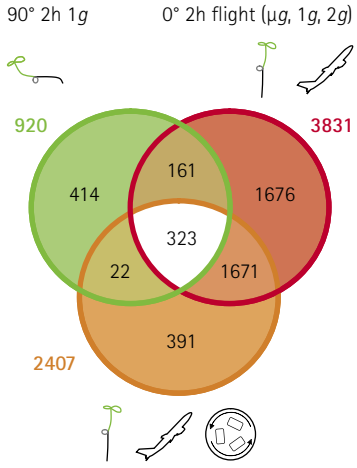

K

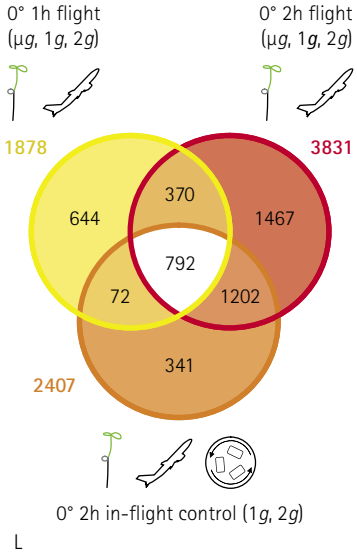

L

3.3.4 Specific sets of genes were differentially expressed in response to reorientation of the plant and in response to changes in gravitational conditions

The Venn diagram analyses of the data, obtained by the different ground and flight experiments, resulted in specific sets of genes which were differentially expressed due to changes in the plant orientation or in acceleration conditions (Fig. 24).

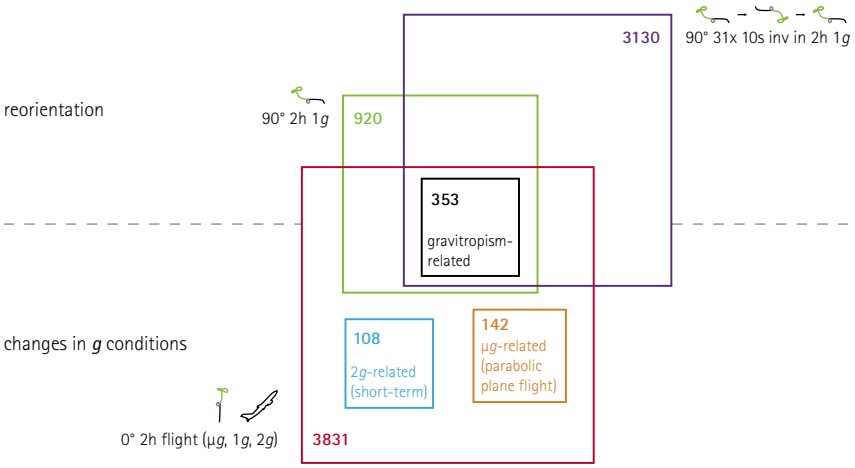

Fig. 24. The data of ground and flight experiments displayed sets of genes, which were significantly regulated due to changes in plant orientation and/or changes in gravity conditions. Stimulation by 90° revealed 353 gravitropism-related genes, which were also affected by parabolic flight conditions. During flight, 108 genes were differentially expressed because of the repeated short-term 2*g* stimuli. A set of 142 genes was detected, whose gene products were regulated due to the µ*g* phases of parabolic flight. The numbers of differentially expressed genes are indicated for the corresponding experimental conditions.

The horizontal reorientation of plant seedlings, which were additionally inverted or not, induced the differential expression of 353 genes (gravitropism-related genes), which were also significantly affected by the gravitational conditions of parabolic plane flight (0° 2h flight µ*g*, 1*g*, 2*g*).

Hyper-*g* related genes were affected in their regulation during centrifugation and in flight. A set of 108 genes was significantly altered in its expression due to the repeated stimulus of 2*g* on ground (0° 62x 20s 2*g* in 2h 1*g*) and in flight (0° 62x 20s 2*g* in 2h flight). Other genes were significantly altered in transcript abundances due to continuous 2*g* stimulation for 2 h (755 genes in horizontally positioned plants).

The repeated µ*g* phases induced the significant up-/down-regulation of 142 genes (µ*g*-related genes) in flight samples compared to the in-flight controls which did not experience microgravity.

3.3.4.1 Gravitropism-related genes, differentially expressed due to 90° reorientation on ground, were also affected by parabolic flight conditions

The transcript abundances of the 353 gravitropism-related genes, which were differentially expressed due to the reorientation by 90° at 1*g* conditions in inverted and in non-inverted seedlings, were analyzed for horizontally and vertically positioned plant seedlings in flight (Fig. 25). More than 66% (234) of these genes were also significantly up- and down-regulated in horizontally positioned plants during a 1-h flight. In contrast to the ground samples (0° 2h 1*g*), in the vertically orientated flight samples 165 of the 353 gravitropism-related genes were significantly altered in their expression. In the vertical plant seedlings during a 2-h parabolic flight all of the 353 genes were differentially expressed compared to ground controls (0° 2h 1*g*). Those of the 353 genes, which were minimum twice down-regulated in seedlings reorientated by 90° on ground, were not only significantly down-regulated in horizontally but also in vertically positioned plants during 1-h parabolic flights (Fig. 27). The same was detected for up-regulated gravitropism-related genes (see also Table IV in the appendix). Therefore, no significant differences in transcript abundances for the horizontally stimulated seedlings versus the vertically growing plants were found (Fig. 26, D). Clustering of the 353 gravitropsim-related genes revealed 12 clusters with up to 56 genes pro cluster (Fig. 28).

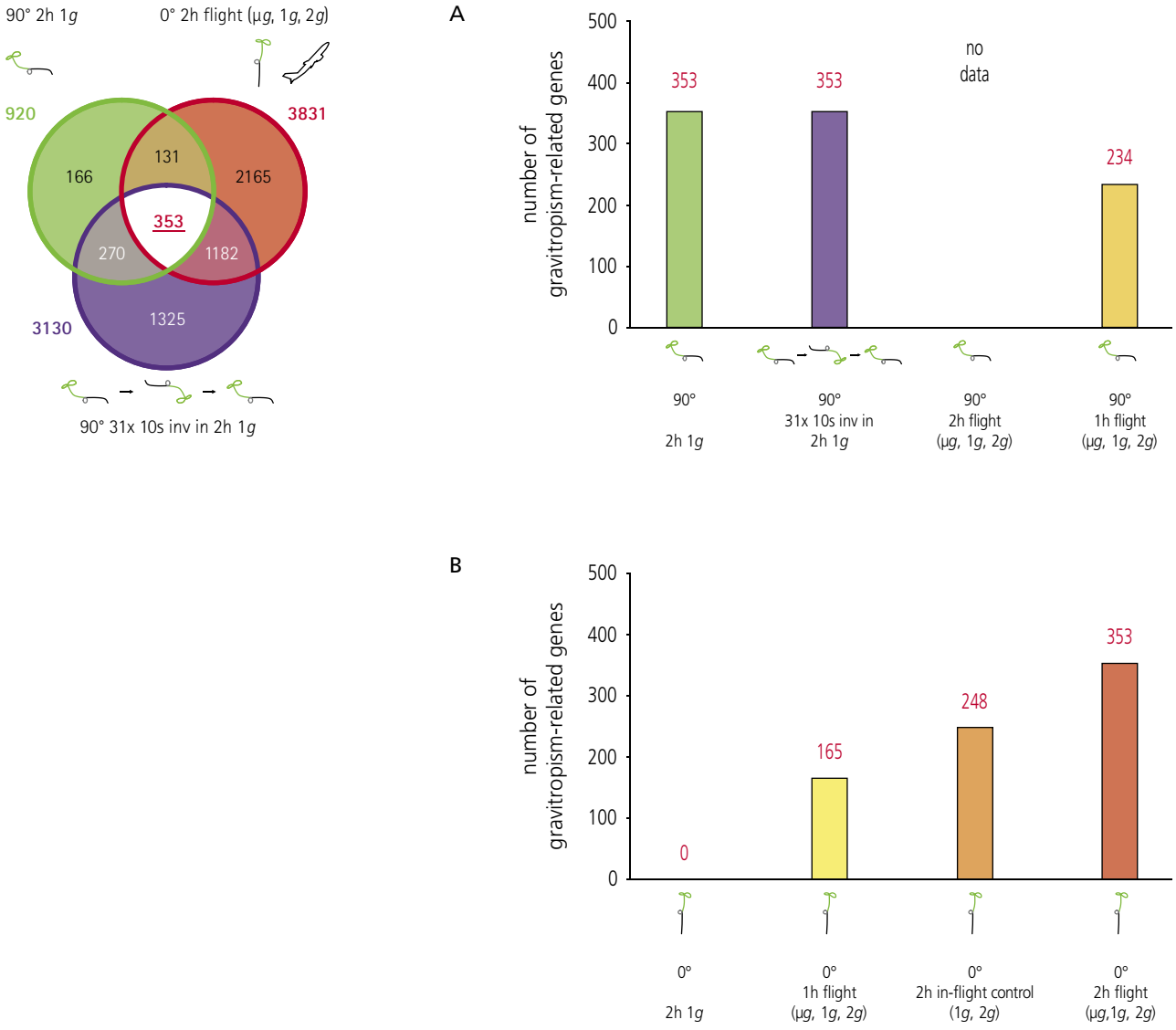

Fig. 25. Gravitropism-related genes were siginificantly affected in their expression level by the conditions of parabolic plane flights. The expression of the 353 genes, which were at least 2-fold up- and down-regulated at horizontal stimulation under 1*g* conditions in inverted and in non-inverted seedlings (see venn diagram on the left), was analyzed for horizontally and vertically orientated plants in the experiment groups. In comparison to the vertically positioned ground controls, in the vertically orientated samples of the 2-h flight all of the 353 genes were differentially expressed. The conditions of 1-h parabolic flights yielded in the minimum twice up-/down-regulation of about half of the 353 gravitropism-related genes (165).

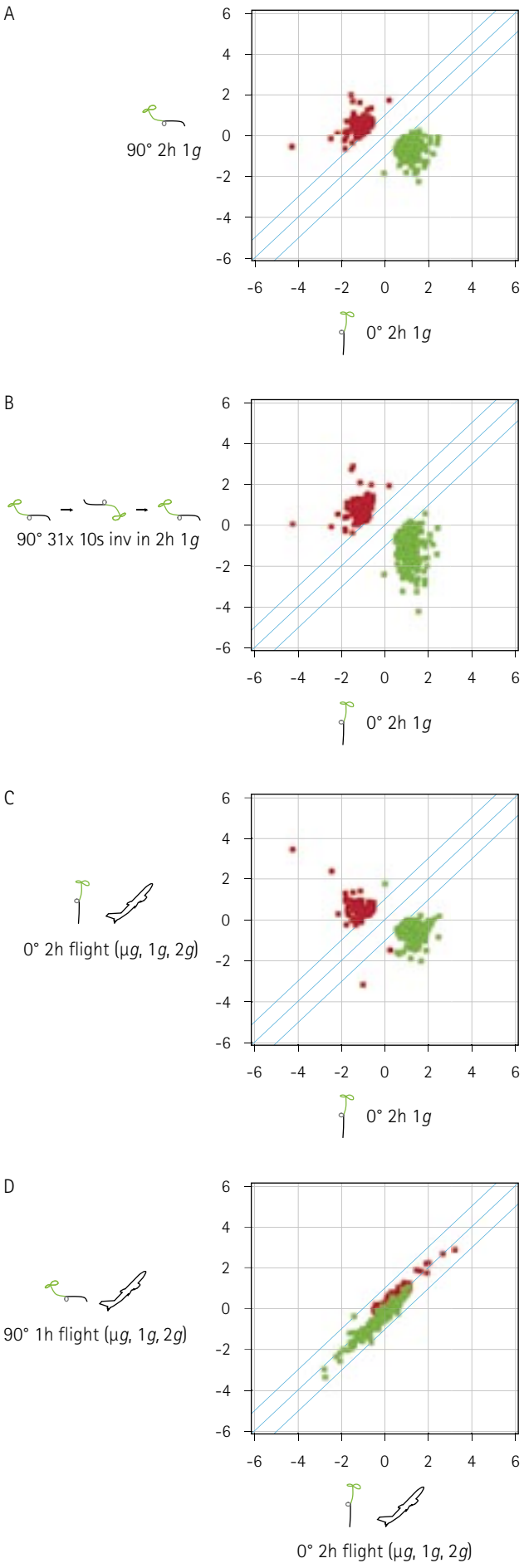

Fig. 26. Scatter-plot graphics illustrating the expression levels of the 353 gravitropism-related genes, which were at least two-fold differentially expressed in plants, whose orientation was changed by horizontal stimulation. The transcript abundances for the 353 genes were plottet against each other for ground (A, B) and flight experiments (C, D). The spot color is defined by scatter plot A (green for down-regulation, red for up-regulation; for more details about-scatter plot graphics, see Fig. 19). At 1*g* conditions, the horizontal stimulation of the plant seedlings induced the differential expression of the 353 genes in horizontally versus vertically orientated plants (A, B). However, during 1-h parabolic flight, a differential expression of these genes in horizontally positioned plants versus vertical flight samples was not observed (D).

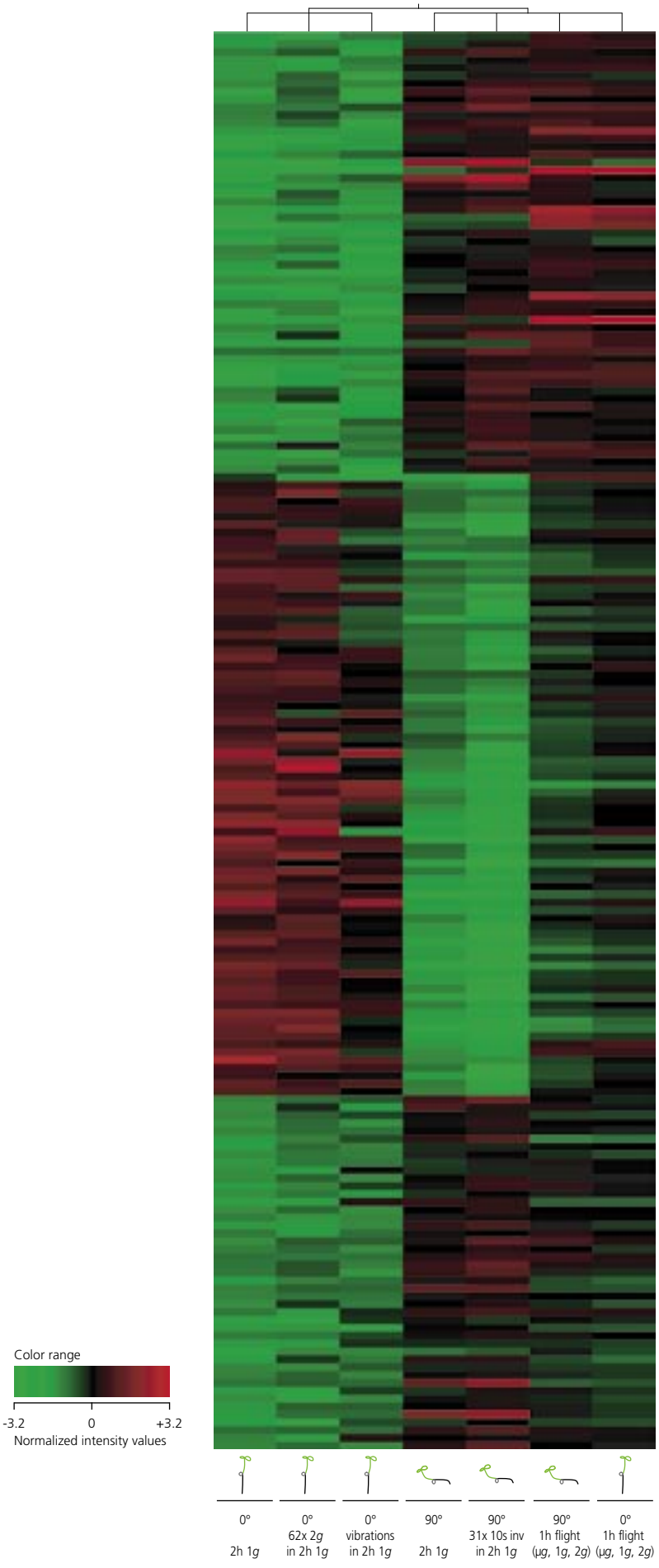
Color range
-3.2
0
+3.2
Normalized intensity values
0°
2h 1g
0°
62x 2g
in 2h 1g
0°
vibrations
in 2h 1g
90°
2h 1g
90°
31x 10s inv
in 2h 1g
90°
1h flight
(µg, 1g, 2g)
0°
1h flight
(µg, 1g, 2g)

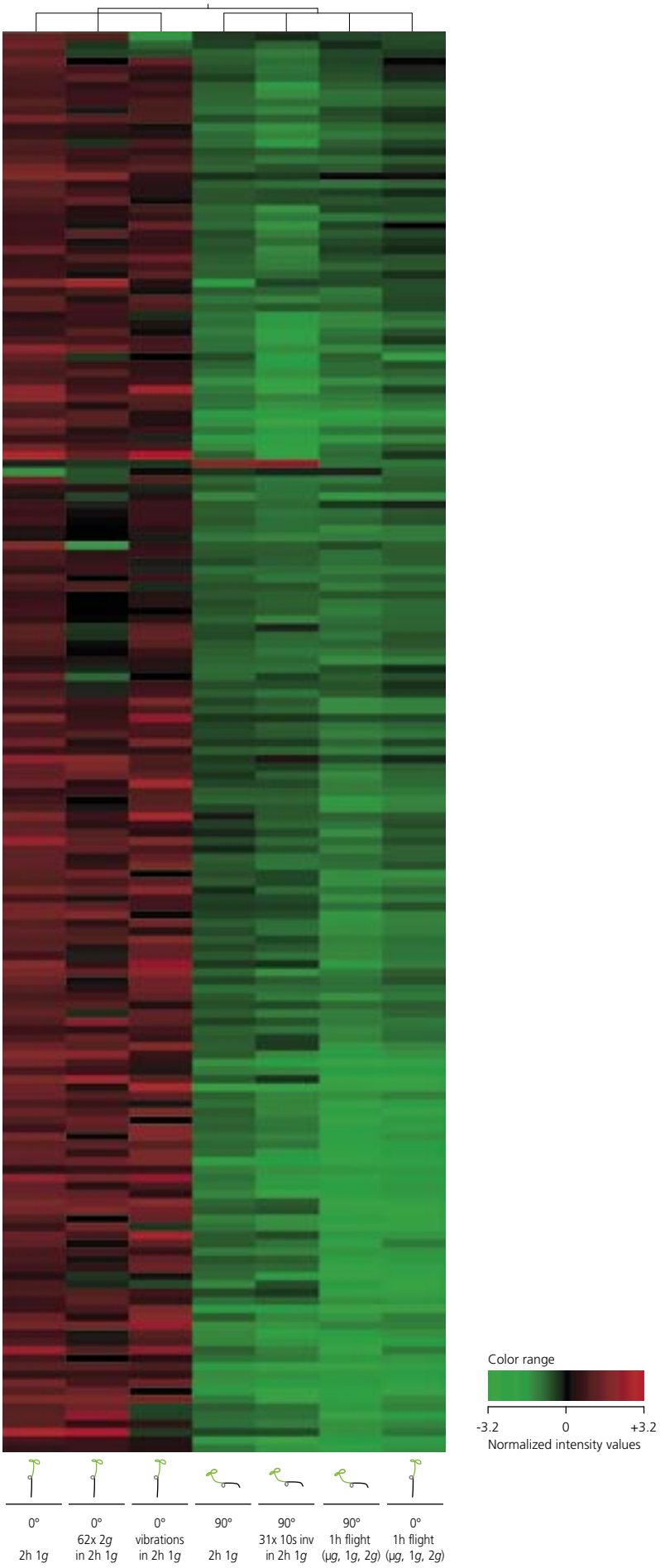

Fig. 27 (pp 47 - 48). Cluster analysis showing the expression ratios of the 353 gravitropism-related genes, which were differentially expressed due to horizontal stimulation under 1*g*. Changes in transcript abundances are illustrated for vertically and horizontally positioned plant seedlings in ground and flight experiments. Intensities of red reflect the degree of up-regulation while intesities of green reflect the degree of down-regulation compared to the vertical control at 1*g* (0° 2h 1*g*). Those of the 353 gravitropism-related genes, which were at least 2-fold down-regulated in horizontally positioned seedlings on ground, were not only significantly down-regulated in horizontally positioned plant samples during flight but also in vertically growing flight samples (1 h). The same was observed for up-regulated genes.

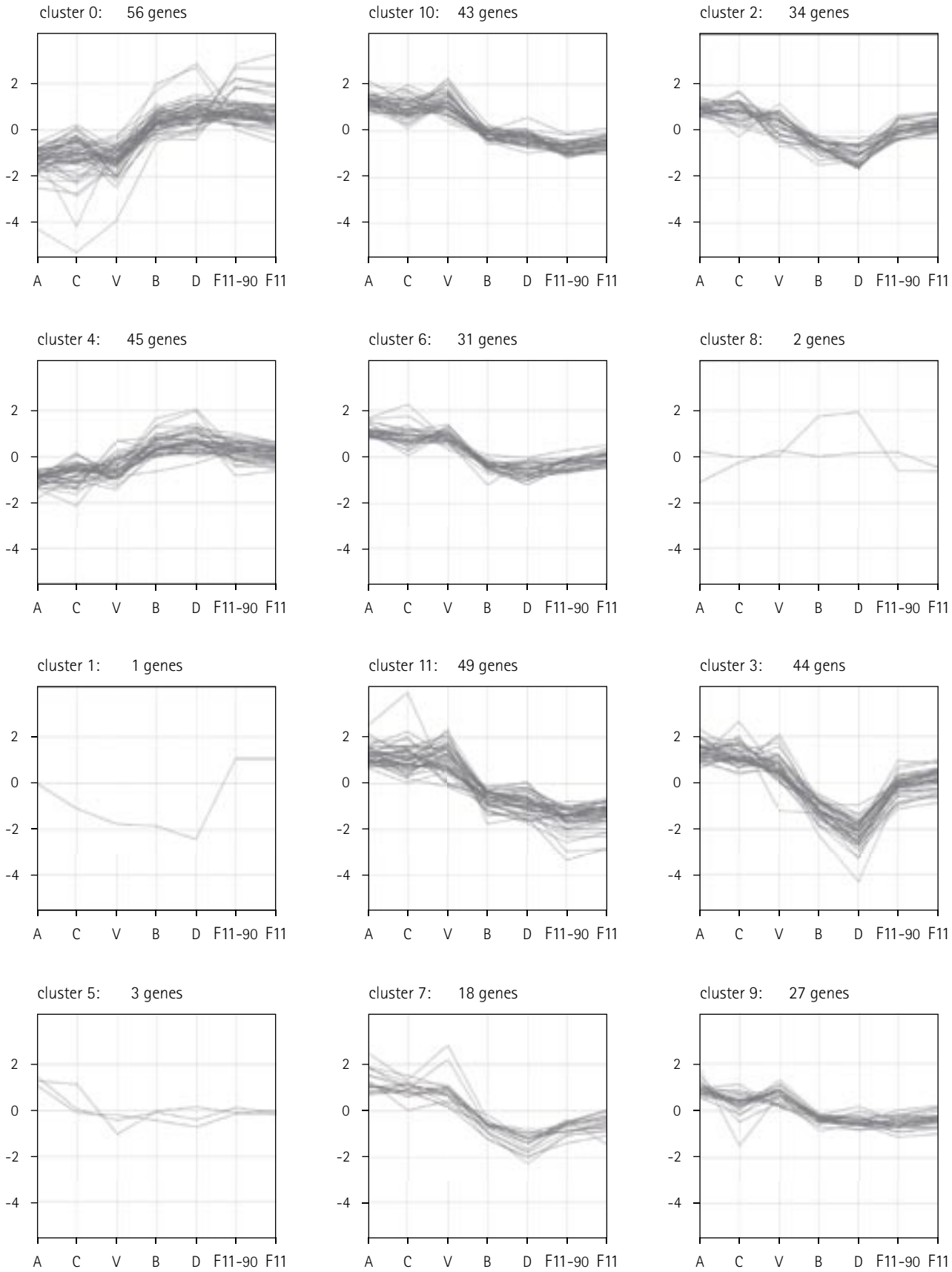

A	0° 2h 1*g*				
C	0° 62x 20s 2*g* in 2h 1*g*	B	90° 2h 1*g*	F11-90	90° 1h flight
V	0° 2h vibrations in 2h 1*g*	D	90° 31x 10s inversion in 2h 1*g*	F11	0° 1h flight

3.3.4.2 Differential gene expression due to 2*g* stimulation

The gene-expression analyses for the plant samples exposed to the parabolic flight conditions and ground centrifugation (0° 62x 2*g* in 2h 1*g*) resulted in a set of 108 genes, which were at least 2-fold changed in their expression particularly due to the repeated short-term 2g stimuli (Fig. 29). These 2*g*-specific genes were not significantly altered in their expression during the typical gravitropic repsonse at 1*g* (90° 2h 1*g*) (Fig. 29, A). However, during the repeated short-term 2*g* centrifugation, 90% of the 108 genes were at least 2-fold down-regulated and 10% of these genes were minimum 2-fold up-regulated compared to the non-centrifuged controls (Fig. 29, B). The effect of the 2*g* phases of the parabolic flight profile on the expression regulation of these 108 genes was very similar to the centrifugation-induced changes in the ground experiment (Fig. 29, C and Fig. 30, see also Table VI in the appendix).

Fig. 28. Single clusters for the gravitropism-related 353 genes. The differentially expressed genes were clustered using a self-organization map algorithm (Agilent GeneSpring® GX). The y axis indicates the relative expression for all of the genes in that cluster, and the x axis indicates the experimental conditions (see figure legend). The number of genes in each cluster is indicated at the top center of each cluster graph.

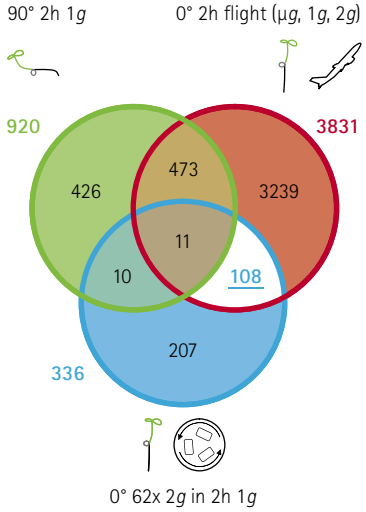

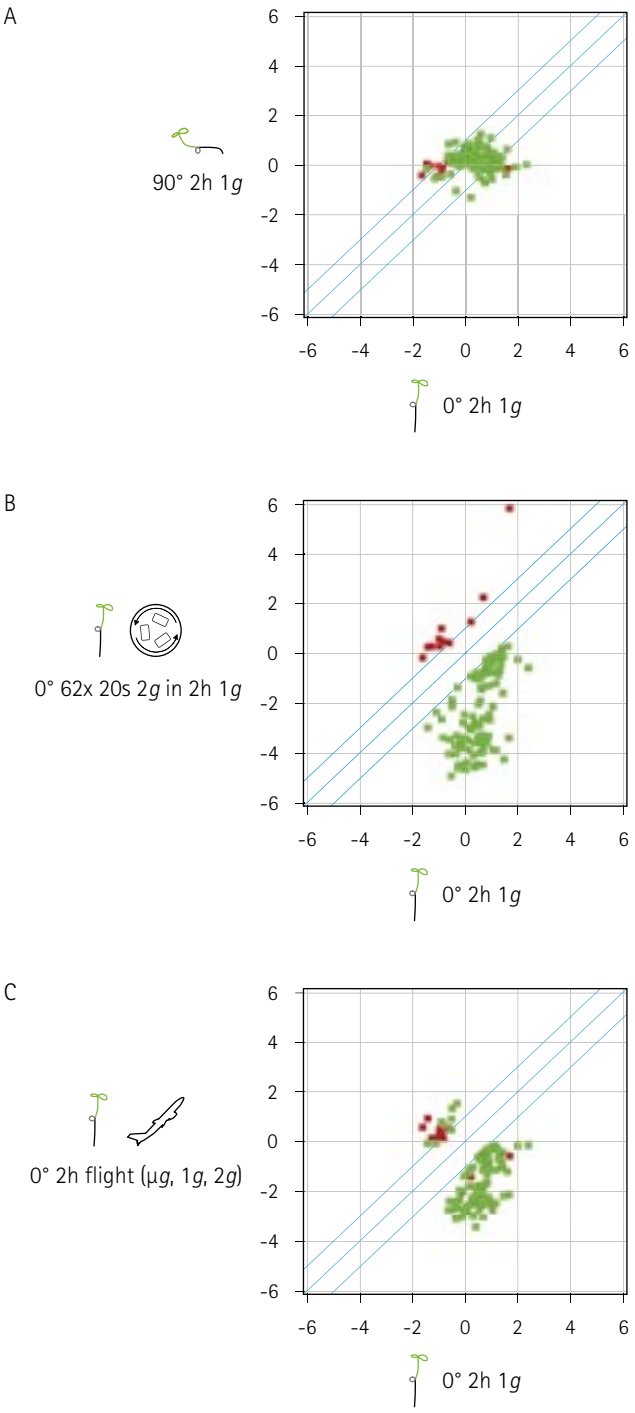

Fig. 29. Scatter-plot graphics illustrating the expression levels of the 108 2*g*-related genes, which were regulated due to the repeated short-term 2*g*-stimuli by centrifugation on ground or during parabolic flight (see Venn diagram on the left). The transcript abundances for the 2*g*-related genes were plottet against each other for ground (A, B) and flight experiments (C). The spot color is defined by scatter plot B (green for down-regulation, red for up-regulation; for more details about scatter-plot graphics, see Fig. 19). During repeated short-term 2*g* centrifugation, 90% of the 2*g*-related genes were at least twice down-regulated and 10% were minimum twice up-regulated compared to the 1*g* control (B). During parabolic flight, the 2*g*-induced changes in transcript abundances were quite similar to the effects by 2*g* centrifugation on ground (C).

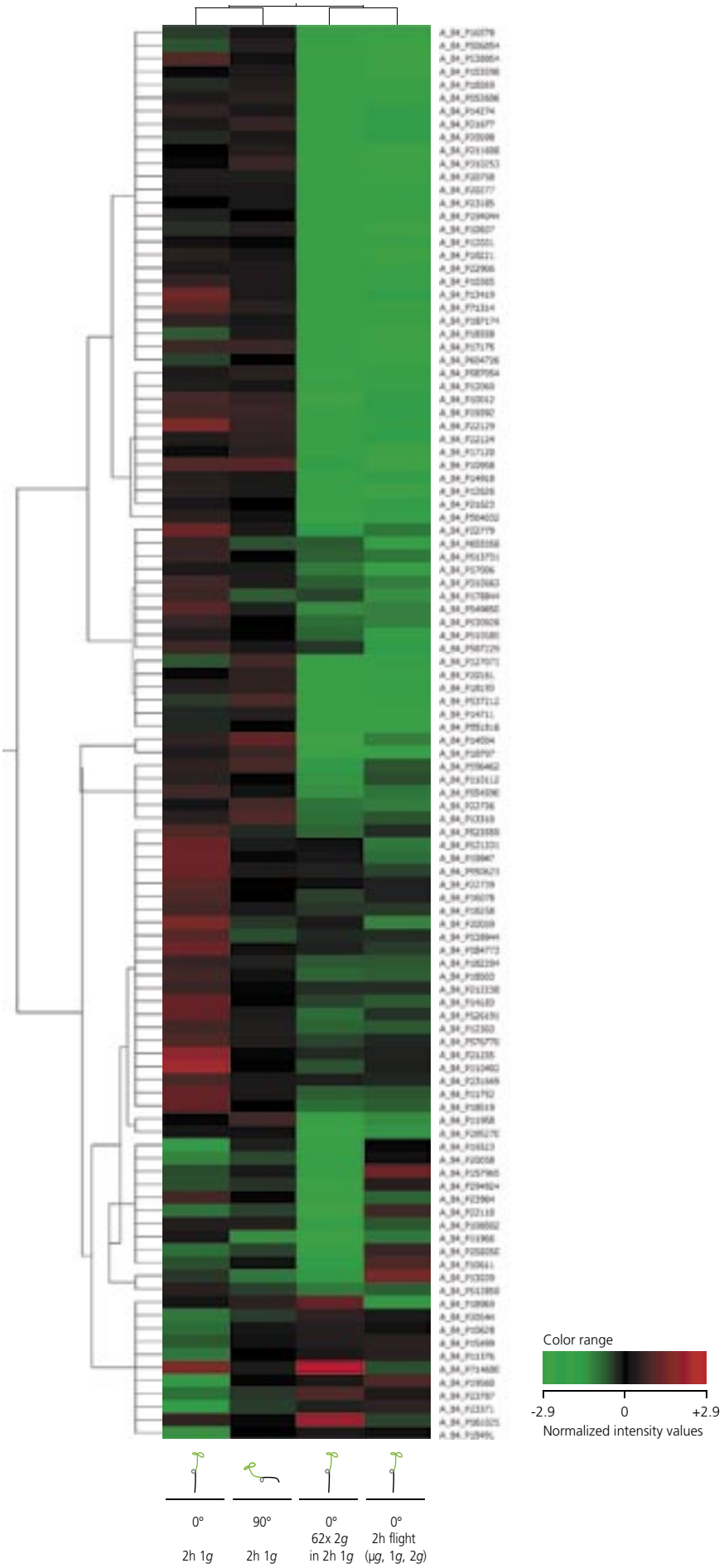

Fig. 30. Cluster analysis showing the expression ratios of the 108 2*g*-related genes, which were regulated at repeated short-term hyper-*g* centrifugation (62x 20s 2*g* in 2h 1*g*) and under 2-h flight conditions (µ*g*, 1*g*, 2*g*). Changes in transcript abundances are illustrated for plant seedlings in 1*g*- and 2*g*-ground experiments as well as for flight samples. Intensities of red reflect the degree of up-regulation while intesities of green reflect the degree of down-regulation compared to the vertical control at 1*g* (0° 2h 1*g*).

3.3.4.3 Gene-expression changes due to the additional stimuli by the repeated short-term µ*g* phases during parabolic plane flight

The gene-expression analyses revealed the 2-fold and higher differential expression of 142 genes in the flight samples, which were exposed to all acceleration changes of a 2-h parabolic flight including the µ*g*-phases, versus the in-flight controls, which did not experienced µ*g* as they were centrifuged with 1*g* during microgravity (Fig. 31, A and Fig. 32). The regulation of these µ*g*-related genes was not significantly altered neither by 2-h horizontal stimulation at 1*g* nor by repeated short-term inversion during horizontal stimulation at 1*g* (Fig. 31, B and C). In the same way, the regulation of these µg-related genes was not altered in horizontal positioned plant seedlings during flight compared to vertically growing flight samples (Fig. 31, D, see also Table VII in the appendix).

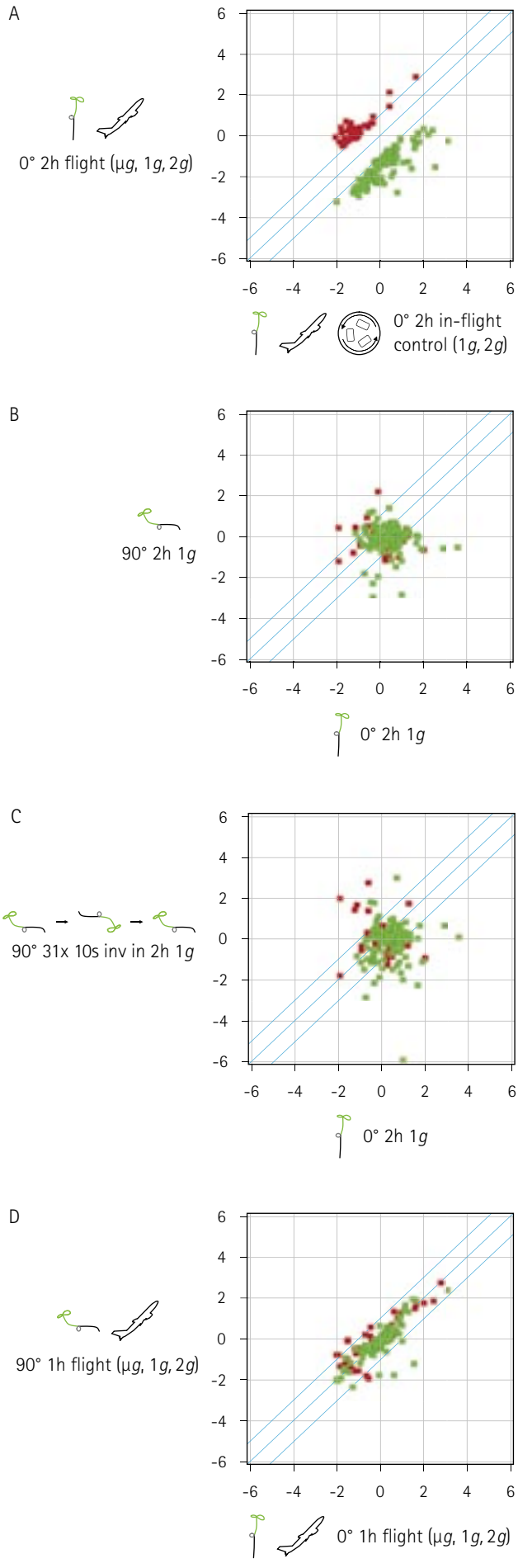

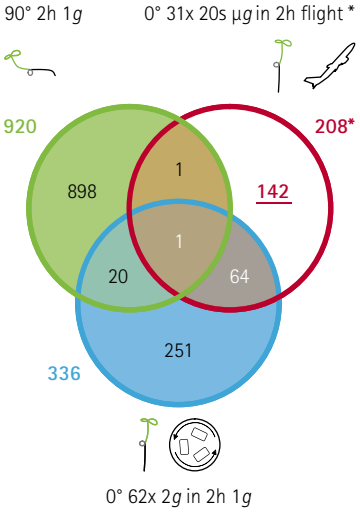

*at least 2-fold differential expression in flight samples (µg, 1g, 2g) versus in-flight controls (1g, 2g)

Fig. 31. Scatter-plot graphics illustrating the expression levels of the 142 µg-related genes, which were particularly regulated due to the repeated short-term µg phases during parabolic flight (see Venn diagram on the left). The transcript abundances for the µg-related genes were plottet against each other for ground (B, C) and flight experiments (A, D). The spot color is defined by scatter plot A (green for down-regulation, red for up-regulation; for more details about scatter-plot graphics, see Fig. 19). Independent of the plants orientation during flight (0° or 90°, D) a set of 142 genes was at least 2-fold differentially expressed in the flight samples, which experienced all acceleration levels including the µg-phases, compared to the in-flight controls, which were centrifuged with 1g during microgravity (A). No significant up-/down-regulation of the 142 µg-related genes is observed in horizontally stimulated seedlings (non-inverted or inverted) versus vertically positioned seedlings at 1g (B, C).

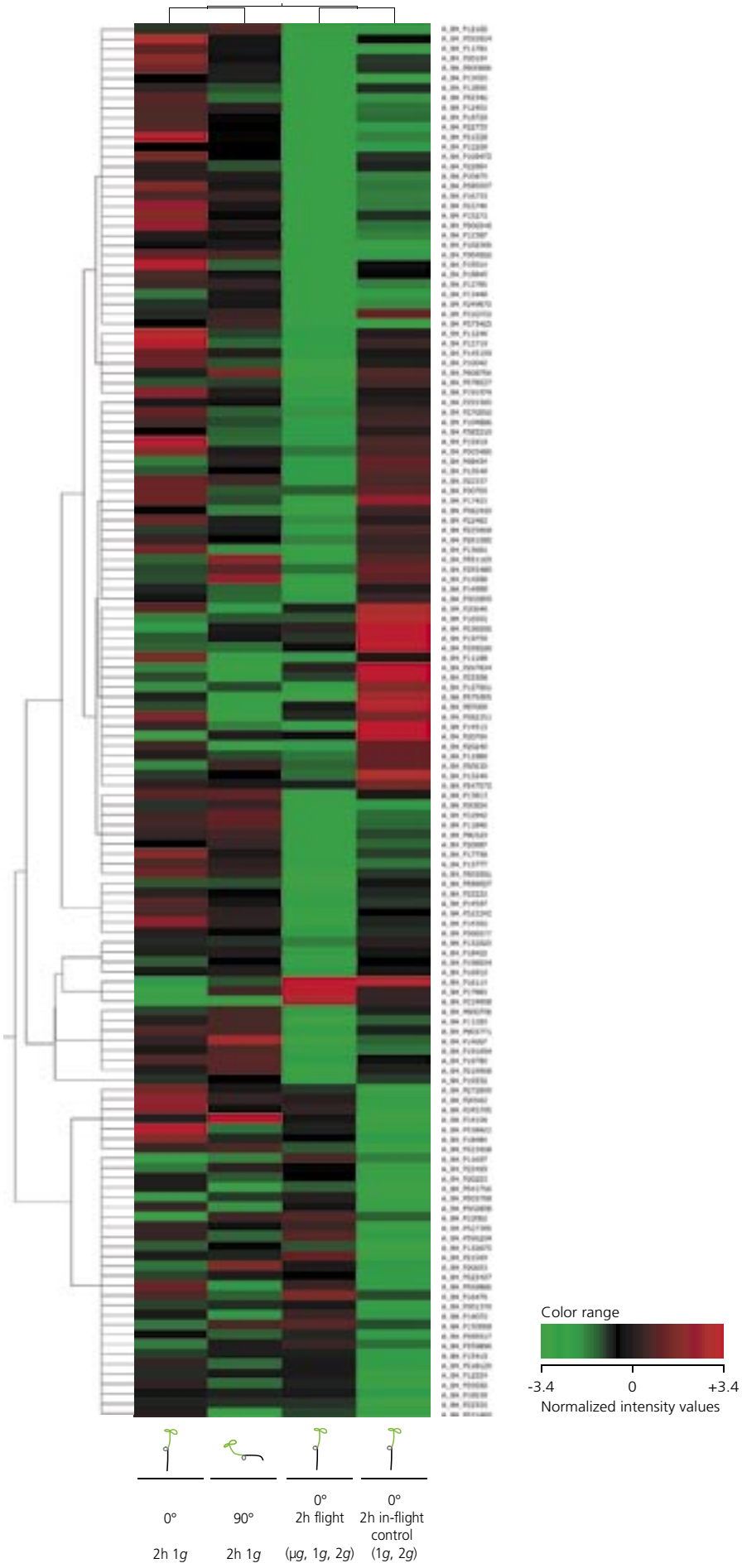

Fig. 32. Cluster analysis showing the expression ratios of the 142 µ*g*-related genes, which were regulated due to the µ*g*-conditions of the parabolic flight. Changes in transcript abundances are illustrated for plant seedlings in 1*g*-ground experiments as well as for flight samples. Intensities of red reflect the degree of up-regulation while intesities of green reflect the degree of down-regulation compared to the vertical control at 1*g* (0° 2h 1*g*).

3.3.4.4 Functional categorization of gravitropism-, 2*g*- and µ*g*-related genes

The insufficient annotation details of approximately one-third to half of the genes, whose differential expression was analyzed in the experiments of the present study, did not afford any classification into a functional category (Fig. 33, 'unknown'). However, the existing data about the genes' functional role in cell biological processes showed that gene regulation due to gravitropic processes at horizontal plant stimulation was substantially attributed to DNA and protein metabolism, signaling, transporter activities, stress and defense response as well as cell wall modification. A similar classification was found for the 2*g*- and the µ*g*-related genes. Compared to the other gene sets, a noticeable number of genes involved in the response to µ*g* was attributed to lipid metabolic processes. General stress- and defense-related gene regulation processes were highest altered during the gravitropism-related response.

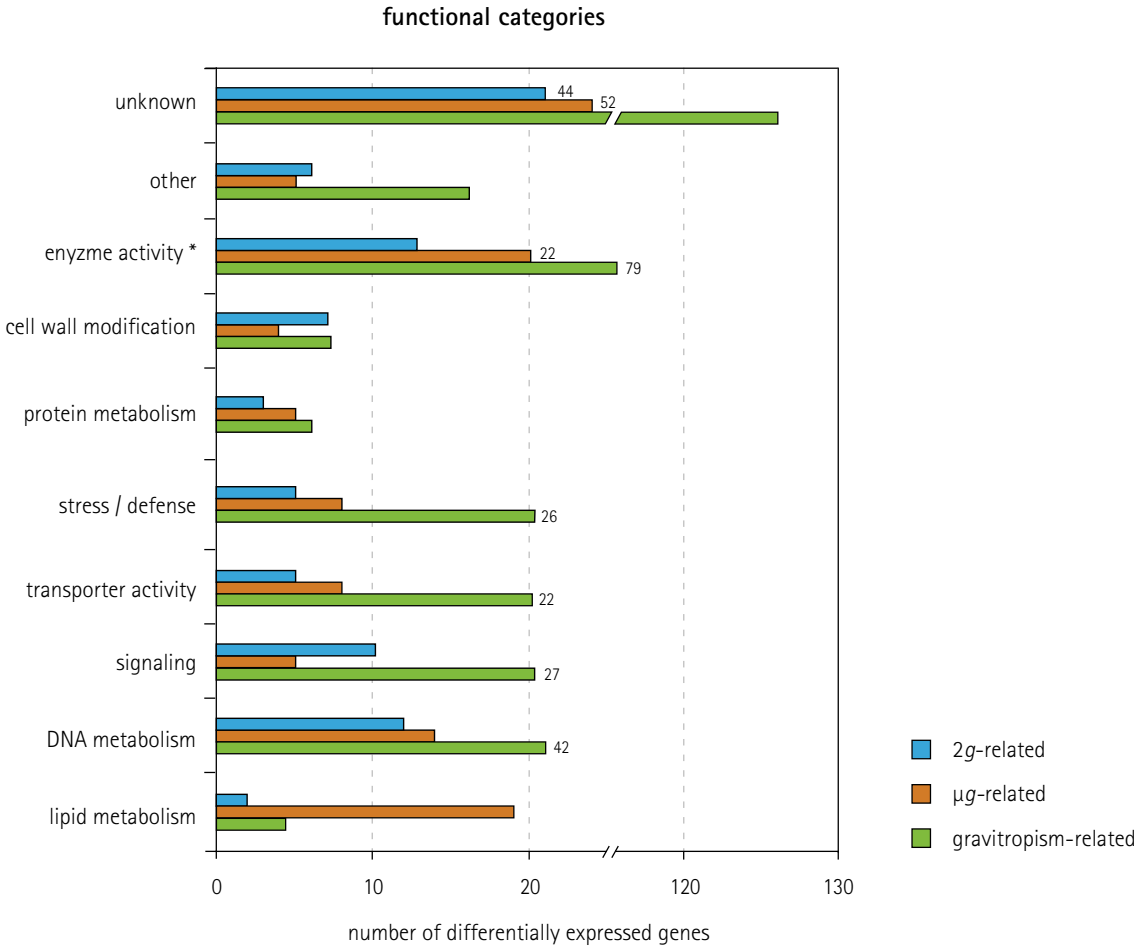

* genes encoding for proteins with enzyme activities unless annotation details allowed more precise functional classification

Fig. 33. The three sets of genes, whose expression was significantly changed at particular gravity conditions, were attributed to functional categories based on the genes' annotation details (TAIR). The 2*g*- and µ*g*-related changes in transcription were quite similar attributed to the different biological processes. The plant orientation by 90° affected stress-related processes, transporter activities, signaling and metabolic processes.

4. DISCUSSION

In the last decades, experiments on microgravity platforms and on ground were performed to increase our knowledge about gravisensing processes and gravitropic responses in plants. Microarray technology was used to study gene-expression in plants after gravitropic stimulation by reorientation, after exposure to hyper-*g* or clinorotation and after exposure to microgravity conditions (sounding-rocket and space-shuttle experiments: Paul et al., 2005; Martzivanou et al., 2006; Salmi and Roux, 2008). However, up to now, no gene-expression studies under the changing gravity conditions of parabolic plane-flights have been conducted. Parabolic plane flights provide the unique opportunity to investigate the impact of different acceleration conditions including 1*g*, 2*g* and µ*g* on biological organisms. In the present study on Arabidopsis seedlings, a whole genome analysis on the response to the gravitational conditions of parabolic flights with the Airbus A300 Zero-G were investigated for the first time. In addition, a comprehensive ground-based experiment series under different gravity conditions at 1*g* and 2*g* was performed in parallel, in order to assess the flight-induced changes. Therefore, this study provides an extensive evaluation on the gravity-dependent gene expression in Arabidopsis.

The molecular data obtained by microarray analyses were complemented by studies on the cellular mechanisms that underly the positioning of statoliths and the statolith sedimentation in Arabidopsis root statocytes and in the unicellular lower plant system, the Chara rhizoids. In particular, the findings from experiments under the altered gravity conditions of parabolic plane and sounding-rocket flights decisively contribute to our understanding of gravity-induced cellular and molecular processes in plants.

4.1 Threshold-acceleration level required for lateral statolith displacement in Chara rhizoids

As the gravisensing statocytes of higher plants are not easily accessible for experimental applications and the signal-transduction and -transmission network from these cells is highly complex, it is not easy to discriminate between the very early processes of gravisusception and -perception in higher plants. In contrast to higher plants, the single-celled rhizoids of the green alga Chara are well suited for various research methods and allow for the investigation of all phases of gravisensing in one single cell. Previous studies on the positively gravitropic rhizoids have already given insights into structural and functional details of statolith sedimentation and gravireceptor activation processes. While studies on the role of actin in gravisensing of higher plant statocytes have given scarce and partly contradictory

results (Blancaflor and Hasenstein, 1997; Nick et al., 1997; Yamamoto and Kiss; 2002; Hou et al., 2003, 2004), for characean rhizoids, it is undisputable that actomyosin is essentially involved in the positioning of statoliths and in the statolith-sedimentation processes (Sievers et al., 1991; Braun et al. 2002). In vertically oriented Chara rhizoids, basipetally acting actomyosin forces compensate gravity force keeping the statoliths in a dynamically stable position 10-30 µm above the apex of the cell (Braun et al., 2002). In previous microgravity experiments during sounding-rocket missions, the removal of the gravity force disturbed the balance between this force and the counteracting actomyosin force leading to the transport of the statoliths away from the tip (Buchen et al., 1993; Braun et al., 2002).

Gravisusception in Chara rhizoids is initiated by gravity-induced sedimentation of statoliths. Sedimenting statoliths are actively guided by the actomyosin system of the cell to the gravisensitive membrane site 10-30 µm behind the tip, the only site where gravireceptors are located (Braun, 2002). Statolith sedimentation on the gravisensitive membrane site is required to induce graviperception and to eventually cause a curvature response of the rhizoid. Displacement of statoliths toward the cell flank without settling on the gravisensitive membrane area does not initiate gravitropic response. However, once statoliths are laterally displaced by sufficiently high accelerations toward the cell flank, they inevitably settle on the gravisensitive membrane area where they activate gravireceptors and induce the gravitropic curvature response of the rhizoid (Braun, 2002). Although the molecular nature of the gravireceptor in characean rhizoids is still unknown, the receptor has recently been functionally characterized. Experiments during parabolic plane flights confirmed that contact-interactions between the statoliths surface and the gravireceptor are sufficient for receptor activation in rhizoids. Weightless statoliths, which did not exert pressure but were in contact with the gravireceptors, were still able to activate the receptors (Limbach et al., 2005).

4.1.1 High gravisensitivity provides the basis for an efficient gravisensing system in plant cells

Based on this knowledge about structural and functional details of actomyosin-mediated statolith positioning and sedimentation as well as gravireceptor activation, the interactions between myosins and statoliths are considered to be the molecular basis of the threshold value for the gravisensitivity of characean rhizoids (Limbach et al., 2005). Therefore, the threshold value for gravisensitivity can be determined by the minimum lateral acceleration that is needed to overcome the actomyosin forces and to induce sedimentation of statoliths. Limbach et al. (2005) have already shown that the threshold value for the gravisensitivity of Chara rhizoids is $\leq 0.14g$. In the present study, this approximation of acceleration value required for the lateral displacement of statoliths in characean rhizoids was narrowed down. Lateral centrifugation of vertically growing rhizoids during the microgravity phase of MAXUS-8 demonstrated that a lateral accele-

ration of ≤ 0.08*g* was sufficient to induce a significant displacement of statoliths toward the centrifugal cell flank. A distinct albeit not significant tendency of lateral statolith displacement was observed at even lower accelerations in the range of 0.06*g* to 0.08*g*.

Given a threshold value of lateral statolith displacement of ≤ 0.08*g* (a = 0.78 ms^{-2}), statolith volume V (statolith diameter 2 µm), statolith density ($\rho_{statolith} = \rho_{barium\ sulfate} = 4.5\ g\ cm^{-3}$), and cytoplasmic density ($\rho_{cytoplasm} = 1.03\ g\ cm^{-3}$), the cytoskeletal force F that has to be exceeded to displace a single statolith in lateral direction, is in the range of:

$F = \Delta\rho$ (statolith-cytoplasm) x V x a = 1.14 x 10^{-14}N.

This value represents the cytoskeletal forces that restrict lateral displacement of statoliths. It is more than one tenth of the actomyosin forces (1*g*) acting on a statolith in the basal direction to keep statoliths in a dynamically stable resting position at the level of the gravisensitive membrane site (Buchen et al., 1993; Cai et al., 1997; Braun et al., 2002). Considering the threshold level of ≤ 0.08*g* and an average distance (s) between a statolith and the plasma membrane of 15 µm, the mechanical work (W) required for a complete sedimentation of a single statolith onto the gravisensitive membrane site is:

W = F x s = 1.71 x 10^{-19} J.

This value represents the energetic concept that underlies gravisusception processes in Chara rhizoids. The general threshold of gravisensitivity in Chara rhizoids (between 0.06*g* and 0.08*g*) is considerably below those for ciliates (> 0.16*g*, ≤ 0.3*g*; Hemmersbach et al., 1996), flagellates (≤ 0.16*g*; Häder et al., 1995) and statocytes of higher plants (≤ 0.1*g;* Brown et al., 1995). The high sensitivity is the fundamental basis for an extremely efficient gravisensing system in characean rhizoids. In contrast to the highly controlled statoliths' position in axial direction, the little restriction of statoliths' movements in lateral direction ensures a relatively free and fast sedimentation of statoliths onto the graviperception site of the cell membrane. Thus, the gravisensing apparatus is highly efficient so that even very small deviations from the genetically determined set-point angle are rapidly corrected by the cell.

4.2 Statolith-mediated graviperception in Arabidopsis root statocytes

In contrast to Chara rhizoids (Limbach et al., 2005), no functional characterization of graviperception has yet been published for higher plants. However, recent results of parabolic plane-flight experiments on Arabidopsis root statocytes suggest that higher plant gravirecep-

tors are not mechanosensitive, since they are still activated by sedimented but weightless statoliths, which do not exert pressure on the receptor molecules (Greuel, 2007; Hauslage, 2008). This notion has been made under the assumption that during the microgravity phases of the parabolic plane flight, statoliths remain sedimented on the physical lower cell flank and are not displaced from the gravisensitive membrane by actomyosin forces, which continously act on statoliths. In the present study, this assumption was tested by analyzing the position of sedimented statoliths in the root statocytes of Arabidopsis seedlings during the different acceleration phases of the parabolic plane flights.

4.2.1 In terms of gravireceptor activation, root statocytes and characean rhizoids share the same mechanism

In contrast to Chara rhizoids, which allow for in vivo video-microscopic tracking of statoliths, microscopic observation of statolith movements in columella cells of roots is impaired by the lower level of microscopic resolution in the multicellular plant organ. In the present study, Arabidopsis root statocytes were fixed by $KMnO_4$ and statolith position was statistically analyzed in semithin sections. No significant displacement of statoliths during the short microgravity phases of parabolic plane flights was observed. Recent studies demonstrated, that the final curvature angles of primary Arabidopsis roots, which were flown on 12 parabolic flight days, were similar or higher but not smaller as compared to in-flight controls, which experienced all parabolic flight conditions except the µ*g*-phases (Greuel, 2007; Hauslage, 2008). Considering these findings and the observation that the positions of sedimented statoliths at the beginning and at the end of the 22-s microgravity phases were not significantly different, it is concluded that graviperception is not interrupted by the µ*g*-phases of the parabolic plane flights.

In contrast to the flight experiments, inversion of Arabidopsis roots resulted in the interruption of contact between sedimented statoliths and the gravireceptors terminating graviperception within seconds. Sedimentation of statoliths that were initially settled onto the lower statocyte flank of a horizontally positioned Arabidopsis root, which was then inverted from 90° to the 270° position, resulted in doubling of the distance between the statoliths and the primarily lower statocyte flank within 10 s. This finding and the observation of recent studies that repeated inversion of gravistimulated Arabidopsis roots for at least 10 s from 90° to 270° significantly reduced the final growth curvature response (Greuel, 2007; Hauslage, 2008) demonstrates that 20 s are long enough to interrupt graviperception.

The results are complemented by the observation that increasing the weight of statoliths, which were sedimented onto the lower cell flank of gravitropically stimulated Arabidopsis root statocytes, does not affect the gravitropic response (Greuel, 2007; Hauslage, 2008). These findings strongly suggest that higher plant gravireceptors are acti-

vated by direct interactions with sedimented statoliths upon contact rather than by mechanical forces exerted by the weight of statoliths as was also shown for characean rhizoids (Limbach et al., 2005). Once the statoliths approach the gravisensitive membrane, no pressure or tension forces mediated by the weight of the statoliths are required to initiate the graviperception processes. In this respect, higher plant root statocytes principally use the same statolith-mediated gravireceptor-activation mechanism as the lower plant model Chara rhizoid.

4.2.2 Findings are contradictory to hypotheses on mechanosensitive gravireceptors

The conclusions of this study support the hypothesis that amyloplasts induce graviperception by directly interacting with receptors in the ER membrane (Volkmann and Sievers, 1979). Root statocytes show a specific structural polarity, i.e. in the upper proximal half of root statocytes, the cell cytoskeleton stabilizes the nucleus and, therefore, prevents the nucleus from sedimentation. In contrast to the nucleus, the amyloplasts are typically located in the lower distal half of the cell and are relatively free to sediment in the direction of gravity due to a less dense actin cytoskeleton in this part of the cell (Sievers and Volkmann, 1977). Therefore, in the statocytes of vertically oriented downward-growing roots, the amyloplasts sediment along the gravity vector and typically settle on a very prominent structure, the distal ER complex in the lower half of the cell (Sievers and Volkmann, 1972; 1977). Since amyloplasts have not been localized in direct contact with the plasma membrane so far, it appears most likely that sedimented amyloplasts interact with gravireceptors located in the ER membrane (Leitz et al., 2009). Since electron microscopic studies identified at least one ER cisterna located at the statocyte flanks (Wendt et al., 1987), statoliths do not necessarily interact with gravireceptors located in the membrane of the distal ER complex but in general with gravireceptors located in the membrane of ER cisternae. Cress roots, which were treated with the actin-disrupting drug Cytochalasin D and were then centrifuged, showed a complete spatial separation of statoliths from the distal ER complex. Although statoliths had no contact with the distal ER complex, horizontal stimulation of the treated and centrifuged cress roots resulted in a gravitropic curvature response (Wendt et al., 1987). Thus, statolith sedimentation onto gravireceptors in the distal ER complex is not required but onto gravireceptors in lateral ER cisternae is sufficient to induce graviperception in statocytes. Furthermore, earlier studies revealing a correlation between increased latent periods of the graviresponse and the time for restoration of polarity after centrifugation (Sievers and Heyder-Caspers, 1983) support the idea that the structural polarity of statocytes, in particular the location of the ER and the position of statoliths, is of vital importance for the gravisensing mechanisms in higher plants.

The findings on the statolith-mediated graviperception in higher plant statocytes and in Chara rhizoids, obtained in the present study and during previous parabolic plane-flight experiments (Limbach et

al., 2005; Greuel, 2007; Hauslage, 2008), are contrary to models of gravisensing that postulate a receptor activation by tension or shearing forces generated by statolith sedimentation and transferred to the receptors via actin microfilaments (Zheng and Staehelin, 2001; Boonsirichai et al., 2002, Sievers et al., 2002; Blancaflor and Masson, 2003; Perbal and Driss-Ecole, 2003). It is undisputable that during the gravity-induced statolith sedimentation, actin plays an important role since the molecular interactions between the statoliths' myosins and the actin microfilaments ensure the most beneficial and efficient statolith sedimentation onto the gravisensitive membrane (Sievers et al., 1989; Sievers et al., 1991; Volkmann et al., 1991). In addition to modulating the statolith sedimentation, actin interactions with statoliths also facilitate the appropriate resting position for statoliths. For example, plant root statocytes showed an actin-dependent distribution of statoliths in microgravity (Driss-Ecole et al., 2000; Blancaflor, 2002).

However, if the actin cytoskeleton was a prerequisite for gravisensing in higher plant cells, e.g. as transducer of tension or shearing forces, it would be expected that the curvature response of roots, which were treated with actin-disrupting drugs like Latrunuclin B (LatB), would be inhibited. In contrast to this assumption, studies reported on promoted gravitropic responses of LatB-treated roots, which had been stimulated by reorientation for a short time and then rotated on a 1 rpm (rounds per minute) clinostat (Hou et al., 2004). Furthermore, it was demonstrated that an intact actin cytoskeleton is not essentially needed for the establishment of the auxin gradient (Muday, 2001). Therefore, actomyosin obviously optimizes the statolith sedimentation and statolith positioning in statocytes, but is not per se needed for the processes of graviperception in higher plants. As the results of the parabolic plane-flight and inversion experiments in the present study demonstrated, no pressure or tension forces potentially mediated by actin microfilaments are required but contact-interactions between sedimented statoliths and the gravireceptors are needed for the initiation of graviperception.

4.3 Gravity-dependent gene expression in plants

The experimental findings on the cellular mechanisms of gravisusception and -perception processes in plants revealing a highly sensitive and efficient gravisensing system were complemented by a comprehensive whole genome analysis on the effect of altered gravity conditions in Arabidopsis seedlings. With regard to large-scale gene-expression analyses, until now, only a few studies have focused on gravity-induced changes in plants (Moseyko et al., 2002; Martzivanou and Hampp, 2003; Kimbrough et al., 2004; Paul et al., 2005). The present study is the first to combine parabolic plane-flight experiments and a large set of experiments on ground to investigate

gene-expression patterns under various gravitational conditions. The highly sensitive Agilent Arabidopsis thaliana 60-mer oligonucleotide microarray that has already been successfully applied in other gene-expression studies on plants (Miura et al., 2010; Walley et al., 2010), covers the entire Arabidopsis genome and allowed for large-scale identification of genes in this study. In the experiments, the technical replicates were of high quality and the expression levels of selected prominent housekeeping genes were not affected during the changing experimental conditions. Therefore, the data presented in this study are highly reproducible. An earlier study has already reported on different classes of genes including (i) those insensitive to changes in gravitational conditions, (ii) those that are regulated in an opposite manner by different gravity conditions and (iii) those that are sensitised or desensitised dependent upon a sequence of changes in gravitational forces (Centis-Aubay et al., 2003). In the present study, the gene-expression analyses of Arabidopsis seedlings, which were exposed to the changing gravitational forces in parabolic plane flights and to different gravity conditions on ground, confirmed that, in principal, there are specific sets of genes that are differentially expressed in response to specific changes in the gravitational conditions. For each set, comparison of the gene-expression profiles in ground and flight experiments indicated the existence of several clusters of coregulated genes.

4.3.1 Hyper-*g* affects the expression of genes involved in stress response, metabolic pathways and cell-wall modifications

In this study, when 3-d-old Arabidopsis seedlings were gravistimulated by 90° reorientation for two hours, at least 920 genes were at least twice up- or down-regulated. A previous study focusing on the gene expression in three-week old Arabidopsis seedlings using oligonucleotide probe microarrays that provided 8300 genes, detected the differential expression of 141 genes after 30 min of horizontal stimulation (Moseyko et al., 2002). One hour of stimulation by 135° reorientation significantly changed the transcript abundance of 1730 genes in Arabidopsis root apices of 7-d-old seedlings (Kimbrough et al., 2004). In the present study and in the mentioned previous works, the reorientation at 1*g* conditions affected genes, whose products are suggested to be involved in gravitropism, i.e. Ca^{2+}-binding proteins, calmodulin or calmodulin-like proteins, cell wall modifying components, auxin-induced proteins, ethylene-responsive element binding factors and plant-defense proteins. The gene regulation processes are mainly attributed to the functional categories metabolism, transcription, transport, signal transduction and response to stress, as was also shown by Moseyko et al. (2002) and Kimbrough et al. (2004).

For the first time, the quantitative effect of continuous (2h 2*g*) and repeated short-term (62x 20s 2*g* in 2h 1*g*) hyper-*g* conditions on the whole genome expression pattern of Arabidopsis was evaluated. The number of 2*g*-affected genes was lower (204 at 2h 2*g* and 336 at 62x 20s 2*g* in 2h 1*g*) as compared to the number of genes, which were

differentially expressed during gravitropic response at 1*g* conditions (920). Up to now, only little is known about the effect of hyper-*g* on gene regulation in plants. Findings of earlier studies on the impact of gravitational fields between 1*g* and 10*g* on callus cultures of Arabidopsis (Martzivanou and Hampp, 2003) show similarities to the results of the centrifugation experiments in this study. The microarray analysis using a commercial chip with 4105 selected genes revealed an up-regulation of 200 transcripts in Arabidopsis callus cultures, which had been exposed to 7*g* for 1 h. The study not only reported on alterations as part of a general stress response, but also on a high number of genes, which were changed due to hyper-*g* induced metabolic processes and cell-wall modifications. The authors assumed that *g*-forces above a threshold of about 5*g* for 1 h cause distinct metabolic plant responses, which are regulated by gene expression (Martzivanou and Hampp, 2003). The results of the present study clearly demonstrate that – in terms of cell wall rearrangement amino acid and secondary metabolism as well as defense response – continuous centrifugation with 2*g* for 2 h leads to similar alterations. Genes exhibiting significantly changed levels of transcripts encoded for diverse proteins, which are involved in metabolic processes, e.g. phosphoglycerate dehydrogenase, arginine methyltransferase, diverse amino acid transporters and diverse enzymes of the carbohydrate biosynthetic metabolism. Furthermore, non-stop centrifugation with 2*g* for 2 h induced the differential expression of heat shock proteins and other stress-responsive proteins, e.g. cytochrome P450, as was also shown in the previous study on Arabidopsis callus cultures. Genes encoding for expansins, extensins and other cell wall modifying enzymes as well as diverse transporters, e.g. ammonium, nitrate and sugar transportes, were also significantly altered in their transcript abundances.

While the transcript level of all 200 7*g*-related genes analyzed in callus cultures was significantly increased, approximately 70% of the above mentioned 2*g*-related genes were significantly down-regulated in this study. As the duration of hyper-*g* stimulation was 2 h in this study versus 1 h in the previous study, these differences in orientation of gene expression might be explained by temporal expression pattern changes that were already observed in other studies on gravity-related gene-expression changes (Moseyko et al., 2002; Kimbrough et al., 2004). For example, the study by Moseyko et al. (2002) reported on temporal expression patterns for gravitropism-related genes that showed down-regulation at the 15-min time point and up-regulation at the 30-min time point. The author's conclusion that this observation does not fit into a simple 'switch on/switch off' model, implicates the idea that, during gene regulation in response to a stimulus, genes are not simply up- or down-regulated but reoriented in expression over time. Because there was only one time point for plant fixation in the ground experiments (2 h), the question of expression changes over time can not be answered by this study. However, it was demonstrated that the regulatory pathways during 2*g* centrifugation for 2 h and 7*g*

centrifugation for 1 h share some common key components. Therefore, it was shown that *g*-forces less than 5*g* cause distinct metabolic responses on genetic level.

Furthermore, a set of 108 genes was detected, which was particularly regulated in response to repeated short-term 2*g* centrifugation on ground (62x 20s 2*g* in 2h 1*g*) and in response to repeated 2*g*-phases during parabolic plane flights (62x 20s 2*g* in 2h flight). Similar to the continuous 2*g*-centrifugation experiment, nearly all of the 108 genes (90%) were significantly down-regulated. However, except for 5 genes (including glucosamine/galactosamine-6-phosphate isomerase and myb121 transcription factor), this set of genes responding to successively applied 2*g* stimuli, was independent of the regulation by non-stop 2*g* centrifugation. This finding indicates that successively applied short-time 2*g* stimuli may induce other gene-regulation pathways in plants compared to continuous 2*g* conditions. This assumption is supported by the previously mentioned study on different classes of genes which were regulated dependent of the sequence of changes in gravity conditions (Centis-Aubay et al., 2003). Investigations of the expression pattern of selected genes from Arabidopsis grown either at 1*g* or on a clinostat (1 rpm), and either used directly or after hyper-*g* stimulation (5 *g* for 30 min), suggest that the expression of gravity-sensitive genes involves 'complex interacting and/or independent regulatory pathways, including sensitisation/desensitisation' (Centis-Aubay et al., 2003). Taking into account that already 5 s of gentle back and forth movements significantly alter the expression of hundreds of genes in Arabidopsis root apices (Kimbrough et al., 2004), it appears most likely that the repeated 20-s 2*g* phases during centrifugation or during parabolic plane flights have not only an effect on the regulation of specific genes in general but also cause a kind of sensitisation/desensitisation over time. This might explain two independent gene expression patterns at continuous and at successive 2*g* centrifugation.

Although Arabidopsis seedlings responded differently to continuous versus interrupted 2*g* stimulation, the gene set, which was specifically altered at 62x 2*g*, included genes that encode for putative key components in gravity-sensitive pathways. An auxin-repressed dormancy-associated protein (At1g54870), extensin (At1g22420, At5g43770) and pectin methylesterase (At4g03930) were highly differentially expressed (up to fold change (FC) = -31), as was already shown for Arabidopsis seedlings exposed to 5*g* for 30 min (Centis-Aubay et al., 2003). In summary, considering the findings of the present study and those of previous works, hyper-*g* related changes in gene-expression definitely involve alterations in secondary metabolism, in particular amino acid metabolic processes, which in turn require an enhanced carbohydrate biosynthetic metabolism, e.g. glycolysis. General plant stress responses are induced by hyper-*g* conditions, but also more specific modifications, in particular, the formation of cell-wall components.

4.3.2 Hypergravity-induced gene-expression changes are independent from gravitropism-induced changes

In this study, it was shown that those genes involved in the response to reorientation at 1*g* were not significantly affected by hyper-*g* conditions. Under hyper-*g* conditions, other genes were differentially expressed than during the typical gravitropic response at 1*g* (90° 2h 1*g*). These results are in line with growth analyses in the presence of mechanoreceptor blockers showing that in Arabidopsis hypocotyls the gravity-induced processes in hypergravity-induced growth inhibition is independent of those of gravitropism (Soga et al., 2004). Furthermore, the gene-expression data obtained in this study go with the experimental findings on the cellular gravisensing processes in root statocytes and in characean rhizoids postulating a gravireceptor that is activated by contact-interactions with sedimented statoliths rather than by pressure mediated by the weight of the statoliths (Limbach et al., 2005; Greuel, 2007; Hauslage, 2008). Considering both, the molecular and the cellular data on gravity-induced responses of plants, it is most likely that the hyper-*g* induced processes are independent of those during gravitropism.

4.3.3 Plants are highly sensitive to gentle mechanical perturbations

Previous microarray analyses on Arabidopsis by Moseyko et al. (2002) identified genes specifically responding to 90° reorientation (30 min) and genes that were specifically changed in their expression by very gentle mechanical perturbations, i.e. 360° rotation within 10 s and then resting for 30 min. It was shown that 40% of the transcripts, which were differentially expressed during the gravitropic response in the 90° position, were also significantly up-/down-regulated in response to the mechanical perturbations. These findings were supported by results of the whole genome microarray study by Kimbrough et al. (2004) showing that even 5 s of gentle back and forth movement in the horizontal plane had a significant effect on the regulation of hundreds of genes in Arabidopsis root apices. More than 96% of the transcripts, which were differentially expressed during gravitropic response in 135° position (1h), exhibited also significant changes in expression levels after mild movement for 5 s (then stationary for 1h). Both studies showed that plant seedlings are extreme sensitive to gentle mechanical perturbations in terms of mild movements in the horizontal plane or rather slow rotation. Some kind of intersection between the gravitropic response and the response to the mechanical perturbations was indicated, as numerous genes were commonly differentially expressed after both stimuli.

In the present study, analyses of the inversion experiments underline the observations on the high sensitivity to mechanical perturbations at the genomic level. Stimulation of horizontally positioned Arabidopsis seedlings in terms of repeated (31x) short-term (10 s) inversions from 90° to the 270° resulted in 3130 genes, that were minimum 2-fold changed in expression compared to non-inverted vertically positioned controls (total experiment time was 2h). As

observed in the mechanical-perturbation studies by Moseyko et al. (2002) and Kimbrough et al. (2004), many genes (623) were differentially expressed under both conditions, during stimulation by 90° and in the inversion experiment. Stimulation by gentle shaking, transient movements or transient reorientations, e.g. inversion, obviously affects gene regulation that is also involved in the processes during plant gravitropic response. However, as the data of the present study demonstrated, the stimuli by repeated inversion had an additional effect on the regulation of numerous other genes (2507), which were not involved in the regulatory pathways during the plant response to horizontal stimulation without inversion. Almost half of these additionally affected genes were also differentially expressed under the conditions of a 2-h parabolic flight. Correlations in gene regulation processes for seedlings exposed to the conditions of inversion or parabolic flight were mainly attributed to a lot of stress- and defense-related signaling pathways including the activity of numerous heat shock proteins (HSPs) and other stress-responsive proteins. However, not all of the common gene products involved in the plants response to inversion and flight conditions were part of a general stress response, as will be discussed in the following chapter.

4.3.4 Effects of the repeated short-term µ*g* phases during parabolic flights on gene-expression

With regard to the number of genes affected by the conditions of the ground experiments, the strongest effect was observed in the inversion experiments. Only the conditions of a 2-h parabolic flight significantly altered the transcript abundances of more genes (3831) with 30% of these transcripts (1162) being already significantly regulated after 1-h parabolic flight. No time-dependent reorientation of expression was detected for these genes. All of the 1162 differentially expressed genes, which were down-/up-regulated at the 1-h time point, were similarly down-/up-regulated at the 2-h time point. Because of insufficient annotation details (TAIR, status April 2010), more than one-third of the transcripts significantly regulated during the plant response to flight conditions could not be reliably attributed to specific biological processes. However, four main functional categories became apparent comprising gene products involved in stress and defense responses, protein metabolism and other metabolic processes, transcription and transport activities.

The comparative analysis of the gene expression patterns of the flight samples and the in-flight control samples, which experienced all flight conditions except the µ*g*-phases, revealed a set of 142 µ*g*-related genes. The expression of these genes was significantly altered in plants exposed to the µ*g*-phases of a 2-h flight but was not affected in plants, which were accelerated with 1*g* by means of on-board centrifugation during microgravity. Most of these 142 µ*g*-related genes (80%) were down-regulated in the flight samples including the largest functional group of genes, whose products are suggested to be involved in lipid signaling as possible mediators of the gravity-related signals (Fischer

et al., 2004). The results confirmed the µ*g*-induced down-regulation (up to FC = -10) of numerous lipid transfer proteins (LTPs), as was also shown for *Ceratopteris richardii* during a recent space-flight experiment (Salmi and Roux, 2008). In contrast to studies on long-term exposure to µ*g*, reporting on numerous HSPs involved in plant stress-responses during space-shuttle flights (Paul et al., 2001, 2005; Salmi and Roux, 2008), no HSP-coding gene was among the 142 µ*g*-related genes in this study. In general, the impact on stress-related processes by the repeated µ*g*-phases was less than by repeated inversion stimuli or by the conditions of a whole 2-h flight (1*g*, 62x 20s 2*g* and 31 x 20s µ*g*).

4.3.5 Effect of parabolic flight conditions on gravitropism-related genes

Comparing results from experiments on ground and on parabolic flights, Venn diagram analyses revealed the highest match in gene-expression responses between the two experimental groups '2-h horizontal stimulation at 1*g* interrupted by repeated short-term inversion' and '2-h parabolic flight'. Half of the genes (1535) responding to the repeated inversions were also differentially expressed in the vertically oriented flight samples of a 2-h parabolic flight. These findings suggest that mechanical perturbations as they occur during transient inversion may also be induced by parabolic plane-flight conditions. Interestingly, those 353 gravitropism-related genes, which were part of the plant response to horizontal stimulation with or without inversion and to flight conditions, were not differentially expressed in horizontally versus vertically oriented flight samples (1-h flight). The opposite was observed for horizontally versus vertically positioned seedlings at 1*g* conditions. Since the comparative analyses of the expression values for the gravitropism-related genes clearly revealed the significant up- or down-regulation in horizontally positioned plants versus vertical controls at 1*g*, the horizontal stimulation during parabolic flight was expected to show the same effect. However, cluster analyses confirmed that those genes, which were down-regulated during 90° but not during 0° positioning on ground, were down-regulated during both, 90° and 0° positioning in flight. The same was observed for the up-regulated genes. These findings explain why significant differences in gene-expression ratios were not detected in horizontal versus vertically oriented seedlings during parabolic flights (1 h). In particular, because of insufficient knowlegde about functional details of many gene products, data currently do not allow precise evaluation of the impact by the acceleration profile of parabolic plane flight. Concerning the gravitropism-related genes, it is hard to say what aspect of the flight conditions resulted in the reorientation of gene expression in vertical oriented Arabidopsis seedlings.

Previous experiments during parabolic flights with the aircraft A300 Zero-G demonstrated that during flights, vibrations are generated particularly by the aircraft engines (Schmidt, 2004). Furthermore, it was shown that these vibrations were transmitted to experiment hardware and experiment samples, respectively. In order to

test whether parabolic flight-induced vibrations cause some kind of mechanical perturbations during flight potentially affecting the expression of gravity-related genes, the data by Schmidt (2004) were used to simulate the vibration-flight profile in ground experiments. More than 500 genes were significantly up- or down-regulated in seedlings exposed to the vibrations in the simulation experiment (2 h). Only 100 of the total 3831 genes, which were affected by the conditions of a 2-h flight, were also part of the plant response to the vibrations in the ground experiment. Although these data are based upon a simulation of flight vibrations, it is most likely that the strong effect on gene-expression level by the changing acceleration conditions during flight is almost independent of effects induced by vibrations. Current efforts on live-recording of the vibrations during a parabolic plane flight will possibly allow an even more realistic run of vibration experiments on ground and will allow for further testing of the hypothesis that the flight-induced vibrations affect gravity-related gene-expression. However, the data of the present study showed that the 353 gravitropism-related genes, which were significantly affected in their regulation during flight, were not differentially expressed in response to the simulated flight-vibration profile. Concerning these gravitropism-related genes, the expression pattern of the vibrated Arabidopsis plants was nearly identical to that of non-vibrated controls. Therefore, it is concluded that flight vibrations did not predominantly trigger the regulation of gravitropism-related genes in vertical growing seedlings during flight.

It appears likely that the specific parabolic flight sequence by itself (1*g*, 62x 20s 2*g* and 31x 20s µ*g*) affected gene expression in general and, in particular, gravitropism-related gene expression. Not only variations from normal 1*g* conditions, e.g. hypergravity or microgravity conditions, for a longer continuous time period (e.g. centrifugation experiments, sounding-rocket flights) affect complex gene regulatory pathways, but also the specific conditions of a sequence of changes like that one during parabolic plane flights. In this respect, the effects on gene regulation by continuous and successive stimulation are rather different. Non-stop hyper-*g* centrifugation, for example, resulted in a gene expression pattern that considerably differed from that at repeated short-term centrifugation. The successive changes between 1*g*, 2*g* and µ*g* during parabolic plane flights provide unusual conditions that have never been experienced by biological organisms during evolution. These special stimuli not only induce general plant stress responses and complex changes in metabolic processes, they obviously affect gene regulation processes that are typically involved in plant gravitropism, even in seedlings which are not stimulated with respect to their orientation, i.e. are vertically oriented. Since vertically oriented plants do not have to gravitropically respond in terms of reorientating their organs relative to the gravity vector, this finding may, at a first glance, seem incompatible with physiological or energetic explanations. It is worth mentioning that, of course, in contrast to the horizontally positioned Arabidopsis seedlings, the prima-

ry roots and shoots of the plants in 0° position never showed any gravitropic curvature response during parabolic flight. The observations become more coherent when considering that even plant seedlings, whose organs are correctly oriented with respect to their genetically determined set-point angle, continuously respond to gravity. In order to establish straight growth of the primary root and shoot, plants not only have to permanently sense but also respond to deviations from the set-point angle. The result of this permanent response to gravity is actually well known as the circumnutation of roots and shoots (for review, see Johnsson 1979) and is based on a very efficient gravisensing mechanism 'guiding' the plant organs to the position with the most beneficial environmental conditions. To what extent the conditions provided by parabolic plane flights might influence the cellular processes of gravisensing, so that even vertically oriented seedlings showed the differential expression of gravitropism-related genes, is discussed in the following.

4.4 High gravisensitivity and great efficiency on cellular and genomic level ensures the most beneficial gravitropic response of plants

The present new findings on gravity-related cellular and molecular processes point to a gravisensing system in plant cells that substantially bases upon two principles, i.e. a high sensitivity to gravistimuli and an '*always at the ready*' status. The results of the MAXUS-8 experiment showed an extremely high gravisensitivity for characean rhizoids. A threshold acceleration of $\leq 0.08g$ is sufficient to overcome the cytoskeleton forces acting on statoliths in lateral direction and, therewith, to induce sedimentation of statoliths toward the gravireceptors. From the energetic point of view, the high level of gravisensitivity is not only ensured by the low acceleration threshold for lateral statolith displacement but also by the mechanism of gravireceptor activation depending on contact between statoliths and gravireceptors (Limbach et al., 2005). The highly functional organization of the actomyosin system in Chara rhizoids allows for a relatively free statolith sedimentation in lateral direction onto the gravireceptors on the one hand, and, on the other hand, controls the statoliths position in basal direction by keeping them at the level of the gravisensitive membrane site (for review, see Braun et al. 2002). This actomyosin-mediated mechanisms are the basic prerequisite for the '*always at the ready*' status in rhizoids. The effective combination of both, the high sensitivity in terms of a very low threshold and the readiness to continuously sense and respond, facilitates not only a fast and most beneficial gravitropic response during reorientation but also during normal orientation of the rhizoid. Of course, from the three-dimensional point of view, in a downward-growing rhizoid, the statoliths distributed in the gravisensitive belt-like area (10-30 µm behind the tip) permanently trigger graviperception by activating gravirecep-

tors. By this means, a symmetric signal in terms of a symmetric Ca^{2+} gradient is established in the tip growing cell. Tilting of rhizoids leads to the activation of gravireceptors in only one cell flank, the physical lower one, on which the statoliths are sedimented. The influx of Ca^{2+} is locally inhibited directly or indirectly by the activation of the gravireceptors causing differential growth of the opposite cell flanks and, therewith, the gravitropic curvature of the rhizoid (for review, see Braun, 1997, 2002).

In higher plant organs, the situation is far more complex, as the individual signals from numerous gravisensing statocytes have to be integrated and translated into a common signal, which is transmitted by means of growth hormones. In terms of the most beneficial orientation of plant organs and energetic aspects, respectively, the ability of plants to avoid unfavorable gravitropic responses to only transient stimuli, e.g. by wind or rain, and, on the other hand, to respond to consistent reorientation is crucial. To ensure such a highly functional gravisensing system, the integration of the signals from all statocytes has to allow for effective differentiation between transient stimuli and consistent stimulation. In this regard, the actomyosin-mediated saltatory movements of statoliths (Sack et al., 1986; Yamamoto et al., 2002; Palmieri et al., 2005; Saito et al., 2005) and the structural polarity of statocytes are essential. Findings of several studies indicate that sedimented amyloplasts interact with gravireceptors in the ER membrane, not necessarily with receptors located in the membranes of the distal ER complex but of ER cisternae in general (Sievers and Volkmann, 1972; 1977; Wendt et al., 1987). Results of a recent study demonstrated that the membrane of the cortical ER network was deformed by the kinetic energy of sedimented statoliths. The author supposed that an elastic lift force exerted by the ER could push the statoliths out of their normal 'resting position' in downward growing roots when stimulated by reorientation (Leitz et al., 2009). Independent of this hypothesis, the ER membranes represent a large sensitive surface for sedimented statoliths in plant statocytes. Because of the cone-shaped geometry of statocytes and because of the statoliths' permanent saltatory movements, at least a few statoliths are always in contact with ER membranes initiating graviperception. Gravireceptor activation most likely affects the activity of Ca^{2+} channels causing a distal Ca^{2+} influx into the statocytes that in turn activates auxin efflux proteins (Fig. 34, B). With regard to the multi-cellular section of the gravisensing tissues in roots and shoots, the signals from all statocytes are integrated and a symmetric signal in terms of the growth-hormone auxin is established during straight growth of roots (Fig. 34) and shoots. Reorientation of plant organs leads to the sedimentation of the statoliths along the gravity vector and the gravireceptor activation in the physical lower statocyte flank. The resulting asymmetric signal from the gravisensing tissues to the responding cells by means of a lateral gradient of auxin leads to the differential growth of the opposite flanks of the reoriented organ (Cholodny, 1928; Went, 1933).

Earlier studies have already distinguished two types of gravistimulation, the static and the dynamic one (Sievers et al., 1991; Sievers and Hejnowicz, 1992). Static stimulation occurs in normally oriented plants at a constant gravity field, and is connected with the 'resting position' of the statoliths interacting with the gravireceptors in the ER membranes. Dynamic stimulation involves the displacement of statoliths along the gravity vector during plant reorientation. It is likely that a continuous graviperception triggered by persistent actomyosin-mediated permanent saltatory movements of statoliths underlies both, static and dynamic stimulation. In a recent study it was demonstrated that the rapid (< 1 s) and short-range (< 1µm) statolith movements are randomly-oriented and characterized by a high variance (Leitz et al., 2009). It appears most likely that these random actomyosin-mediated movements of statoliths lead to a successive activation of gravireceptors in the ER membrane inducing a triggered gravitropic signal and, thus, providing a constant source of noise level to gravisensing statocytes (Fig. 34, B). The magnitude of this random noise level determines the limit for the ability of statocytes to sense the signals generated by statolith sedimentation (Leitz et al., 2009). The increase of noise level by a triggered signaling would amplify information-carrying signals generated by statolith sedimentation (Hänggi, 2002; Ma and Hasenstein, 2006; Leitz et al., 2009). Such a triggering would provide the basis for a gravisensing system that is very sensitive to even small deviations from the genetically determined set-point angle of plant organs. In addition, such a mechanism would prevent plants from unfavorable responses to only transient stimuli, e.g. to strong shaking by wind, since the signals generated by these transient stimuli are immediately superimposed by signals attributed to static stimulation. Thus, transduction of gravistimuli into physiological signals only leads to the initiation of gravitropic response when gravistimulation persists for a sufficient time period. A gravisensing system based upon a triggered gravitropic signaling mediated by the saltatory movements of statoliths might also explain, why the gravisensitivity of starch-less mutants is strongly reduced, but reorientation in response to gravity is still existent (Caspar and Pickard, 1989; Kiss et al. 1996; Weise and Kiss, 1999). Although, the increasing density of plastids by increasing the starch content promotes the gravisusception and -perception processes in statocytes, gravisensing does not require starch-filled plastids. The plastid-based gravisensing in starch-less mutants is strongly supported by the saltatory movements of statoliths in statocytes.

The findings of the present gene-expression study on Arabidopsis seedlings are in line with this model of a triggered gravitropic signaling as the basis of a highly sensitive gravisensing mechanism in plants. It is conceivable that the special conditions provided by a parabolic plane flights, in particular the fast and successive changes of the acceleration conditions, enhance the saltatory movements of statoliths. The results of the present study indicate that flight conditions cause mechanical perturbations, which most likely lead to an increased motility of statoliths (Fig. 34, B.2) but not to a significant statolith

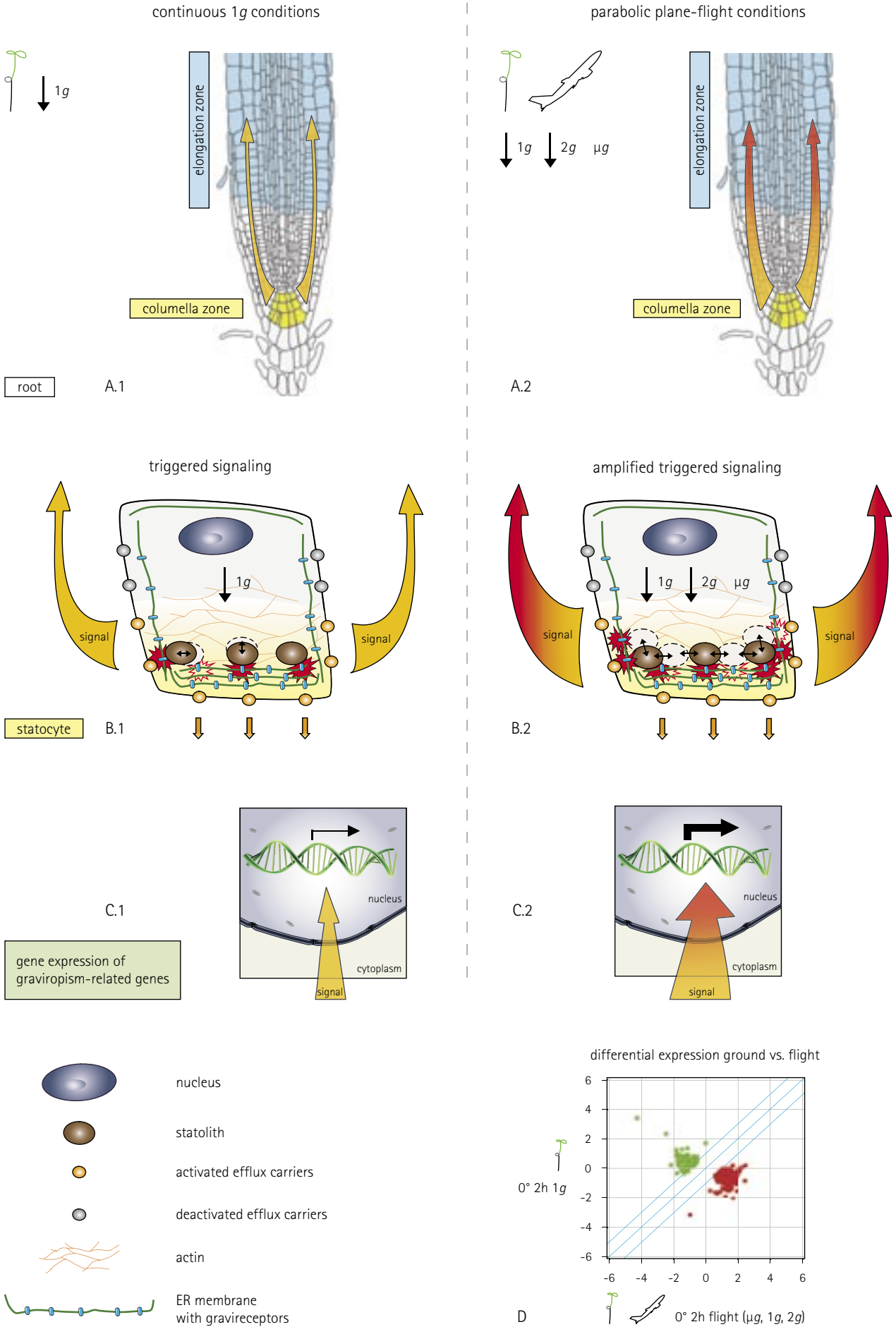
continuous 1g conditions
parabolic plane-flight conditions
1g
elongation zone
columella zone
root
A.1
1g
2g
µg
elongation zone
columella zone
A.2
triggered signaling
amplified triggered signaling
1g
signal
signal
statocyte
B.1
1g
2g
µg
signal
signal
B.2
C.1
gene expression of graviropism-related genes
nucleus
cytoplasm
signal
C.2
nucleus
cytoplasm
signal
nucleus
statolith
activated efflux carriers
deactivated efflux carriers
actin
ER membrane with gravireceptors
differential expression ground vs. flight
0° 2h 1g
6
4
2
0
-2
-4
-6
-6
-4
-2
0
2
4
6
D
0° 2h flight (µg, 1g, 2g)

displacement, as was demonstrated by the analyses on the position of sedimented statoliths during parabolic plane flights. Assuming that, during flight, an enhanced statolith motility results in a strongly increased signal triggering, which in turn provides an amplified noise level to the statocytes, it appears likely that the threshold for the initiation of gravitropic responses is considerably lower in flight samples compared to 1*g* controls – at least concerning the activation of gene regulatory pathways. This would give an explanation for the differential expression of gravitropism-related genes in vertically oriented Arabidopsis seedlings under flight conditions versus vertically positioned ground controls (Fig. 34, D). Thus, the extremely amplified static gravistimulation during flight induced the up- and down-regulation of genes, which are actually involved in the plant response to reorientation at normal 1*g* conditions on Earth. Of course, a gravitropic curvature response was not observed, since the direction of acting gravity forces during flight (1*g*, 2*g*) was parallel to the vertically positioned seedlings.

Fig. 34. Model for graviperception in normally positioned plant organs using the example of roots. During static stimulation in normally oriented roots at constant 1*g* conditions, the actomyosin-mediated statoliths' movements avoid resting of the sedimented statoliths and lead to the triggered activation (red stars) of gravireceptors in the ER membranes (B.1). Gravireceptor activation most likely affects the activity of Ca^{2+} channels causing a distal Ca^{2+} influx (yellow area in the statocyte), which in turn activates auxin-efflux proteins. In vertically oriented roots, the integration of the signals from all statocytes of the columella zone results in the basipetal signaling in terms of a symmetric flux of auxin (arrows) (A). The gravitropic signaling finally induces the expression of gravitropism-related genes (C.1) whose products are involved in gravity-related growth processes – managing straight growth in vertically oriented roots and differential growth during curvature response in reoriented roots, respectively. Mechanical perturbations caused by the conditions of parabolic plane flights (1*g*, 2*g*, µ*g*) lead to a strongly increased motility of statoliths (B.2). The resulting amplified triggering provided to the statocytes enhances the gravity-induced signals and, in comparison to 1*g* controls, the threshold for initiation of gravitropic response – in terms of gene-expression regulation – is considerably lower (C.2). Thus, the extremely amplified static stimulation during flight results in the significant up-/down-regulation of gravitropism-related genes compared to 1*g* controls (D).

5. SUMMARY

The present study focused on the cellular and molecular gravisensing-related processes in Arabidopsis and in the unicellular rhizoids of the green alga Chara. Experiments during sounding-rocket and parabolic plane flights were conducted in order to assess the effect of altered gravity conditions on gravitropism-related processes in plant cells. The cellular findings on statolith-mediated gravisusception and graviperception processes in characean rhizoids and higher plant root statocytes as well as the obtained data on gene-expression regulation during altered gravitational conditions considerably extend our knowledge about gravity-related mechanisms in plants.

During the sounding rocket experiment of MAXUS-8, determination of the minimum acceleration that is required to induce lateral displacement of statoliths revealed a low threshold value ($\leq 0.08g$) for the gravisensitivity in Chara rhizoids. This high level of gravisensitivity ensures a gravisensing mechanism that is highly efficient so that even small deviations from the genetically determined set-point angle are rapidly corrected by the cell. The positioning of sedimented statoliths in the statocytes of horizontally stimulated Arabidopsis root seedlings during the different acceleration phases of parabolic plane flights have been analyzed. The findings revealed the missing evidence that graviperception in higher plants is accomplished by contact-interactions between statoliths and gravireceptors rather than by mechanical pressure. Once the statoliths are sedimented onto the gravireceptors, no pressure mediated by the weight of the statoliths is required for activation of the gravireceptors. In this respect, higher plant root statocytes and Chara rhizoids apparently share the same mechanism of graviperception.

The findings about cellular graviperception mechanisms in plant cells were complemented by new results on the gravity-related gene-expression in Arabidopsis. At the level of gene expression, plants are not only sensitive to changes in orientation at $1g$ conditions but also to the altered conditions provided by parabolic plane flight. It was demonstrated that, in principle, plants are highly sensitive to even transient changes in gravity conditions. The rapidly changing acceleration conditions of parabolic plane flights ($1g$, $2g$ and μg) significantly affected the gene regulation of thousands of genes including gravitropism-related genes, which were actually involved in the plant response to 90° reorientation on ground. Furthermore, it was demonstrated that gravitational conditions differing from $1g$ conditions on Earth not only induced general stress responses but also more specific modifications, like e.g. the rearrangement of cell-wall components durring hyper-g conditions. Findings on gene-expression level confirmed hypergravity-induced processes which are independent of gravitropism-related mechanisms in plants, and, therefore, support the assumption that gravireceptor activation is independent of pressure or tension forces.

In summary, findings on cellular and molecular level, presented in this study, demonstrated that a high gravisensitivity and a great efficiency provide the fundamental basis of plant gravisensing in order to allow for a most beneficial gravitropic plant response.

6. OUTLOOK

The analyses of the present study on gravity-related gene expression in Arabidopsis provide the basis for further molecular investigations in order to improve our knowledge on gravitropism-related processes in plants. Future experiments should build on the findings of this study and of previous works comprising the general effects on gene- and protein-expression patterns by plant reorientation and by altered gravitational conditions. The findings on the main regulatory pathways, which are supposed to play a role during gravitropism-related processes, should be narrowed down to potential key components. In this respect, the present study has confirmed the importance of considering both, molecular findings and cellular findings. Our increasing knowledge about structural and functional details of gravity-induced cellular processes will probably allow for new molecular approaches and vice versa. Until now, cellular or biochemical approaches on the statocytes of higher plants are rare because of the complex tissues of gravisensing plant organs, and the transparent single-celled Chara rhizoids and protonemata are more easily accessible and, therefore, better suited for investigations at the cellular level. However, reliable research methods for molecular and biochemical studies in the rhizoid and the protonema have yet to be established. Thus, there is urgent need to integrate findings from different model systems in order to develop a more complete idea of plant gravisensing. By unraveling the common principle of contact-dependent gravireceptor activation in Chara rhizoids and higher-plant statocytes, the present study has demonstrated the power of integrating the findings from different model systems. It will be an important task of future studies to characterize the molecular nature of the gravireceptors and to identify the crucial components in the statolith membrane as the interaction partners with gravireceptor molecules in plant cells.

7. REFERENCES

7.1 Literature

ALONI, R., LANGHANS, M., ALONI, E. & ULLRICH, C. (2004): Role of cytokinin in the regulation of root gravitropism. Planta, 220, 177-182.

BARJAKTAROVIĆ, Z., NORDHEIM, A., LAMKEMEYER, T., FLADERER, C., MADLUNG, J. & HAMPP, R. (2007): Time-course of changes in amounts of specific proteins upon exposure to hyper-*g*, 2-D clinorotation, and 3-D random positioning of Arabidopsis cell cultures. J Exp Bot, 58 (15/16), 4357-4363.

BARJAKTAROVIĆ, Z., BABBICK, M., NORDHEIM, A., LAMKEMEYER, T., MAGEL, E. & HAMPP, R. (2009): Alterations in protein expression of Arabidopsis thaliana cell cultures during hyper- and simulated micro-gravity. Microgravity Sci Technol, 21, 191-196.

BARJAKTAROVIĆ, Z., SCHÜTZ, W., MADLUNG, J., FLADERER, C., NORDHEIM, A. & HAMPP, R. (2009): Changes in the effective gravitational field strength affect the state of phosphorylation of stress-related proteins in callus cultures of Arabidopsis thaliana. J Exp Bot, 60 (3), 779-789.

BELYAVSKAYA, N.A. (2004): Changes in calcium signalling, gravitropism, and statocyte ultrastructure in pea roots induced by calcium channel blockers. J Gravit Physiol, 11(2), 209-210.

BLANCAFLOR, E. & HASENSTEIN, K. (1997): The organization of the actin cytoskeleton in vertical and graviresponding primary roots of maize. Plant physiol, 113, 1447-1455.

BLANCAFLOR, E. (2002): The cytoskeleton and gravitropism in higher plants. J Plant Growth Regul, 21, 120-136.

BLANCAFLOR, E. & MASSON, P. (2003): Plant gravitropism. Unraveling the ups and downs of a complex process. Plant Physiol, 133, 1677-1690.

BLILOU, I., XU, J., WILDWATER, M., WILLEMSEN, V., PAPONOV, I., FRIML, J., HEIDSTRA, R., AIDA, M., PALME, K. & SCHERES, B. (2005): The PIN auxin efflux facilitator network controls growth and patterning in Arabidopsis roots. Nature, 433(6), 39-44.

BOONSIRICHAI, K., GUAN, C., CHEN, C., CHEN, R. & MASSON, P. (2002): Root gravitropism: an experimental tool to investigate basic cellular and molecular processes underlying mechanosensing and signal transmission in plants. Annu Rev Plant Biol, 53, 421-447.

BRAUN, M. (1996): Anomalous gravitropic response of Chara rhizoids during enhanced accelerations. Planta, 199, 443-450.

BRAUN, M. (1997): Gravitropism in tip-growing cells. Planta, 203, 11-19.

BRAUN, M. & Richter, P. (1999): Relocalization of the calcium gradient and a dihydropyridine receptor is involved in upward bending by bulging of Chara protonemata, but not in downward bending by bowing of Chara rhizoids. Planta, 209, 414 - 423.

BRAUN, M. (2001): Association of spectrin-like proteins with the actin-organized aggregate of endoplasmic reticulum in the Spitzenkörper of gravitropically tip-growin plant cells. Plant Physiol, 125, 1611 -1620.

BRAUN, M. (2002): Gravity perception requires statoliths settled on specific plasma membrane areas in characean rhizoids and protonemata. Protoplasma, 219, 150-159.

BRAUN, M., BUCHEN, B. & SIEVERS, A. (2002): Actomyosin-mediated statolith positioning in gravisensing plant cells studied in microgravity. J Plant Growth Regul, 21, 137-145.

BRAUN, M., HAUSLAGE, J., CZOGALLA, A. & LIMBACH, C. (2004): Tip-localized actin polymerization and remodeling, reflected by the localization of ADF, profilin and villin, are fundamental for gravity-sensing and polar growth in characean rhizoids. Planta, 205, 39-50.

BRAUN, M. & LIMBACH, C. (2005): Actin-based gravity-sensing mechanisms in unicellular plant model systems. ESA-SP, 590, 41-45.

BROCK, T. & KAUFMANN, P. (1988): Altered growth response to exogenous auxin and gibberellic acid by gravistimulation in pulvini of Avena sativa. Plant physiol, 87, 130-133.

BROWN, A.H., CHAPMAN, D.K., JOHNSSON, A., HEATHCOTE, D. (1995): Gravitropic responses of the Avena coleoptile in space and on clinostats. I. Gravitropic response thresholds. Physiol Plant, 95, 27-33.

BUCHEN, B., BRAUN, M., HEJNOWICZ, Z. & SIEVERS, A. (1993): Statoliths pull on microfilaments. Protoplasma, 172, 38-42.

BUCHEN, B., BRAUN, M. & SIEVERS, A. (1997): Statoliths, cytoskeletal elements and cytoplasmic streaming of Chara rhizoids under reduced gravity during TEXUS flights. Life sciences experiments performed on sounding rockets (1985-1994). ESA-SP, 1206, 71-75.

BUER, C., SUKUMAR, P. & MUDAY, G. (2006): Ethylene modulates flavonoid accumulation and gravitropic responses in roots of Arabidopsis. Plant Physiol, 140, 1384-1396.

CAI, W., BRAUN, M. & SIEVERS, A. (1997): Displacement of statoliths in Chara rhizoids during horizontal rotation on clinostats. Acta Bot Exp Sinica, 30 (2), 147-155.

CASPAR, T. & PICKARD, B.G. (1989): Gravitropism in a starchless mutant of Arabidopsis: implications for the starch-statolith theory of gravity sensing. Planta, 177, 185-197.

CENTIS-AUBAY, S., GASSET, G., MAZARS, C., RANJEVA, R. & GRAZIANA, A. (2003): Changes in gravitational forces induce modifications of gene expression in A. thaliana seedlings. Planta, 218(2), 179-185.

CHOLODNY, N. (1928): Beiträge zur hormonalen Theorie von Tropismen. Planta, 6, 118–134.

CHOMCZYNSKI, P. & SACCHI, N. (1987): Single-step method of RNA isolation by acid guanidinium thiocyanate-phenol-chloroform extraction. Anal Biochem, 162(2), 156-159.

DRISS-ECOLE, D., VASSY, J., REMBUR, J., GUIVARC'H, A., PROUTEAU, M., DEWITTE, W. & PERBAL, G. (2000): Immunolocalization of actin in root statocytes of Lens culinaris L.. J Exp Bot, 51, 521-528.

FASANO, M.J., SWANSON, S.J., BLANCAFLOR, E.B., DOWD, P.E., TEHHUI, K. & GILROY, S. (2001): Changes in root cap pH are required for the gravity response of the Arabidopsis root. Plant Cell, 13, 907-922.

FISCHER, U., MEN, S. & GREBE, M. (2004): Lipid function in plant cell polarity. Curr Opin Plant Biol, 7, 670–676.

FRIML, J., WISNIEWSKA, J., BENKOVA, E., MENDGEN, K. & PALME, K. (2002): Lateral relocation of auxin efflux regulator PIN3 mediates tropism in Arabidopsis. Nature, 415, 806-809.

FRIML, J. (2003): Auxin transport - shaping the plant. Curr Opin Plant Biol, 6, 7-12.

GIRKE, T., TODD, J., RUUSKA, S., WHITE, J., BENNING, C & OHLROGGE, J. (2000): Microarray analysis of developing Arabidopsis seeds. Plant Physiol, 124, 1570-1581.

GREUEL, N. (2007): Molecular and functional analyses of the early mechanisms of graviperception studied in characean rhizoids and Arabidopsis roots. Diploma thesis, IMBIO, University of Bonn, Germany.

GREUEL, N.; HAUSLAGE, J. & BRAUN, M. (2007): Early mechanisms of gravity sensing in plants. ESA-SP, 647, 469-472.

GODA, H., SASAKI, E., AKIYAMA, K., MARUYAMA-NAKASHITA, A., NAKABAYASHI, K., LI, W., OGAWA, M., YAMAUCHI, Y., PRESTON, J., AOKI, K., KIBA, T., TAKATSUTO, S., FUJIOKA, S., ASAMI, T., NAKANO, T., KATO, H., MIZUNO, T., SAKAKIBARA, H., YAMAGUCHI, S., NAMBARA, E., KAMIYA, Y., TAKAHASHI, H., YOKOTA HIRAI, M., SAKURAI, T., SHINOZAKI, K., SAITO, K., YOSHIDA, S. & SHIMADA, Y. (2008): The AtGenExpress hormone and chemical treatment data set: experimental design, data evaluation, model data analysis and data access. The Plant J, 55, 526-542.

HABERLANDT, G. (1900): Über die Perzeption des geotropischen Reizes. Ber. Dtsche. Bot. Ges., 18, 261-272.

HÄDER, D.P., ROSUM, A., SCHÄFER, J. & HEMMERSBACH, R. (1995): Gravitaxis in the flagellate Euglena gracilis is controlled by an active gravireceptor. J Plant Physiol, 146, 474 - 480.

HANANO, S. & DAVIS, S. (2007): Mind the clock. Plant Signal Behav, 2(6), 477-479.

HÄNGGI, P. (2002): Stochastic resonance in biology. How noise can enhance detection of weak signals and help improve biological information processing. Chemphyschem, 3(3), 285-290.

HAUSLAGE, J. (2008): Funktionelle Charakterisierung von frühen Graviperzeptionsmechanismen in Pflanzen. Doctoral thesis, IMBIO, University of Bonn, Germany.

HEJNOWICZ, Z., HEINEMANN, B. & SIEVERS, A. (1977): Tip growth: pattern of growth rate and stress in the Chara rhizoid. Zeitschr Pflanzenphysiol, 81, 409-424.

HEMMERSBACH, R.; VOORMANNS, R.; BRIEGLEB, W.; RIEDER, N. & HÄDER, D.P. (1996): Influence of accelerations on the spatial orientation of Loxodes and Paramecium. Biotechnol, 47 (2-3), 271-278.

HODICK, D., BUCHEN, B. & SIEVERS, A. (1998): Statolith positioning by microfilaments in Chara rhizoids and protonemata. Adv Space Res, 21, 1183-1189.

HORN, A. (2007): Design, construction and testing of a new shock freezing system during parabolic flight. Master thesis, Julius Maximilian Universität, Würzburg, Germany.

HOSON, T., KAMISAKA, S., MASUDA, Y., YAMASHITA, M. & BUCHEN, B. (1997): Evaluation of the three-dimensional clinostat as a simulator of weightlessness. Planta, 203, 187-197.

HOU, G., MOHAMALAWARI, D. & BLANCAFLOR, E. (2003): Enhanced gravitropism of roots with a disrupted cap actin cytoskeleton. Plant Physiol, 131, 1360-1373.

HOU, G., KRAMER, V., WANG, Y., CHEN, R., PERBAL, G., GILROY, S. & BLANCAFLOR, E. (2004): The promotion of gravitropism in Arabidopsis roots upon actin disruption is coupled with the extended alkalinization of the columella cytoplasm and a persistent lateral auxin gradient. Plant J, 39, 113-125.

JOHNSSON, A. & HEATHCOTE, D (1973): Experimental evidence and models in circumnutation. Zeitschrift fur Pflanzenphysiologie, 70, 371-405.

KILIAN, J., WHITEHEAD, D., HORAK, J., WANKE, D., WEINL, S., BATISTIC, O., D'ANGELO, C., BORNBERG-BAUER, E., KUDLA, J. & HARTER, K. (2007): The AtGenExpress global stress expression data set: protocols, evaluation and model data analysis of UV-B light, drought and cold stress responses. The Plant J, 50, 347-363.

KIM, S., CHANG, S., LEE, E., CHUNG, W., KIM, Y., HWANG, S. & SEUNG LEE, J. (2000): Involvement of brassinosteroids in the gravitropic response of primary root of maize. Plant physiol, 123, 997-1004.

KIMBROUGH, J., MONDRAGON, R., BOSS, W., BROWN, C. & SEDEROFF, H. (2004): The fast and transient transcriptional network of gravity and mechanical stimulation in the Arabidopsis root apex. Plant Physiol, 136, 2790-2805.

KISS, J.Z., WRIGHT, J.B., CASPAR, T. (1996): Gravitropism in roots of intermediate-starch mutants of Arabidopsis. Physiologia Plantarum, 97, 237-244.

KUZNETSOV, O.A. & HASENSTEIN, K.H. (1996): Magnetophoretic induction of root curvature. Planta, 198, 87–94.

KUZNETSOV, O.A. & HASENSTEIN, K.H. (1997): Magnetophoretic induction of curvature in coleoptiles. J Exp Bot, 48, 1951–1957.

KUZNETSOV, O.A., SCHUCHOW, F.D., SACK, F.D. & HASENSTEIN, K.H. (1999): Curvature induced by amyloplast magnetophoresis in protonemata of the moss Ceratodon Purpureus. Plant Physiol, 119, 645–650.

LEE, J., CHANG, W. & EVANS, M. (1990): Effects of ethylene on the kinetics of curvature and auxin redistributaion in gravistimulated roots of zea mays. Plant physiol, 94, 1770-1775.

LEGUÉ, V., BLANCAFLOR, E., WYMER, C., PERBAL, G., FANTIN, D. & GILROY, S. (1997): Cytoplasmic free Ca^{2+} in Arabidopsis root changes in response to touch but not gravity. Plant physiol, 114(3), 789-800.

LEITZ, G.; SCHNEPF, E. & GREULICH, K.O. (1995): Micromanipulation of statoliths in gravity-sensing Chara rhizoids by optical tweezers. Planta, 197, 278-288.

LEITZ, G., KANG, B., SCHOENWAELDER, M. & STAEHELIN, L. (2009): Statolith sedimentation kinetics and force transduction to the cortical endoplasmic reticulum in gravity-sensing Arabidopsis columella cells. Plant Cell, 21, 843-860.

LI, L., XU, J., XU, Z. & XUE, H. (2005): Brassinosteroids stimulate plant tropisms through modulation of polar auxin transport in Brassica and Arabidopsis. The Plant Cell, 17, 2738-2753.

LIMBACH, C., HAUSLAGE, J., SCHÄFER, C. & BRAUN, M. (2005): How to activate a plant gravireceptor. Early mechanisms of gravity sensing studied in characean rhizoids during parabolic flights. Plant physiol, 139, 1-11.

LIMBACH, C., STAEHELIN, L., SIEVERS, A. & BRAUN, M. (2008): Electron tomographic characterization of a vacuolar reticulum and of six vesicle types that occupy different cytoplasmic domains in the apex of tip-growing Chara rhizoids. Planta, 227, 1101-1114.

LU, Y.T. & Feldman, L.J. (1997): Light-regulated root gravitropism: a role for, and characterization of, a calcium/calmodulin-dependent protein kinase homolog. Planta, 203, 91-97.

MA, Z. & HASENSTEIN, K. (2005): The onset of gravisensitivity in the embryonic root of flax. Plant Phys, 140, 159-166.

MACCLEERY, S. & KISS, J.Z. (1999): Plastid sedimentation kintetics in roots of wild-type and starch-deficient mutants of Arabidopsis. Plant physiol, 120, 183-192.

MADLUNG, A., BEHRINGER, F. & LOMAX, T. (1999): Ethylene plays multiple nonprimary roles in modulating the gravitropic response in tomato. Plant physiolol, 120, 897-906.

MARTZIVANOU, M. & HAMPP, R. (2003): Hyper-gravity effects on the Arabidopsis transcriptome. Physiol Plant, 118, 221-231.

MARTZIVANOU, M., BABBICK, M., COGOLI-GREUTER, M. & HAMPP, R. (2006): Microgravity-related changes in gene expression after short-term exposure of Arabidopsis thalana cell cultures. Protoplasma, 229, 155-162.

MIURA, E., KATO, Y. & SAKAMOTO, W. (2010): Comparative transcriptome analysis of green/white variegated sectors in Arabiodpsis yellow variegated2: responses to oxidative and other stresses in white sectors. J Exp Bot, April, 1-13.

MOSEYKO, N., ZHU, T., CHANG, H., WANG, X. & FELDMANN, L. (2002): Transcription profiling of the early gravitropic response in Arabidopsis using high-density oligonucleotide probe microarrays. Plant Physiol, 130, 720-728.

MUDAY, G.K. (2001): Auxin and tropisms. J Plant Growth Regul, 20, 226-243.

NĚMEC, B. (1900): Über die Art der Wahrnehmung des Schwerkraftreizes bei den Pflanzen. Ber. Dtsche. Bot. Ges., 18, 241-245.

NICK, P., GODBOLE, R. & WANG, Q. (1997): Probing rice gravitropism with cytoskeletal drugs and cytoskeletal mutants. Biol bull, 192, 141-143.

OTTENSCHLÄGER, I., WOLFF, P., WOLVERTON, C., BHALERAO, R., SANDBERG, G., ISHIKAWA, H., EVANS, M. & PALME, K. (2003): Gravity-regulated differential auxin transport from columella to lateral root cap cells. PNAS, 100(5), 2987-2991.

PALMIERI, M. & KISS, J. (2005): Disruption of the F-actin cytoskeleton limits statolith movement in Arabidopsis hypocotyls. J Exp Bot, 56(419), 2539-2550.

PAUL, A., DAUGHERTY, C., BIHN, E., CHAPMAN, D., NORWOOD, K. & FERL, R. (2001): Transgene expression patterns indicate that spaceflight affects stress signal perception and transduction in Arabidopsis. Plant Physiol, 126, 613-621.

PAUL, A., POPP, M., GURLEY, W., GUY, C., NORWOOD, K. & FERL, R. (2005): Arabidopsis gene expression patterns are altered during spaceflight. Adv Space Res, 36, 1175-1181.

PERBAL, G. & DRISS-ECOLE, D. (2003): Mechanotransduction in gravisensing cells. Trends in Plant Science, 8(10), 498-504.

PERERA, I., HEILMANN, I., CHANG, S., BOSS, W. & KAUFMANN, P. (2001): A role for inositol 1,4,5-trisphosphate in gravitropic signaling and the retention of cold-perceived gravistimulation of oat shoot pulvini. Plant Physiol, 125, 1499-1507.

PERERA, I., HUNG, C., BRADY, S., MUDAY, G. & BOSS, W. (2006): A universal role for inositol 1,4,5-trisphosphate-mediated signaling in plant gravitropism. Plant Physiol, 140, 746-760.

PLIETH, C. & TREWAVAS, A. (2002): Reorientation of seedlings in the earth's gravitational field induces cytosolic calcium transients. Plant physiol, 129, 786-796.

SACK, F.D., SUYEMOTO, M.M., & LEOPOLD A.C. (1986): Amyloplast sedimentation and organelle saltation in living corn columella cells. Am J Bot, 73, 1692–1698.

SACKS, J. von (1887): Lectures on the physiology of plants. Translated by MARSHALL WARD, H. Oxford Clarendon Press.

SAITO, C., MORIITA, M., KATO, T. & TASAKA, M. (2005): Amyloplasts and vacuolar membrane dynamics in the living grarvipercepti-ve cell of the Arabidopsis inflorescence stem. Plant Cell, 17, 548-558.

SALMI, M. & ROUX, S. (2008): Gene expression changes induced by space flight in single-cells of the fern Ceratopteris richardii. Planta, 229, 151-159.

SCHMIDT, W. (2004): Quickly changing acceleration forces (QCAFs) vibration analysis on the A300 Zero-G. Microgravity Sci Technol, 15(1), 42-48.

SCHRÖTER, K., LÄUCHLI, A. & SIEVERS, A. (1975): Mikroanalytische Identifikation von Bariumsulfat-Kristallen in den Satolithen der Rhizoide von Chara fragilis, Desv Planta, 122, 213-225.

SCOTT, A. & STRÖMGREN ALLEN, N. (1999): Changes in cytosolic pH within Arabidopsis root columella cells play a key role in the early signaling pathway for root gravitropism. Plant Physiol, 121, 1291-1298.

SIEVERS, A. & VOLKMANN, D. (1972): Verursacht differentieller Druck der Amyloplasten auf ein komplexes Endomembransystem die Geoperzeption in Wurzeln? Planta, 102, 160–172.

SIEVERS, A. & VOLKMANN, D. (1977): Ultrastructure of gravity-perceiving cells in plant roots. Proceedings of the Royal Society of London. Series B, Biological Sciences, 199, 525-536.

SIEVERS, A.; HEINEMANN, B. & RODRIGUEZ-GARCIA, M.I. (1979): Nachweis des subapikalen differenziellen Flankenwachstums im Chara-Rhizoid während der Graviresponse. Zeitschr Pflanzenphysiol, 91, 435-442.

SIEVERS, A. & HEYDER-CASPERS, L. (1983): The effect of centrifugal accelerations on the polarity of statocytes and on the graviperception of cress roots. Planta, 157, 64-70.

SIEVERS, A., KRUSE, S., KUO-HUANG, L. & WENDT, M. (1989): Statoliths and microfilaments in plant cells. Planta, 179, 275-278.

SIEVERS, A., BUCHEN, B., VOLKMANN, D. & HEJNOWICZ, Z. (1991): Role of the cytoskeleton in gravity perception. Academic Press, London, 169-182.

SIEVERS, A. & HEJNOWICZ, Z. (1992): How well does the clinostat mimic the effect of microgravity on plant cells and organs? ASGSB Bull, 5, 69-75.

SIEVERS, A; HODICK, D. & BUCHEN, B. (1996): Gravity sensing in tip-growing cells. Trends Plant Sci, 1, 273-279.

SIEVERS, A., BRAUN, M. & MONSHAUSEN, G.B. (2002): Root cap: structure and function. In: WAISEL, Y. et al. (eds) Plant roots - the hidden half. Ed 3. Marcel Dekker, New York, 33-47.

SOGA, K., WAKABAYASHI, K., KAMISAKA, S. & HOSON, T. (2004): Graviperception in growth inhibition of plant shoots under hypergravity conditions produced by centrifugation is independent of that in gravitropism and may involve mechanoreceptors. Planta, 218, 1054–1061.

VOLKMANN, D. & SIEVERS, A. (1979): Graviperception in multicellular organs. In: HAUPT, W. & FEINLEIB, M.E., Editors, Encycl Plant Physiol N.S., Springer, Berlin, 7, 573–600.

VOLKMANN, D., BUCHEN, B., HEJNOWICZ, Z., TEWINKEL, M. & SIEVERS, A. (1991): Oriented movement of statoliths studied in a reduced gravitational field during parabolic flights of rockets. Planta, 185, 153-161.

WALLEY, J., KELLEY, D., NESTOROVA, G., HIRSCHBERG, D. & DEHESH, K. (2010): Arabidopsis deadenylases AtCAF1a and AtCAF1b play overlapping and distinct roles in mediating environmental stress responses. Plant physiol, 152, 866-875.

WANG, H., ZHENG, H.Q., SHA, W., ZENG, R. & Xia, Q.C. (2006): A proteomic approach to analysing responses of Arabidopsis thaliana callus cells to clinostat rotation. J Exp Bot, 57, 8274-835.

WEISE, S.E. & Kiss, J.Z. (1999): Gravitropism of inflorescence stems in starch-deficient mutants of Arabidopsis. Int J Plant Sci, 160, 521-527.

WEISE, S.E., KUZNETSOV, O.A., HASENSTEIN, K.H. & Kiss, J.Z. (2000): Curvature in Arabidopsis inflorescences stem is limited to the region of amyloplast displacement. Plant Cell Physiol, 41, 702-709.

WENDT, M., KUO-HUANG, L. & SIEVERS, A. (1987): Gravitropic bending of cress roots without contact between amyloplasts and complexes of endoplasmic reticulum. Planta, 172, 321-329.

WENT, F. (1928): Wuchstoff und Wachstum. Rec Trav Bot Neerl, 25, 1-116.

YAMAMOTO, K. & KISS, J. (2002): Disruption of the actin cytoskeleton results in the promotion gravitropism in inflorescence stems and hypocotyls of Arabidopsis. Plant Physiol, 128, 669-681.

YODER, T., ZHEN, H., TODD, P. & STAEHELIN, A. (2001): Amyloplast sedimentation dynamics in maize columella cells support a new model for the gravity-sensing apparatus of roots. Plant Physiol, 125, 1045-1060.

ZHENG, H. & STAEHELIN, L. (2001): Nodal endoplasmic reticulum, a specialized form of endoplasmic reticulum found in gravity-sensing root tip columella cells. Plant Physiol, 125, 252-265.

7.2 Web sources

TAIR databases, Bulk Data Retrieval, GO annotations.
URL: http://www.arabidopsis.org/tools/bulk/go/index.jsp

8. APPENDIX

8.1 Experiment overview

Table III. Overview about all flight and ground experiments peformed for the analyses on gravity-dependent gene expression in plants (see 2.3.2). Numerous biological replicates of the same experimental conditons were analyzed to achieve good reproducibility of the experiments. Samples were hybridized on seperate slides (technical replicates). One Arabidopsis thaliana slide provided 4 arrays (4x 44K slide format, Agilent Technologies, Germany). The Arabidopsis seedlings for all experiments were cultivated from 3 different harvests.

icons	experiment conditions	biological replicates	set of seeds (harvests)	technical replicates
	0° 2h 1*g* (control)	A7.1	1	slide 1, array 1
		A6.1	1	slide 2, array 1
		A2.2	2	slide 5, array 1
		A2.3	3	slide 7, array 1
		A3.3	3	slide 7, array 2
	90° 2h 1*g*	B6.1	1	slide 1, array 2
		B1.1	1	slide 2, array 2
		B3.2	2	slide 3, array 1
		B4.2	2	slide 5, array 2
		B1.3	3	slide 7, array 3
		B3.3	3	slide 7, array 4
	0° 62x 20s 2*g* in 2h 1*g*	C6.1	1	slide 1, array 3
		C1.1	1	slide 2, array 3
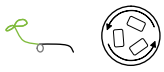	90° 62x 20s 2*g* in 2h 1*g*	E1.2	2	slide 10, array 1
		E2.2	2	slide 10, array 2
		E3.2	2	slide 10, array 3
	90° 2h 2*g*	G1.2	2	slide 10, array 4
		G3.3	3	slide 9, array 1
	90° 31x 10s inversion (inv) in 2h 1*g*	D2.1	1	slide 1, array 4
		D1.1	1	slide 2. array 4
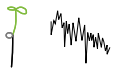	0° 2h vibrations in 2h 1*g*	V1.3	3	slide 9, array 2
		V2.3	3	slide 9, array 3
		V3.3	3	slide 9, array 4
	0° 2h flight, 31 parabolas (µ*g*, 1*g*, 2*g*)	F(31P)-a-FD1	1	slide 3, array 2
		F(31P)-b-FD1	1	slide 5, array 3
		F(31P)-FD2	1	slide 4, array 1
		F(31P)-FD3	2	slide 6, array 1
	0° 1h flight, 11 parabolas (µ*g*, 1*g*, 2*g*)	F(11P)-FD5	2	slide 3, array 4
		F(11P)-FD6	3	slide 6, array 3
	0° 2h in-flight control, 31 parabolas (1*g*, 2*g*)	IFC(31P)-a-FD1	1	slide 3, array 3
		IFC(31P)-b-FD1	1	slide 5, array 4
		IFC(31P)-FD2	1	slide 4, array 2
		IFC(31P)-FD3	2	slide 6, array 2
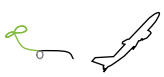	90° 1h flight, 11 parabolas (µ*g*, 1*g*, 2*g*)	F(11P)-FD5-90°	2	slide 3, array 4
		F(11P)-FD6-90°	3	slide 6, array 4

8.2 Gravitropism-related genes – annotations and normalized values

Table IV (pp 88 - 95). Normalized intensity values of the 353 gravitropism-related genes which were differentially expressed due to stimulation by 90° reorientation on ground. The fold change (FC) denotes the ratio of intensity value of the respective treatement to vertical control at 1*g* (0° 2h 1*g*). Annotation details (description and other names) sourced by TAIR.

		normalized intensity values		FC	normalized intensity values		FC		
functional category	At No.	control 0° 2h 1*g*	exp. 90° 31x inv in 2h 1*g*	exp. vs. control	control 0° 2h 1*g*	exp. 0° 2h flight	exp. vs. control	description	other names
DNA metabolism	At1g74660	1.47	-0.03	**-2.83**	1.47	-0.40	**-3.67**	zinc finger homeobox family protein	F1M20.34, MIF1
	At5g26170	-1.22	1.16	**5.20**	-1.22	0.00	**2.34**	WRKY family transcription factor	
	At5g52020	0.93	-1.03	**-3.88**	0.93	-0.56	**-2.80**	AP2 domain-containing protein	MSG15.10
	At2g25820	1.68	-0.09	**-3.41**	1.68	-2.00	**-12.80**	transcription factor, putative similar to TINY	F17H15.15
	At5g22630	0.76	-1.42	**-4.51**	0.76	-0.84	**-3.03**	prephenate dehydratase family protein	ADT5, MDJ22.5
	At2g44940	1.01	-0.94	**-3.88**	1.01	-0.48	**-2.82**	AP2 domain-containing transcription factor TINY	T13E15.25
	At4g28530	0.91	-2.34	**-9.53**	0.91	-0.88	**-3.47**	no apical meristem (NAM) family protein	F17H15.15
	At5g11190	-2.17	0.55	**6.62**	-2.17	0.30	**5.57**	AP2 domain-containing transcription factor	F2I11.80, SHINE3, SHN3
	At1g14490	1.43	-0.14	**-2.97**	1.43	-0.58	**-4.02**	DNA-binding protein-related	F14L17.27
	At4g20970	-1.32	0.40	**3.30**	-1.32	-0.07	**2.39**	basic helix-loop-helix (bHLH) family protein	T13K14.130
	At2g29660	0.99	-0.35	**-2.52**	0.99	-0.24	**-2.35**	zinc finger (C2H2 type) family protein	T27A16.24
	At1g68360	1.17	-0.65	**-3.52**	1.17	-0.47	**-3.10**	similar to zinc finger protein	F14L17.27
	At3g60530	0.95	-0.51	**-2.74**	0.95	-0.47	**-2.67**	identical to cDNA for GATA transcription factor 4	T13K14.130
	At2g47900	0.55	-0.82	**-2.58**	0.55	-0.47	**-2.02**	F-box family protein	ATTLP3, F17A22.29
	At4g01460	-0.69	0.42	**2.15**	-0.69	0.44	**2.19**	basic helix-loop-helix (bHLH) family protein	F11O4.13
	At5g39610	0.89	-0.63	**-2.86**	0.89	-0.38	**-2.40**	no apical meristem (NAM) family protein	ANAC092, ATNAC2, ATNAC6
	At1g76410	1.10	-0.98	**-4.24**	1.10	-0.74	**-3.58**	zinc finger (C3HC4-type RING finger) protein	ATL8, F15M4.9
	At1g67970	-0.64	1.32	**3.90**	-0.64	0.65	**2.45**	heat shock factor protein, putative (HSF5)	AT-HSFA8, HSFA8, T23K23.18
	At4g12080	0.87	-0.61	**-2.79**	0.87	-0.65	**-2.87**	DNA-binding family protein (AT hook motif)	AHL1, ATAHL1, F16J13.150
	At4g27310	1.54	-1.03	**-5.92**	1.54	-0.56	**-4.28**	zinc finger (B-box type) family protein	M4I22.120
	At5g49700	1.40	-0.16	**-2.96**	1.40	-0.65	**-4.16**	DNA-binding protein	K2I5.6
	At5g23730	0.92	-0.48	**-2.63**	0.92	-0.39	**-2.48**	WD-40 repeat family protein	MRO11.23
	At5g59550	1.00	-0.36	**-2.57**	1.00	-0.25	**-2.37**	zinc finger (C3HC4-type RING finger) protein	F2O15.22
	At1g67370	-1.15	0.59	**3.33**	-1.15	0.05	**2.29**	meiotic asynaptic mutant 1 (ASY1)	ASY1, ATASY1,F1N21.19
	At3g09160	-0.81	0.30	**2.15**	-0.81	0.64	**2.72**	RNA recognition motif (RRM)-containing protein	
	At1g47655	1.17	-0.54	**-3.28**	1.17	0.02	**-2.22**	Dof-type zinc finger domain-containing protein	
	At4g31640	-1.34	0.75	**4.24**	-1.34	0.37	**3.26**	transcriptional factor B3 family protein	
	At1g67030	1.07	-1.03	**-4.29**	1.07	-0.01	**-2.12**	zinc finger (C2H2 type) family protein (ZFP6)	F1O19.8, ZFP6
	At3g56970	-2.49	-0.07	**5.33**	-2.49	2.40	**29.58**	basic helix-loop-helix (bHLH) family protein	BHLH038, ORG2, T8M16.7
	At5g16350	-1.10	1.09	**4.57**	-1.10	0.04	**2.21**	expressed protein	MQK4.7
	At1g62910	-1.08	0.18	**2.40**	-1.08	0.07	**2.22**	pentatricopeptide (PPR) protein	F16P17.6
	At4g11400	-0.76	1.54	**4.93**	-0.76	0.44	**2.29**	ARID/BRIGHT DNA-binding protein	F25E4.20
	At5g43200	0.66	-1.19	**-3.60**	0.66	-1.66	**-4.98**	zinc finger (C3HC4-type RING finger) protein	MNL12.2
	At2g40520	-1.10	0.24	**2.53**	-1.10	0.51	**3.05**	nucleotidyltransferase family protein	T2P4.13
	At3g20475	-1.39	0.01	**2.63**	-1.39	0.48	**3.65**	DNA mismatch repair MutS family protein	ATMSH5, MQC12.27, MSH5
	At4g17800	1.58	-0.97	**-5.84**	1.58	-0.35	**-3.80**	DNA-binding protein	DL4935C, FCAALL.129
	At2g37060	1.09	-0.14	**-2.36**	1.09	-0.29	**-2.60**	CCAAT-box binding transcription factor	T2P4.13
	At4g31900	0.23	1.94	**3.27**	0.23	-1.46	**-3.23**	chromatin remodeling factor CHD3 (PICKLE)	F11C18.100, PKR2
	At5g44260	1.27	-1.26	**-5.78**	1.27	-0.97	**-4.73**	zinc finger (CCCH-type) family protein	K9L2.1
	At3g60080	1.25	-0.61	**-3.62**	1.25	-0.45	**-3.25**	zinc finger (C3HC4-type RING finger) protein	T2O9.60
	At1g14200	1.21	-0.64	**-3.61**	1.21	-0.52	**-3.32**	zinc finger (C3HC4-type RING finger) protein	F7A19.29

functional category	At No.	normalized intensity values: control 0° 2h 1*g*	normalized intensity values: exp. 90° 31x inv in 2h 1*g*	FC: exp. vs. control	normalized intensity values: control 0° 2h 1*g*	normalized intensity values: exp. 0° 2h flight	FC: exp. vs. control	description	other names
DNA metabolism	At5g43190	1.01	-0.34	**-2.56**	1.01	-0.45	**-2.74**	F-box family protein (FBX6)	MNL12.1
	At1g75080	0.67	-0.46	**-2.18**	0.67	-0.46	**-2.18**	brassinosteroid signaling positive regulator	BZR1, F9E10.7
signaling	At4g27260	0.69	-0.97	**-3.16**	0.69	-0.50	**-2.29**	auxin-responsive GH3 family protein	GH3.5, M4I22.70, WES1
	At4g27450	0.85	-0.41	**-2.40**	0.85	-0.34	**-2.28**	auxin down-regulated protein ARG10	F27G19.50
	At2g45210	1.04	-0.83	**-3.64**	1.04	-0.55	**-3.00**	auxin-responsive protein-related	F4L23.28
	At1g43040	1.42	-0.87	**-4.90**	1.42	-0.57	**-3.96**	auxin-responsive protein	F2H10.1
	At5g47530	1.03	-1.41	**-5.41**	1.03	-0.43	**-2.73**	auxin-responsive protein	MNJ7.12
	At1g72430	1.14	-0.52	**-3.14**	1.14	-0.09	**-2.34**	auxin-induced protein TGSAUR22	T10D10.10
	At5g59940	0.84	-0.61	**-2.74**	0.84	-0.42	**-2.39**	UV-B light-insensitive protein	
	At1g14920	0.99	-0.81	**-3.49**	0.99	-0.49	**-2.80**	gibberellin response modulator (GAI) (RGA2)	
	At1g55430	0.86	-2.39	**-9.49**	0.86	-0.55	**-2.65**	DC1 domain-containing protein	T5A14.18
	At2g44840	1.20	0.20	**-2.01**	1.20	-0.49	**-3.24**	ethylene-responsive element-binding protein	ATERF13, EREBP, ERF13
	At4g36580	-0.86	1.28	**4.40**	-0.86	0.54	**2.65**	AAA-type ATPase family protein	AP22.32
	At2g34650	1.12	-0.53	**-3.15**	1.12	-0.43	**-2.94**	protein kinase PINOID (PID)	ABR, PINOID, T31E10.1
	At5g25350	1.52	-0.20	**-3.29**	1.52	-0.36	**-3.68**	F-box family protein	EBF2, F18G18.90
	At1g66145	0.56	-0.59	**-2.23**	0.56	-1.58	**-4.41**	CLAVATA3/ESR-Related 18 (CLE18)	CLE18
	At3g46890	1.49	-1.04	**-5.79**	1.49	-0.42	**-3.75**	hypothetical protein F2I9.20	T6H20.80
	At4g08620	0.87	-3.27	**-17.63**	0.87	-0.24	**-2.16**	sulfate transporter	SULTR1.2
	At4g37580	1.59	-0.30	**-3.69**	1.59	-1.23	**-7.03**	N-acetyltransferase, putative / hookless1 (HLS1)	COP3, F19F18.70, HLS1
	At1g66830	-0.93	0.33	**2.39**	-0.93	0.38	**2.48**	leucine-rich repeat transmembrane protein	F4N21.23
	At3g02880	0.85	-0.69	**-2.91**	0.85	-0.58	**-2.69**	leucine-rich repeat transmembrane protein	F13E7.17
	At4g34930	0.98	-0.70	**-3.23**	0.98	-0.16	**-2.20**	1-phosphatidylinositol phosphodiesterase	
	At3g04720	0.99	-0.81	**-3.48**	0.99	-0.51	**-2.83**	hevein-like protein (HEL)	F7O18.21, HEL, PR-4
	At2g42060	1.04	0.04	**-2.01**	1.04	-0.99	**-4.08**	CHP-rich zinc finger protein	T6D20.5
	At5g65800	0.79	-0.77	**-2.93**	0.79	-0.43	**-2.32**	1-aminocyclopropane-1-carboxylate synthase	ACS5, CIN5, ETO2, MPA24.15
	At1g71090	0.93	-0.48	**-2.66**	0.93	-0.16	**-2.13**	auxin efflux carrier family protein	F23N20.8
	At5g02060	1.32	-0.73	**-4.15**	1.32	-0.45	**-3.41**	ethylene responsive element binding protein	T7H20.110
	At5g24470	-0.76	0.58	**2.54**	-0.76	0.90	**3.17**	pseudo-response regulator 5 (APRR5)	APRR5, PRR5, T31K7.5
stress / defense response	At4g27320	1.24	-0.17	**-2.65**	1.24	-0.02	**-2.39**	universal stress protein (USP) family protein	ATPHOS34, M4I22.130, PHOS34
	At3g62550	-1.17	0.57	**3.34**	-1.17	0.99	**4.47**	universal stress protein (USP) family protein	T12C14.250
	At5g42510	1.92	-2.70	**-24.50**	1.92	-0.56	**-5.58**	disease resistance-responsive family protein	MDH9.21
	At3g13950	1.10	-0.69	**-3.46**	1.10	-0.43	**-2.90**	expressed protein	MDC16.7
	At3g30390	1.17	-0.75	**-3.76**	1.17	-0.65	**-3.51**	amino acid transporter family protein	T6J22.19
	At3g23240	1.63	0.09	**-2.91**	1.63	-0.49	**-4.33**	ethylene response factor 1 (ERF1)	ATERF1, ERF1, K14B15.4
	At1g30660	-1.37	0.72	**4.25**	-1.37	-0.25	**2.17**	toprim domain-containing protein	T5I8.11
	At3g47420	1.55	-1.21	**-6.77**	1.55	-0.84	**-5.21**	glycerol-3-phosphate transporter	ATPS3, T21L8.170
	At1g61070	1.35	-0.04	**-2.61**	1.35	0.02	**-2.51**	plant defensin-fusion protein (PDF2.4)	LCR66, PDF2.4, T7P1.20
	At3g15700	1.14	-1.11	**-4.76**	1.14	-0.07	**-2.32**	NBS/LRR disease resistance protein	LCR66, PDF2.4,T7P1.20
	At5g44900	1.01	-0.52	**-2.90**	1.01	-0.40	**-2.66**	disease resistance protein (TIR class)	K21C13.8
	At4g11650	0.81	-0.94	**-3.37**	0.81	-0.65	**-2.75**	osmotin-like protein (OSM34)	ATOSM34, OSMOTIN 34, T5C23.80
	At1g78210	-0.92	0.57	**2.82**	-0.92	0.27	**2.29**	hydrolase, alpha/beta fold family protein	T11I11.15
	At3g05370	-1.66	1.11	**6.81**	-1.66	0.99	**6.24**	disease resistance family protein	
	At5g43740	-0.67	0.99	**3.16**	-0.67	0.66	**2.52**	disease resistance protein (CC-NBS-LRR class)	MQD19.7
	At5g22410	1.03	-1.91	**-7.65**	1.03	-0.39	**-2.66**	peroxidase ATP14a	MWD9.21, RHS18
	At1g13860	-0.99	0.17	**2.23**	-0.99	0.34	**2.51**	dehydration-responsive protein	F16A14.7
	At5g42500	1.44	-2.72	**-17.87**	1.44	-1.05	**-5.61**	disease resistance-responsive family protein	MDH9.20
	At5g36270	1.10	-2.57	**-12.74**	1.10	-0.52	**-3.08**	dehydroascorbate reductase	T30G6.13

functional category	At No.	normalized intensity values: control 0° 2h 1*g*	normalized intensity values: exp. 90° 31x inv in 2h 1*g*	FC: exp. vs. control	normalized intensity values: control 0° 2h 1*g*	normalized intensity values: exp. 0° 2h flight	FC: exp. vs. control	description	other names
stress / defense response	At5g51270	1.00	-1.02	**-4.05**	1.00	-0.49	**-2.82**	protein kinase family protein	MWD22.22
	At1g05250	1.44	-1.81	**-9.53**	1.44	-0.32	**-3.39**	peroxidase ATP11a	YUP8H12.14
	At4g22212	1.60	-2.10	**-12.97**	1.60	-0.66	**-4.79**	expressed protein	
	At1g05240	1.65	-1.84	**-11.24**	1.65	-0.39	**-4.11**	peroxidase ATP11a	YUP8H12.15
	At2g28670	1.14	-1.80	**-7.66**	1.14	-0.78	**-3.77**	disease resistance-responsive family protein	T8O18.4
	At4g33730	1.53	-2.93	**-22.12**	1.53	-0.63	**-4.47**	pathogenesis-related protein	T16L1.220
	At5g40020	0.80	-0.67	**-2.76**	0.80	-0.83	**-3.10**	pathogenesis-related thaumatin family protein	MYH19.180
transporter activity	At1g16370	1.30	-0.03	**-2.51**	1.30	-0.50	**-3.48**	similarity to organic cation transporter OCTN1	ATOCT6, F3O9.17, OCT6
	At3g01930	1.08	-0.99	**-4.22**	1.08	-0.91	**-3.97**	nodulin family protein	F28J7.26
	At3g29590	-1.41	0.01	**2.68**	-1.41	0.93	**5.07**	transferase family protein	AT5MAT, MTO24.5
	At5g43370	1.88	-0.92	**-6.99**	1.88	-1.04	**-7.56**	inorganic phosphate transporter (PHT2)	APT1, MWF20.6, PHT2
	At3g20460	0.72	-2.25	**-7.83**	0.72	-0.40	**-2.17**	sugar transporter	MQC12.5
	At1g31820	1.29	-0.57	**-3.63**	1.29	-0.27	**-2.94**	similarity to asc-type amino acid transporter 2	F16B22.32, UCC2
	At2g44790	1.54	-1.34	**-7.36**	1.54	-1.40	**-7.68**	uclacyanin II	F16B22.32, UCC2
	At4g14030	0.73	-0.49	**-2.32**	0.73	-0.56	**-2.43**	selenium-binding protein	DL3055C, FCAALL.79, SBP1
	At5g09950	-1.34	0.20	**2.90**	-1.34	0.48	**3.54**	pentatricopeptide (PPR) protein	MYH9.16
	At3g05165	0.72	-0.30	**-2.04**	0.72	-0.74	**-2.75**	sugar transporter	
	At4g25640	1.06	-0.50	**-2.95**	1.06	-0.09	**-2.22**	MATE efflux family protein	ATDTX35, FFT, L73G19.20
	At1g08070	-1.10	0.55	**3.13**	-1.10	0.22	**2.49**	pentatricopeptide (PPR) protein	OTP82, T6D22.15
	At3g27290	-0.90	0.28	**2.25**	-0.90	0.28	**2.25**	F-box family protein-related	K17E12.11
	At5g60660	1.88	-2.29	**-18.09**	1.88	-0.84	**-6.60**	major intrinsic family protein	PIP24, PIP2F, mup24.9
	At1g80760	0.74	-0.58	**-2.50**	0.74	-0.60	**-2.52**	major intrinsic family protein	AtNIP6, F23A5.11, NIP6,NLM7
	At2g32270	1.37	-1.56	**-7.63**	1.37	-1.47	**-7.16**	zinc transporter (ZIP3)	T32F6.21, ZIP3
	At5g43350	1.81	-0.79	**-6.07**	1.81	-0.89	**-6.52**	inorganic phosphate transporter (PHT1)	ATPT1, MWF20.4, PHT1 1
	At4g30700	-0.91	0.63	**2.92**	-0.91	0.35	**2.40**	pentatricopeptide (PPR) protein	T10C21.50
	At4g19680	1.61	-4.25	**-58.39**	1.61	-0.93	**-5.81**	iron-responsive transporter (IRT2)	ATIRT2, IRT2, T16H5.40
	At4g15720	-0.93	0.57	**2.83**	-0.93	0.38	**2.48**	pentatricopeptide (PPR) protein	DL3900W, FCAALL.369
	At1g48640	0.99	-0.82	**-3.50**	0.99	-0.35	**-2.53**	lysine and histidine specific transporter	F11I4.17
	At2g39130	0.74	-0.38	**-2.17**	0.74	-0.36	**-2.15**	amino acid transporter family protein	T7F6.1
cell wall modification	At2g20520	1.16	-2.35	**-11.39**	1.16	-0.47	**-3.09**	fasciclin-like arabinogalactan-protein (FLA6)	FLA6, T13C7.11
	At5g44130	1.50	-0.05	**-2.92**	1.50	-0.04	**-2.91**	fasciclin-like arabinogalactan-protein	FLA13, MLN1.5
	At3g55820	-0.74	0.94	**3.20**	-0.74	0.44	**2.27**	hypothetical protein	F1I16.230
	At3g16920	0.69	-0.59	**-2.44**	0.69	-0.86	**-2.93**	glycoside hydrolase family 19 protein	ATCTL2, CTL2, K14A17.26
	At3g10960	1.30	-0.64	**-3.81**	1.30	-0.26	**-2.93**	xanthine/uracil permease family protein	ATAZG1, AZG1, F9F8.22
	At3g10710	1.09	-1.90	**-7.96**	1.09	-0.70	**-3.47**	pectinesterase family protein	RHS12, T7M13.21
	At5g57070	0.98	-0.93	**-3.76**	0.98	-0.38	**-2.57**	hydroxyproline-rich glycoprotein family protein	RHS12, T7M13.21
lipid metabolism	At4g22460	1.51	-1.77	**-9.73**	1.51	-1.18	**-6.45**	lipid transfer protein (LTP) family protein	F7K2.40
	At2g18370	1.56	-2.30	**-14.46**	1.56	-1.11	**-6.35**	lipid transfer protein (LTP) family protein	T30D6.12
	At3g22570	0.81	-1.51	**-4.97**	0.81	-0.45	**-2.38**	lipid transfer protein (LTP) family protein	F16J14.13
	At1g45201	0.58	-1.46	**-4.09**	0.58	-0.52	**-2.13**	lipase class 3 family protein	ATTLL1, TLL1
	At1g28590	1.03	-1.51	**-5.84**	1.03	-0.33	**-2.57**	lipase	F1K23.17
protein metabolism	At3g07070	1.14	-2.54	**-12.81**	1.14	-0.45	**-3.02**	protein kinase family protein	F17A9.25
	At4g25240	0.79	-1.02	**-3.51**	0.79	-0.59	**-2.60**	multi-copper oxidase type I family protein	F24A6.80, SKS1
	At3g17790	0.96	-1.62	**-5.97**	0.96	-0.79	**-3.35**	acid phosphatase type 5 (ACP5)	ATACP5, ATPAP17, MEB5.10, PAP17

functional category	At No.	normalized intensity values: control 0° 2h 1*g*	normalized intensity values: exp. 90° 31x inv in 2h 1*g*	FC: exp. vs. control	normalized intensity values: control 0° 2h 1*g*	normalized intensity values: exp. 0° 2h flight	FC: exp. vs. control	description	other names
other	At4g23530	1.11	-0.54	**-3.14**	1.11	-0.09	**-2.29**	expressed protein	F16G20.230
	At1g54530	1.02	-1.02	**-4.10**	1.02	-0.39	**-2.66**	calcium-binding EF hand family protein	F20D21.45
	At5g28150	0.94	-0.18	**-2.17**	0.94	-0.14	**-2.12**	expressed protein	ATACP5, ATPAP17, MEB5.10, PAP17
	At5g14670	2.30	-0.97	**-9.67**	2.30	0.07	**-4.72**	ADP-ribosylation factor	ATARFA1B, T15N1.160
	At2g27610	-1.03	1.04	**4.21**	-1.03	0.38	**2.66**	pentatricopeptide (PPR) protein	F15K20.29
	At4g22970	-1.10	0.11	**2.31**	-1.10	-0.08	**2.04**	peptidase C50 family protein	AESP, ESP, F7H19.150, RSW4
	At1g18970	1.76	-0.91	**-6.38**	1.76	-0.68	**-5.45**	germin-like protein (GLP1) (GLP4)	F14D16.12, GLP4
	At1g18980	1.62	-1.63	**-9.51**	1.62	-0.81	**-5.39**	germin-like protein	F14D16.13
	At5g64900	0.66	-1.21	**-3.67**	0.66	-0.56	**-2.33**	expressed protein	ATPEP1, MXK3.13, PEP1, PROPEP1
	At1g18350	2.52	-0.17	**-6.43**	2.52	0.19	**-5.01**	mitogen-activated protein kinase kinase	ATMKK7, BUD1, F15H18.14, MKK7
	At3g01900	1.20	-1.15	**-5.10**	1.20	-0.76	**-3.88**	cytochrome P450 family protein	CYP94B2, F1C9.32
	At2g34500	1.20	-1.71	**-7.50**	1.20	-1.88	**-8.44**	cytochrome P450 family protein	CYP710A1, F13P17.35
	At2g34490	0.79	-2.05	**-7.13**	0.79	-0.90	**-3.21**	cytochrome P450 family protein	ATMKK7, BUD1, F15H18.14, MKK7
	At4g39950	0.84	-0.44	**-2.43**	0.84	-0.21	**-2.08**	cytochrome P450 79B2	CYP79B2, T5J17.120
	At1g16410	-0.00	-2.43	**-5.39**	-0.00	1.78	**3.45**	cytochrome P450	
	At4g00210	1.35	-0.94	**-4.88**	1.35	-0.65	**-3.98**	lateral organ boundaries domain protein 31	F6N15.25, LBD31
enzyme activity *	At5g19930	0.95	-0.57	**-2.85**	0.95	-0.17	**-2.17**	integral membrane family protein	F6N15.25, LBD31
	At2g42530	-4.29	0.05	**20.26**	-4.29	3.45	**214.97**	cold-regulated protein (cor15b)	COR15B, F14N22.20
	At2g26740	1.17	-0.11	**-2.42**	1.17	-0.06	**-2.34**	epoxide hydrolase, ATsEH	ATSEH, F18A8.11
	At2g37450	-1.25	0.59	**3.58**	-1.25	0.87	**4.35**	nodulin MtN21 family protein similar to MtN21	F3G5.24
	At1g65570	1.46	-2.03	**-11.23**	1.46	-0.48	**-3.84**	polygalacturonase 5	F5I14.10
	At1g10760	-1.08	0.64	**3.28**	-1.08	0.95	**4.09**	starch excess protein (SEX1)	GWD1, SEX1, SOP1, T16B5.10
	At2g29750	1.06	-1.23	**-4.91**	1.06	-0.77	**-3.56**	UDP-glucosyl transferase family protein	T27A16.15, UGT71C1
	At2g02990	0.79	-0.56	**-2.55**	0.79	-0.73	**-2.87**	ribonuclease 1 (RNS1)	ATRNS1, T17M13.16
	At5g42650	0.88	-0.73	**-3.04**	0.88	-0.44	**-2.49**	cytochrome P450 74A (CYP74A)	AOS, CYP74A, DDE2
	At1g31130	1.37	-0.28	**-3.13**	1.37	-0.50	**-3.66**	expressed protein	F28K20.6
	At1g47480	1.03	-0.32	**-2.55**	1.03	-0.00	**-2.05**	expressed protein	F16N3.25
	At2g39980	1.15	-0.10	**-2.38**	1.15	-0.55	**-3.26**	transferase family protein	T28M21.14
	At2g20800	-1.13	2.09	**9.29**	-1.13	0.35	**2.78**	pyridine nucleotide-disulphide oxidoreductase	F5H14.23, NDB4
	At2g47050	-1.49	-0.39	**2.14**	-1.49	1.36	**7.21**	invertase/pectin methylesterase inhibitor	F14M4.12
	At5g26310	1.25	-2.72	**-15.65**	1.25	-1.12	**-5.19**	UDP-glucoronosyl/UDP-glucosyl transferase	F9D12.4,UGT72E3
	At4g26770	0.65	-1.37	**-4.05**	0.65	-0.39	**-2.05**	phosphatidate cytidylyltransferase	F10M23.110
	At2g40230	1.42	-0.84	**-4.80**	1.42	-0.82	**-4.75**	transferase family protein	F14M4.12
	At4g14130	0.85	-1.33	**-4.52**	0.85	-1.55	**-5.28**	xyloglucan:xyloglucosyl transferase	DL3105C, FCAALL.173, XTR7
	At5g61350	1.36	-2.08	**-10.83**	1.36	-0.72	**-4.22**	protein kinase family protein	MFB13.1
	At2g40880	-0.88	0.95	**3.56**	-0.88	0.65	**2.88**	cysteine protease inhibitor	ATCYSA, FL3-27, T20B5.8
	At3g44720	0.74	-1.06	**-3.49**	0.74	-0.80	**-2.89**	prephenate dehydratase family protein	ADT4, T32N15.11
	At3g63010	1.13	-0.55	**-3.22**	1.13	-0.56	**-3.24**	expressed protein similar to PrMC3	ATGID1B, T20O10.110
	At1g79550	1.00	-0.98	**-3.94**	1.00	-0.70	**-3.24**	phosphoglycerate kinase	PGK, T8K14.3
	At2g32400	-1.16	0.64	**3.50**	-1.16	0.46	**3.09**	glutamate receptor family protein (GLR3.7)	ATGLR3.7, GLR5, T32F6.8
	At2g32630	-1.45	0.51	**3.88**	-1.45	0.09	**2.91**	pentatricopeptide (PPR) protein	T26B15.19
	At2g34190	0.93	-0.53	**-2.75**	0.93	-0.31	**-2.36**	xanthine/uracil permease family protein	F13P17.3
	At2g25240	0.84	-1.65	**-5.61**	0.84	-0.29	**-2.19**	serine protease inhibitor	T22F11.17
	At4g25820	0.99	-1.74	**-6.62**	0.99	-0.52	**-2.85**	xyloglucan:xyloglucosyl transferase	ATXTH14, XTH14, XTR9
	At5g06570	1.01	-0.02	**-2.04**	1.01	-0.52	**-2.89**	expressed protein	F15M7.10
	At1g55290	1.04	-1.57	**-6.13**	1.04	-0.10	**-2.20**	oxidoreductase, 2OG-Fe(II) oxygenase	F7A10.24
	At1g09300	-0.67	1.11	**3.42**	-0.67	0.36	**2.04**	metallopeptidase M24 family protein	T31J12.2

* genes encoding for proteins with enzyme activities unless annotation details allowed more precise functional classification

functional category	At No.	normalized intensity values: control 0° 2h 1*g*	normalized intensity values: exp. 90° 31x inv in 2h 1*g*	FC: exp. vs. control	normalized intensity values: control 0° 2h 1*g*	normalized intensity values: exp. 0° 2h flight	FC: exp. vs. control	description	other names
enzyme activity *	At3g44520	1.14	-0.30	**-2.72**	1.14	-0.04	**-2.26**	esterase/lipase/thioesterase family protein	At5g43080
	At4g16260	0.76	-0.99	**-3.36**	0.76	-0.34	**-2.14**	glycosyl hydrolase family 17 protein	DL4170C, FCAALL.386
	At5g43080	-1.17	0.58	**3.36**	-1.17	0.11	**2.43**	cyclin, putative similar to A-type cyclins	CYCA3 1, MMG4.10
	At1g75270	0.77	-0.60	**-2.60**	0.77	-0.60	**-2.60**	dehydroascorbate reductase	DHAR2, F22H5.1
	At3g56620	0.85	-0.40	**-2.38**	0.85	-0.26	**-2.16**	integral membrane family protein	T5P19.270
	At3g60550	1.95	0.58	**-2.58**	1.95	-0.35	**-4.92**	cyclin family protein similar to cyclin 2	CYCP32, T8B10.210
	At4g26220	0.97	-1.60	**-5.91**	0.97	-0.44	**-2.65**	caffeoyl-CoA 3-O-methyltransferase	T25K17.30
	At4g15550	1.07	-0.23	**-2.48**	1.07	-0.24	**-2.49**	beta-D-glucosyltransferase (IAGLU)	DL3815C, FCAALL.103, IAGLU
	At1g35250	0.87	-2.61	**-11.18**	0.87	-0.83	**-3.24**	thioesterase family protein	T9I1.4
	At2g23910	-0.52	1.44	**3.90**	-0.52	0.66	**2.26**	cinnamoyl-CoA reductase	T29E15.11
	At1g63150	-0.83	1.47	**4.93**	-0.83	0.32	**2.22**	pentatricopeptide (PPR) protein	F16M19.13
	At1g77790	0.71	-1.25	**-3.90**	0.71	-0.66	**-2.59**	glycosyl hydrolase family 17 protein	T32E8.12
	At2g23060	1.54	-0.47	**-4.03**	1.54	-0.56	**-4.28**	GCN5-related N-acetyltransferase (GNAT)	
	At3g20015	1.64	-0.02	**-3.16**	1.64	0.22	**-2.67**	aspartyl protease family protein	MZE19.7
	At5g14310	0.64	-0.55	**-2.28**	0.64	-0.50	**-2.19**	expressed protein	ATCXE16, F18O22.100
	At5g26570	-0.84	0.57	**2.66**	-0.84	0.37	**2.31**	glycoside hydrolase starch-binding protein	ATGWD, F9D12.1,OK1, PWD
	At4g30250	-1.30	0.61	**3.78**	-1.30	0.40	**3.27**	AAA-type ATPase family protein	F9N11.100
	At3g55630	-1.08	0.50	**2.99**	-1.08	0.74	**3.54**	dihydrofolate synthetase (DHFS/FPGS4)	ATDFD, F1I16.40
	At3g04340	-0.60	0.84	**2.70**	-0.60	0.64	**2.35**	FtsH protease family protein	
	At3g29250	1.26	-1.23	**-5.62**	1.26	-0.66	**-3.79**	short-chain dehydrogenase/reductase (SDR)	MXO21.10
	At4g12830	-1.85	-0.19	**3.16**	-1.85	1.33	**9.08**	hydrolase, alpha/beta fold family protein	T20K18.180
	At5g06300	0.89	-0.80	**-3.21**	0.89	-0.30	**-2.28**	lysine decarboxylase family protein	MHF15.18
	At5g27320	0.99	-0.24	**-2.34**	0.99	-0.04	**-2.04**	expressed protein similar to PrMC3	ATGID1C, F21A20.30, GID1C
	At3g29635	1.55	-2.30	**-14.39**	1.55	-0.56	**-4.31**	transferase family protein	T13J10.13
	At1g63450	0.97	-0.96	**-3.83**	0.97	-0.18	**-2.22**	exostosin family protein	F2K11.17, RHS8
	At1g34490	1.58	-2.13	**-13.05**	1.58	-0.60	**-4.53**	membrane bound O-acyl transferase (MBOAT)	F12K21.28
	At4g15400	1.25	-0.38	**-3.10**	1.25	-0.46	**-3.28**	transferase family protein	DL3745C, FCAALL.284
	At1g49860	-1.09	1.30	**5.22**	-1.09	0.40	**2.81**	glutathione S-transferase	ATGSTF14,F10F5.9
	At1g23550	-1.12	0.34	**2.75**	-1.12	-0.11	**2.01**	expressed protein	F28C11.18, SRO2
	At4g18440	-0.90	0.86	**3.39**	-0.90	0.44	**2.52**	adenylosuccinate lyase	F28J12.100
	At5g23530	0.88	-0.85	**-3.31**	0.88	-0.84	**-3.29**	expressed protein	ATCXE18, MQM1.21
	At1g65110	-1.49	0.62	**-4.31**	-1.49	0.71	**4.58**	ubiquitin carboxyl-terminal hydrolase	T23K8.2
	At2g16530	1.03	-0.83	**-3.64**	1.03	-0.12	**-2.23**	3-oxo-5-alpha-steroid 4-dehydrogenase	F1P15.9
	At4g27010	-1.01	0.74	**3.37**	-1.01	0.33	**2.54**	expressed protein	F10M23.350
	At4g11655	1.25	-0.61	**-3.61**	1.25	-0.20	**-2.73**	transmembrane protein	
	At3g20830	0.98	-0.69	**-3.19**	0.98	-0.64	**-3.08**	protein kinase family protein	MOE17.13
	At3g19680	1.21	-0.26	**-2.76**	1.21	-0.12	**-2.52**	expressed protein	MMB12.17
	At4g27820	-1.02	0.24	**2.40**	-1.02	0.65	**3.18**	glycosyl hydrolase family 1 protein	
	At3g11810	1.04	-0.33	**-2.57**	1.04	-0.02	**-2.08**	expressed protein	F26K24.10
	At1g78990	1.52	-1.38	**-7.47**	1.52	-0.54	**-4.16**	transferase family protein	YUP8H12R.39
	At2g45610	1.44	-1.44	**-7.34**	1.44	-0.60	**-4.12**	expressed protein low similarity to PrMC3	F17K2.14
	At3g51340	-0.78	1.29	**4.20**	-0.78	0.74	**2.88**	aspartyl protease family protein	F26O13.2
	At5g03490	0.85	-1.13	**-3.94**	0.85	-0.19	**-2.05**	UDP-glucoronosyl/UDP-glucosyl transferase	F12E4.260
	At5g28930	1.31	-1.33	**-6.25**	1.31	-0.87	**-4.53**	hypothetical protein	F3F24.30
	At5g26600	0.99	-0.31	**-2.46**	0.99	-0.45	**-2.72**	expressed protein	
	At1g02570	1.60	-2.65	**-19.01**	1.60	-0.33	**-3.80**	expressed protein	T14P4.23
	At5g38610	1.52	-1.37	**-7.44**	1.52	-0.57	**-4.26**	invertase/pectin methylesterase inhibitor	MBB18.16
	At3g47090	-1.27	0.66	**3.82**	-1.27	0.60	**3.66**	leucine-rich repeat transmembrane kinase	F13I12.140

* genes encoding for proteins with enzyme activities unless annotation details allowed more precise functional classification

functional category	At No.	normalized intensity values: control 0° 2h 1*g*	normalized intensity values: exp. 90° 31x inv in 2h 1*g*	FC: exp. vs. control	normalized intensity values: control 0° 2h 1*g*	normalized intensity values: exp. 0° 2h flight	FC: exp. vs. control	description	other names
unknown	At1g07050	-1.85	0.37	**4.69**	-1.85	0.96	**7.02**	photoperiod sensitivity quantitative trait locus	Hd1, F10K1.24
	At4g34330	0.65	-1.64	**-4.88**	0.65	-0.61	**-2.39**	expressed protein similar to At14a	F10M10.100
	At2g27080	1.64	-0.27	**-3.76**	1.64	-0.22	**-3.62**	harpin-induced protein-related / HIN1	T20P8.13
	At3g09925	0.79	-1.42	**-4.61**	0.79	-0.29	**-2.11**	extensin-like protein precursor (PELP)	
	At1g50040	1.02	-1.04	**-4.19**	1.02	-0.27	**-2.44**	expressed protein	F2J10.8
	At1g13630	-1.72	0.44	**4.48**	-1.72	0.30	**4.06**	pentatricopeptide (PPR) protein	F21F23.6
	At1g75160	0.68	-1.32	**-3.99**	0.68	-0.55	**-2.34**	expressed protein	F22H5.11
	At4g02270	1.30	-1.75	**-8.30**	1.30	-0.61	**-3.75**	pollen Ole e 1 allergen and extensin	RHS13, T2H3.4
	At2g28400	1.37	-1.12	**-5.60**	1.37	-0.63	**-4.00**	expressed protein	T1B3.8
	At4g01410	1.11	-0.11	**-2.32**	1.11	-0.36	**-2.75**	harpin-induced family protein / HIN1	F3D13.5
	At1g52330	1.25	-0.43	**-3.20**	1.25	-0.31	**-2.95**	expressed protein	F19K6.6
	At2g26070	0.96	-0.43	**-2.61**	0.96	-0.56	**-2.86**	expressed protein	RTE1, T19L18.12
	At5g46680	-1.09	0.96	**4.14**	-1.09	0.36	**2.74**	pentatricopeptide (PPR) protein	MZA15.9
	At3g50130	0.93	-0.98	**-3.74**	0.93	-0.45	**-2.60**	expressed protein	F3A4.210
	At3g54040	1.23	-0.58	**-3.50**	1.23	-1.24	**-5.51**	photoassimilate-responsive protein-related	F5K20.340
	At3g57460	-0.53	1.29	**3.55**	-0.53	0.88	**2.66**	expressed protein	T8H10.60
	At5g02640	1.09	-0.62	**-3.29**	1.09	-0.50	**-3.02**	expressed protein	T22P11.230
	At3g52480	1.07	-0.29	**-2.57**	1.07	-0.36	**-2.69**	expressed protein	F22O6.140
	At5g41170	-1.50	0.73	**4.68**	-1.50	0.74	**4.74**	pentatricopeptide (PPR) protein	MEE6.24
	At5g49270	1.17	-2.11	**-9.68**	1.17	-0.71	**-3.67**	phytochelatin synthetase-related	COBL9, DER9, MRH4, SHV2
	At1g04900	-0.54	1.14	**3.21**	-0.54	0.52	**2.08**	expressed protein	F13M7.11
	At4g30320	1.12	-1.82	**-7.68**	1.12	-0.62	**-3.35**	allergen V5/Tpx-1-related family protein	F17I23.340
	At2g27180	1.15	-0.67	**-3.54**	1.15	-0.33	**-2.78**	expressed protein	T22O13.5
	At1g62720	-1.31	0.80	**4.32**	-1.31	0.61	**3.79**	pentatricopeptide (PPR) protein	F23N19.8
	At3g16690	1.56	-0.22	**-3.41**	1.56	-0.01	**-2.96**	nodulin MtN3 family protein	MGL6.16
	At5g62770	1.05	-0.18	**-2.34**	1.05	-0.12	**-2.25**	expressed protein	MQB2.9
	At5g22280	-0.74	0.52	**2.40**	-0.74	0.29	**2.04**	expressed protein	T6G21.7
	At2g18240	-0.76	0.84	**3.04**	-0.76	0.56	**2.50**	RER1 protein	T30D6.25
	At5g64980	-0.87	0.22	**2.12**	-0.87	0.25	**2.17**	expressed protein	MXK3.21
	At3g49030	-0.88	0.81	**3.21**	-0.88	0.50	**2.60**	F-box family protein	T2J13.130
	At3g53010	1.48	-0.64	**-4.36**	1.48	-0.92	**-5.28**	expressed protein	F8J2.180
	At5g46530	1.44	-0.54	**-3.94**	1.44	-0.29	**-3.32**	AWPM-19-like membrane family protein	K11I1.12
	At4g40090	1.30	-2.50	**-13.99**	1.30	-1.02	**-5.01**	arabinogalactan-protein (AGP3)	AGP3, T5J17.1
	At5g13240	0.97	-0.69	**-3.16**	0.97	-0.16	**-2.18**	expressed protein	T31B5.60
	At4g34320	0.63	-1.93	**-5.89**	0.63	-0.68	**-2.47**	expressed protein similar to At14a	F10M10.90
	At5g23030	1.54	-3.28	**-28.19**	1.54	-1.01	**-5.87**	senescence-associated family protein	MYJ24.2, TET12
	At1g72280	-0.71	0.69	**2.63**	-0.71	0.72	**2.70**	endoplasmic reticulum oxidoreductin 1 (ERO1)	ERO1, T9N14.18
	At1g32690	1.40	-0.86	**-4.81**	1.40	-0.81	**-4.63**	hypothetical protein	F6N18.23
	At4g18380	0.89	-0.38	**-2.42**	0.89	-0.23	**-2.17**	F-box family protein	F28J12.40
	At4g26320	2.02	-1.62	**-12.43**	2.02	-0.44	**-5.49**	arabinogalactan-protein (AGP13)	AGP13, T25K17.130
	At1g14150	-1.32	0.06	**2.60**	-1.32	0.62	**3.82**	oxygen evolving enhancer 3 (PsbQ)	F7A19.23
	At1g68450	1.30	-0.21	**-2.85**	1.30	-0.53	**-3.54**	VQ motif-containing protein	T2E12.4
	At3g22160	1.42	0.01	**-2.65**	1.42	-0.29	**-3.27**	VQ motif-containing protein	MKA23.7
	At3g06920	-0.81	0.56	**2.58**	-0.81	0.50	**2.48**	pentatricopeptide (PPR) protein	F17A9.7
	At1g24370	1.25	-1.52	**-6.78**	1.25	-1.17	**-5.35**	hypothetical protein	F21J9.3
	At1g79975	1.04	-0.61	**-3.16**	1.04	-0.07	**-2.16**	expressed protein	
	At3g22290	-0.86	0.58	**2.72**	-0.86	0.22	**2.12**	expressed protein	AT3G22280, MCB17.1
	At1g64580	-0.75	1.10	**3.59**	-0.75	0.29	**2.06**	pentatricopeptide (PPR) protein	F1N19.15
	At5g44140	-0.76	1.14	**3.74**	-0.76	0.25	**2.01**	prohibitin	ATPHB7, MLN1.6

functional category	At No.	normalized intensity values: control 0° 2h 1*g*	normalized intensity values: exp. 90° 31x inv in 2h 1*g*	FC: exp. vs. control	normalized intensity values: control 0° 2h 1*g*	normalized intensity values: exp. 0° 2h flight	FC: exp. vs. control	description	other names
unknown	At4g31330	1.06	-0.71	**-3.42**	1.06	-0.29	**-2.55**	expressed protein	F8F16.150
	At3g23200	1.19	-0.44	**-3.10**	1.19	-0.02	**-2.31**	expressed protein	K14B15.11
	At3g56500	1.35	-0.13	**-2.79**	1.35	-0.38	**-3.31**	serine-rich protein-related	T5P19.150
	At1g69680	0.95	-0.53	**-2.78**	0.95	-0.16	**-2.16**	expressed protein similar to MOG1 isoform A	T6C23.12
	At5g61370	-1.48	1.27	**6.74**	-1.48	0.48	**3.90**	pentatricopeptide (PPR) protein	MFB13.15
	At4g01140	0.91	-1.04	**-3.84**	0.91	-0.42	**-2.50**	expressed protein	F2N1.38
	At1g65900	-1.11	0.27	**2.59**	-1.11	0.47	**2.99**	expressed protein	F12P19.7
	At3g50340	0.78	-0.80	**-2.99**	0.78	-0.77	**-2.91**	expressed protein	
	At3g52360	1.07	-1.19	**-4.81**	1.07	-0.35	**-2.69**	expressed protein	T25B15.130
	At3g21550	1.33	-0.65	**-3.93**	1.33	-0.41	**-3.34**	expressed protein	MIL23.12
	At5g53250	2.48	-1.44	**-15.15**	2.48	-0.84	**-9.95**	arabinogalactan-protein	AGP22, K19E1.5
	At2g41160	0.86	-0.43	**-2.43**	0.86	-0.24	**-2.14**	ubiquitin-associated (UBA)	T3K9.7
	At3g13240	-1.48	1.00	**5.56**	-1.48	0.51	**3.95**	hypothetical protein	MDC11.17
	At2g20540	-1.75	0.87	**6.12**	-1.75	0.46	**4.61**	pentatricopeptide (PPR) protein	T13C7.13
	At5g24170	1.42	-0.33	**-3.37**	1.42	-0.25	**-3.19**	expressed protein	K12G2.6
	At1g07795	2.00	-2.03	**-16.29**	2.00	-0.02	**-4.07**	expressed protein	
	At5g24313	1.39	-1.65	**-8.22**	1.39	-0.30	**-3.22**	expressed protein	
	At1g52640	-0.83	0.73	**2.96**	-0.83	0.52	**2.56**	pentatricopeptide (PPR) protein	F6D8.14
	At2g47540	1.22	-1.55	**-6.84**	1.22	-0.82	**-4.12**	pollen Ole e 1 allergen and extensin protein	T30B22.16
	At2g34655	1.78	0.10	**-3.20**	1.78	-0.54	**-4.99**	expressed protein	
	At4g25190	0.91	-0.55	**-2.77**	0.91	-0.22	**-2.19**	hypothetical protein	
	At2g15280	-0.60	0.86	**2.75**	-0.60	0.47	**2.10**	reticulon family protein (RTNLB10)	F27O10.7
	At2g19320	-1.03	0.90	**3.79**	-1.03	-3.14	**-4.34**	expressed protein	F27F23.12
	At3g28917	1.25	-1.67	**-7.60**	1.25	-0.20	**-2.74**	zinc finger homeobox family protein	MIF2
	At5g56230	1.32	-1.15	**-5.55**	1.32	-0.79	**-4.31**	prenylated rab acceptor (PRA1) family protein	K24C1.4, PRA1.G2
	At2g04860	-1.66	0.78	**5.43**	-1.66	0.25	**3.75**	pentatricopeptide (PPR) protein	F28I8.8
	At2g03330	0.97	-0.15	**-2.16**	0.97	-0.24	**-2.31**	expressed protein	T4M8.24
	At4g27510	-0.94	1.24	**4.52**	-0.94	0.36	**2.45**	expressed protein	F27G19.110
	At2g03230	-1.53	2.73	**19.16**	-1.53	-0.06	**2.78**	hypothetical protein	T18E12.10
	At2g35990	1.00	-2.03	**-8.13**	1.00	-0.47	**-2.75**	hypothetical protein	F11F19.10
	At1g08160	1.16	-0.82	**-3.95**	1.16	-0.77	**-3.81**	harpin-induced protein-related / HIN1	
	At1g52620	-0.95	0.75	**3.25**	-0.95	0.23	**2.27**	pentatricopeptide (PPR) protein	
	At3g50610	-1.74	1.11	**7.21**	-1.74	0.68	**5.35**	hypothetical protein	T20E23.210
	At5g67020	1.15	-1.56	**-6.53**	1.15	-1.39	**-5.82**	expressed protein	K8A10.9
	At5g10890	-1.29	0.86	**4.45**	-1.29	0.02	**2.48**	weak similarity to myosin heavy chain	T30N20.160
	At2g07678	-0.61	1.99	**6.08**	-0.61	0.51	**2.18**	hypothetical protein	T17H1.7
	At2g29830	1.02	-0.18	**-2.29**	1.02	-0.87	**-3.69**	kelch repeat-containing F-box family protein	T27A16.1
	At1g05540	1.10	-0.72	**-3.53**	1.10	-0.16	**-2.40**	expressed protein	T25N20.19
	At1g70985	1.60	0.04	**-2.95**	1.60	-0.68	**-4.86**	hydroxyproline-rich glycoprotein family protein	
	At4g14120	-0.79	0.25	**2.06**	-0.79	0.41	**2.30**	expressed protein	DL3100W, FCAALL.110
	At5g45095	2.16	-0.49	**-6.28**	2.16	-0.09	**-4.75**	expressed protein	
	At1g19160	1.55	-0.16	**-3.26**	1.55	-0.10	**-3.14**	F-box family protein-related	T29M8.3
	At1g28690	-1.27	0.81	**4.21**	-1.27	0.61	**3.67**	pentatricopeptide (PPR) protein	F1K23.11
	At5g27110	-0.82	0.52	**2.54**	-0.82	0.40	**2.33**	pentatricopeptide (PPR) protein	
	At4g21920	-1.24	1.30	**5.85**	-1.24	0.65	**3.71**	expressed protein	F1N20.1
	At2g30760	-1.81	-0.30	**2.84**	-1.81	1.08	**7.42**	hypothetical protein	T11J7.15
	At2g21185	0.90	-1.42	**-5.01**	0.90	-0.60	**-2.84**	expressed protein	
	At5g39640	1.29	0.15	**-2.21**	1.29	-0.32	**-3.07**	hypothetical protein	MIJ24.14
	At3g01580	-1.80	0.41	**4.62**	-1.80	-0.25	**2.93**	pentatricopeptide (PPR) protein	F4P13.34

functional category	At No.	normalized intensity values: control 0° 2h 1*g*	normalized intensity values: exp. 90° 31x inv in 2h 1*g*	FC: exp. vs. control	normalized intensity values: control 0° 2h 1*g*	normalized intensity values: exp. 0° 2h flight	FC: exp. vs. control	description	other names
unknown	At5g61400	-0.95	0.46	**2.67**	-0.95	0.25	**2.31**	pentatricopeptide (PPR) protein	MFB13.18
	At2g36485	1.02	-0.65	**-3.19**	1.02	-0.43	**-2.75**	expressed protein	K15C23.5, MAP18, PCAP2
	At5g44610	1.01	-1.19	**-4.59**	1.01	-0.43	**-2.71**	DREPP plasma membrane polypeptide	K15C23.5, MAP18, PCAP2
	At4g05631	-1.11	1.04	**4.45**	-1.11	0.90	**4.05**	hypothetical protein	
	At1g09220	-0.92	0.77	**3.24**	-0.92	0.30	**2.33**	pentatricopeptide (PPR) protein	T12M4.7
	At1g49330	1.04	-2.42	**-10.96**	1.04	-0.54	**-2.99**	hydroxyproline-rich glycoprotein family protein	
	At3g25240	2.15	-0.78	**-7.62**	2.15	-0.21	**-5.10**	hypothetical protein	MJL12.20
	At2g37035	1.20	-0.28	**-2.79**	1.20	-0.28	**-2.78**	expressed protein	F21O3.6
	At3g43850	1.48	-0.40	**-3.67**	1.48	-0.36	**-3.57**	hypothetical protein	T28A8.140
	At2g12905	-1.45	2.90	**20.42**	-1.45	0.60	**4.15**	expressed protein	
	At2g04800	1.13	-1.42	**-5.85**	1.13	-0.14	**-2.42**	expressed protein	F28I8.16
	At1g59920	1.76	-0.34	**-4.31**	1.76	-0.21	**-3.94**	hypothetical protein	F23H11.23
	At1g51355	0.91	-0.60	**-2.83**	0.91	-0.33	**-2.36**	expressed protein	
	At5g46060	1.89	-1.66	**-11.70**	1.89	-0.78	**-6.38**	expressed protein	MCL19.11
	At5g65480	-0.95	0.59	**2.89**	-0.95	0.31	**2.39**	expressed protein	MNA5.18
	At1g14870	1.42	-0.85	**-4.84**	1.42	-0.85	**-4.85**	expressed protein similar to PGPS/D12	F10B6.27
	At2g16760	0.99	-1.96	**-7.70**	0.99	-1.29	**-4.87**	expressed protein	T24I21.17
	At1g19900	1.91	-2.92	**-28.56**	1.91	-1.49	**-10.54**	similarity to glyoxal oxidase precursor	F6F9.4
	At2g19350	1.58	-0.82	**-5.29**	1.58	-0.56	**-4.41**	expressed protein	F27F23.15
	At4g25790	1.26	-1.82	**-8.45**	1.26	-0.81	**-4.20**	allergen V5/Tpx-1-related family protein	F14M19.70
	At3g50570	1.95	-1.07	**-8.12**	1.95	-0.23	**-4.51**	hydroxyproline-rich glycoprotein family protein	T20E23.170
	At1g72800	1.53	-0.41	**-3.83**	1.53	-0.29	**-3.52**	nuM1-related contains similarity with nuM1	F28P22.1
	At3g28070	-1.14	0.69	**3.58**	-1.14	1.41	**5.89**	nodulin MtN21 family protein similar to MtN21	T20E23.170
	At3g21610	0.94	-0.33	**-2.41**	0.94	-0.24	**-2.26**	expressed protein	MIL23.18
	At3g47840	-0.96	0.67	**3.11**	-0.96	0.21	**2.26**	pentatricopeptide (PPR) protein	T23J7.170
	At2g47360	1.04	-1.47	**-5.67**	1.04	-0.78	**-3.54**	expressed protein	T8I13.20
	At2g22410	-0.86	0.96	**3.52**	-0.86	0.44	**2.46**	pentatricopeptide (PPR) protein	F14M13.19
	At5g05500	1.25	-2.14	**-10.47**	1.25	-0.97	**-4.67**	pollen Ole e 1 allergen and extensin	MOP10.4

8.3 2*g*-related genes – annotations and normalized values

Table V (pp 96 - 97). Normalized intensity values of genes involved in the plants response to continuous 2*g* centrifugation (2h). The table lists only a selection of all 755 2*g*-affected genes, including those genes involved in regulation processes of the most prominent functional groups (for all 755 genes, see enclosed compact disk). The fold change (FC) denotes the ratio of intensity value of the respective treatement to vertical control at 1*g* (0° 2h 1*g*). Annotation details (description and other names) sourced by TAIR.

		normalized intensity values		FC		
functional category	At No.	control 0° 2h 1*g*	exp. 90° 2h 2*g*	exp. vs. control	description	other names
amino acid / secondary metabolism	At1g17745	0.60	-0.45	**-2.07**	D-3-phosphoglycerate dehydrogenase (3-PGDH)	
	At1g48640	0.99	-0.55	**-2.90**	lysine and histidine specific transporter	F11I4.17
	At2g34960	-0.09	-1.76	**-3.19**	cationic amino acid transporter 3	CAT5, F19I3.19
	At5g16740	0.60	-1.32	**-3.79**	amino acid transporter 1	F5E19.80
	At1g04870	-0.59	-1.80	**-2.31**	arginine N-methyltransferase 6	
	At2g23000	-0.94	-2.52	**-2.99**	serine carboxypeptidase S10 family protein	F21P24.6, SCPL10
carbohydrate biosynthetic process	At5g15050	0.16	-1.25	**-2.66**	glycosyltransferase family 14 protein	F2G14.170
	At5g65685	-0.71	0.74	**2.73**	weak similarity to soluble glycogen synthase	
	At1g50580	-0.49	-2.30	**-3.50**	glycosyltransferase family protein	F11F12.10
	At1g66280	0.17	-1.01	**-2.26**	glycosyl hydrolase family 1 protein	BGLU22, T27F4.3
	At1g70090	0.64	-0.54	**-2.26**	glycosyl transferase family 8 protein	F20P5.18, GATL9, LGT8
	At3g60120	0.56	-2.43	**-7.98**	glycosyl hydrolase family 1 protein	BGLU27, T2O9.100
	At4g27820	-1.02	0.44	**2.75**	glycosyl hydrolase family 1 protein	BGLU9, T27E11.60
	At4g38300	-0.97	1.11	**4.23**	glycosyl hydrolase family 10 protein	F22I13.70
	At1g09420	-0.52	0.85	**2.59**	glucose-6-phosphate 1-dehydrogenase	F14J9.8, G6PD4
	At5g54800	0.69	-0.34	**-2.05**	glucose-6-phosphate/phosphate translocator	ATGPT1, GPT1, MBG8.6
	At3g10450	-0.61	0.79	**2.64**	serine carboxypeptidase S10 family protein	F13M14.27, SCPL7
	At1g14360	-0.19	-1.28	**-2.13**	UDP-galactose/UDP-glucose transporter	ATUTR3, F14L17.13, UTR3
stress / defense response	At1g16030	-0.38	3.06	**10.88**	heat shock protein 70	HSP70
	At3g12580	0.81	2.28	**2.77**	heat shock protein 70	HSP70, T2E22.11
	At5g56010	0.64	-0.53	**-2.25**	heat shock protein 81-2 (HSP81-2)	HSP90, HSP81.3, MDA7.5
	At1g77570	-0.38	-1.89	**-2.85**	heat shock transcription factor family protein	T5M16.16
	At3g22830	-0.26	1.52	**3.45**	heat shock transcription factor family protein	HSFA6B, MWI23.20
	At3g46230	-0.12	4.26	**20.81**	17.4 kDa class I heat shock protein (HSP17.4-CI)	HSP17.4
	At1g53540	-0.00	4.13	**17.52**	17.6 kDa class I small heat shock protein (HSP17.6C-CI)	F22G10.20
	At5g12020	0.07	4.02	**15.45**	17.6 kDa class II heat shock protein (HSP17.6-CII)	HSP17.6, F14F18.200
	At5g12030	0.20	4.34	**17.65**	17.7 kDa class II heat shock protein 17.6A (HSP17.7-CII)	HSP17.6
	At5g59720	-0.22	1.86	**4.23**	18.1 kDa class I heat shock protein (HSP18.1-CI)	HSP18.2, MTH12.7
	At3g14200	0.85	-0.41	**-2.39**	DNAJ heat shock N-terminal domain-containing protein	MAG2.19
	At4g19570	-0.41	1.78	**4.56**	DNAJ heat shock N-terminal domain-containing protein	F24J7.130
	At1g52560	-0.78	2.51	**9.78**	26.5 kDa class I small heat shock protein-like (HSP26.5-P)	F6D8.22
	At1g08930	0.45	-1.07	**-2.87**	early-responsive to dehydration stress protein (ERD6)	ERD6, F7G19.19
	At5g38710	0.83	1.88	**2.06**	osmotic stress-responsive proline dehydrogenase	MKD10.10
	At2g23680	0.54	-0.68	**-2.32**	stress-responsive protein	F26B6.33
	At4g25580	0.68	2.02	**2.54**	weak similarity to Low-temperature-induced 65 kDa protein	M7J2.50
	At2g01330	-0.22	1.29	**2.85**	similar to 66kDa stress protein	F10A8.21
	At4g27320	1.24	-0.16	**-2.64**	universal stress protein (USP) family protein	ATPHOS34, M4I22.130, PHOS34
	At5g48657	0.80	-0.43	**-2.33**	defense protein	

functional category	At No.	normalized intensity values: control 0° 2h 1*g*	normalized intensity values: exp. 90° 2h 2*g*	FC: exp. vs. control	description	other names
stress / defense response	At2g30770	-0.07	-3.75	**-12.86**	cytochrome P450 71A13	CYP71A13, T11J7.16
	At3g26830	0.20	-2.54	**-6.69**	cytochrome P450 71B15	CYP71B15, MDJ14.12, PAD3
cell wall modification	At2g15390	0.48	-1.19	**-3.18**	xyloglucan fucosyltransferase	ATFUT4, F26H6.9, FUT4
	At1g69530	0.86	-0.51	**-2.59**	expansin (At-EXP1)	ATEXP1, ATEXPA1, F10D13.18
	At5g38610	1.52	-0.47	**-3.99**	invertase/pectin methylesterase inhibitor family protein	MBB18.16
	At2g47050	-1.49	0.16	**3.15**	invertase/pectin methylesterase inhibitor family protein	F14M4.12
	At3g47670	0.52	-1.58	**-4.30**	invertase/pectin methylesterase inhibitor family protein	F1P2.220
	At1g23200	0.34	-1.07	**-2.65**	pectinesterase family protein	F26F24.2
	At3g06360	0.79	-1.06	**-3.61**	arabinogalactan-protein (AGP27)	F24P17.17
	At1g35230	0.43	-2.12	**-5.85**	arabinogalactan-protein (AGP5)	T9I1.2
	At2g20520	1.16	-0.17	**-2.52**	fasciclin-like arabinogalactan-protein (FLA6)	T13C7.11
	At5g44130	1.50	-0.39	**-3.70**	fasciclin-like arabinogalactan-protein	FLA13, MLN1.5
	At4g08380	1.18	-0.19	**-2.58**	extensin-like family protein	T28D5.70
	At1g55540	0.15	1.26	**2.16**	extensin	EMB1011, T5A14.22
	At4g16140	0.56	-1.21	**-3.41**	extensin domains	DL4110W, FCAALL.289
transporter activity	At1g64780	0.71	-1.27	**-3.96**	ammonium transporter 1, member 2 (AMT1.2)	AMT1 2, ATAMT1 2
	At2g18480	0.80	2.59	**3.45**	mannitol transporter	F24H14.17
	At1g69850	0.18	-0.96	**-2.22**	nitrate transporter (NTL1)	ATNRT1:2, NTL1, T17F3.12
	At1g16390	0.76	-1.22	**-3.95**	organic cation transporter	ATOCT3, F3O9.19
	At1g54730	-0.18	-1.20	**-2.04**	sugar transporter	T22H22.15
	At5g26250	0.80	-0.77	**-2.97**	sugar transporter	T19G15.100
	At4g08620	0.87	-0.77	**-3.13**	sulfate transporter	SULTR1.2, SULTR1 1
	At1g16370	1.30	-0.79	**-4.26**	similarity to organic cation transporter OCTN1	ATOCT6, F3O9.17, OCT6
	At5g22900	-0.05	1.30	**2.54**	putative (CHX3) monovalent cation:proton antiporter family 2 (CPA2) member	ATCHX3, CHX3, MRN17.13
	At1g16820	-0.76	0.92	**3.22**	vacuolar ATP synthase catalytic subunit	F17F16.15
	At5g11230	1.50	-0.35	**-3.62**	organic anion transmembrane transporter (vacuolar proton pump alpha subunit)	F2I11.120

Table VI (pp 98 – 100). Normalized intensity values of the selected set of 108 2*g*-specific genes after exposure to 62x 20s 2*g* in 2h 1*g* and to the flight conditions of a 2h parabolic plane flight. The fold change (FC) denotes the ratio of intensity value of the respective treatement to vertical control at 1*g* (0° 2h 1*g*). Annotation details (description and other names) sourced by TAIR.

		normalized intensity values		FC	normalized intensity values		FC		
functional category	At No.	control 0° 2h 1*g*	exp. 0° 62x 2*g*	exp. vs. control	control 0° 2h 1*g*	exp. 0° 2h flight	exp. vs. control	description	other names
DNA metabolism	At4g35280	-1.51	0.25	**3.38**	-1.51	0.95	**5.51**	zinc finger (C2H2 type) family protein	F23E12.160
	At5g18450	0.48	-3.00	**-11.19**	0.48	-2.41	**-7.41**	AP2 transcription factor, putative DREB2A	F20L16.170
	At3g17010	0.51	-1.08	**-3.00**	0.51	-0.75	**-2.38**	transcriptional factor B3 family protein	K14A17.8
	At2g30420	-1.18	-2.46	**-2.42**	-1.18	-0.08	**2.14**	myb family transcription factor	ETC2, T9D9.23
	At4g08990	1.22	-0.93	**-4.42**	1.22	-0.73	**-3.85**	DNA (cytosine-5-)-methyltransferase (METII)	F23J3.20
	At3g27473	0.95	-0.47	**-2.69**	0.95	-0.28	**-2.35**	DC1 domain-containing protein	K1G2.25
	At5g41450	1.05	-0.28	**-2.52**	1.05	-0.32	**-2.59**	zinc finger (C3HC4-type RING finger)	F20L16.170, MYC6.15
	At3g30210	1.27	-0.74	**-4.01**	1.27	-0.64	**-3.77**	myb family transcription factor (MYB121)	ATMYB121, MIL15.18
	At1g12890	-1.49	-3.09	**-3.04**	-1.49	-0.06	**2.69**	AP2 domain-containing transcription factor	F13K23.25
	At3g19580	1.65	5.90	**19.01**	1.65	-0.59	**-4.70**	zinc finger (C2H2 type) protein 2 (AZF2)	MMB12.27
	At3g22310	-0.68	0.42	**2.15**	-0.68	0.53	**2.32**	DEAD box RNA helicase (RH9)	ATRH9, MCB17.17, PMH1
	At3g22640	0.41	-3.49	**-14.92**	0.41	-2.21	**-6.18**	cupin family protein	MWI23.1, PAP85
signaling	At3g53040	0.83	-3.40	**-18.82**	0.83	-2.27	**-8.58**	late embryogenesis abundant protein	F8J2.210
	At1g67890	-0.97	1.01	**3.96**	-0.97	0.35	**2.51**	protein kinase family protein	T23K23.26
	At2g31650	-0.90	0.46	**2.58**	-0.90	0.14	**2.05**	trithorax-like protein 1 (ATX-1) (TRX1)	SDG27, T9H9.17
	At4g16890	-1.70	-0.20	**2.83**	-1.70	0.59	**4.90**	disease resistance protein (TIR-NBS-LRR class)	BALL, DL4475C, FCAALL.51, SNC1
	At3g12955	0.68	-0.76	**-2.71**	0.68	-1.04	**-3.29**	indole-3-acetic acid induced protein arg7	
	At4g09600	0.87	-2.75	**-12.29**	0.87	-2.40	**-9.64**	gibberellin-regulated protein 3 (GASA3)	GAST1 PROTEIN HOMOLOG 3
	At3g51810	-0.26	-3.77	**-11.42**	-0.26	-2.01	**-3.36**	Em-like protein GEA1 (EM1)	AT3, ATEM1, ATEM 1.6, GEA1
	At2g40170	-0.34	-4.76	**-21.28**	-0.34	-2.75	**-5.32**	Em-like protein GEA6 (EM6)	ATEM6, GEA6, T7M7.23
	At4g09610	1.00	-2.21	**-9.25**	1.00	-2.69	**-13.00**	gibberellin-regulated protein 2 (GASA2)	GAST1 PROTEIN HOMOLOG 2
	At3g09880	-1.35	0.27	**3.07**	-1.35	0.13	**2.79**	serine/threonine protein phosphatase 2A (PP2A)	ATB' BETA, F8A24.7
	At1g54870	0.64	-3.87	**-22.77**	0.64	-3.14	**-13.7**	auxin-regulated protein	F14C21.43
transporter activity	At2g03520	0.61	-2.69	**-9.89**	0.61	-1.15	**-3.39**	similar to SP|Q41706 A3 protein	ATUPS4, T4M8.4
	At5g10000	-0.15	-2.91	**-6.77**	-0.15	-2.08	**-3.81**	ferredoxin family protein	ATFD4, FERREDOXIN 4, MYH9.22
	At3g48270	0.01	-3.59	**-12.16**	0.01	-2.65	**-6.36**	cytochrome P450 71A26	T29H11.210
	At3g03620	-0.27	-3.59	**-9.95**	-0.27	-2.00	**-3.31**	MATE efflux family protein	T12J13.10
	At1g64940	0.49	-0.92	**-2.66**	0.49	-0.65	**-2.2**	cytochrome P450	CYP89A6, F13O11.24
stress / defense response	At5g15970	-0.93	-3.50	**-5.94**	-0.93	0.73	**3.16**	stress-responsive protein (KIN2)	COR6.6, F1N13.110, KIN2
	At3g58450	-0.43	-4.17	**-13.34**	-0.43	-3.21	**-6.87**	universal stress protein (USP) family protein	F14P22.40
	At2g21490	-0.32	-4.60	**-19.41**	-0.32	-3.18	**-7.26**	dehydrin family protein	DEHYDRIN LEA, F3K23.25, LEA
	At1g61300	-1.04	0.27	**2.48**	-1.04	0.52	**2.95**	disease resistance protein (NBS-LRR class)	T1F9.21
	At2g15010	0.09	-3.99	**-16.87**	0.09	-1.83	**-3.78**	putative thionin	T15J14.5
cell wall modification	At4g03930	0.79	-0.47	**-2.40**	0.79	-1.34	**-4.37**	pectin methylesterase	T24M8.6
	At4g02300	0.82	-0.84	**-3.15**	0.82	-0.73	**-2.94**	pectinesterase family protein	T2H3.6
	At1g63540	1.56	0.26	**-2.47**	1.56	-1.21	**-6.82**	hydroxyproline-rich glycoprotein family protein	F2K11.10
	At1g22420	0.70	-0.68	**-2.61**	0.70	-0.65	**-2.56**	extensin	F12K8.23
	At5g43770	1.00	-3.96	**-31.14**	1.00	-2.79	**-13.9**	extensin	MQD19.12

functional category	At No.	normalized intensity values: control 0° 2h 1*g*	normalized intensity values: exp. 0° 62x 2*g*	FC: exp. vs. control	normalized intensity values: control 0° 2h 1*g*	normalized intensity values: exp. 0° 2h flight	FC: exp. vs. control	description	other names
protein metabolism	At5g18340	0.64	2.26	**-13.34**	0.64	-0.49	**-2.19**	U-box domain-containing protein	F20L16.60
	At1g60190	1.11	-1.27	**-5.19**	1.11	-1.14	**-4.75**	armadillo/beta-catenin repeat family protein	T13D8.8
	At2g38920	-0.60	-1.94	**-2.53**	-0.60	0.48	**2.12**	SPX (SYG1/Pho81/XPR1) protein	T7F6.9
cell adhesion	At1g15190	1.31	-0.19	**-2.84**	1.31	-0.49	**-3.49**	hypothetical protein	F9L1.13
	At1g30800	1.10	-0.08	**-2.27**	1.10	-0.18	**-2.43**	expressed protein	T17H7.8
	At3g17520	0.60	-4.07	**-25.60**	0.60	-2.05	**-6.3**	late embryogenesis abundant protein	MKP6.25
lipid metabolism	At3g27660	1.62	-3.48	**-34.21**	1.62	-2.18	**-13.8**	glycine-rich protein / oleosin	MGF10.3, OLE3, OLEO4
	At3g08770	-0.98	-2.75	**-3.40**	-0.98	0.81	**3.46**	lipid transfer protein 6 (LTP6)	F17O14.24
other	At1g22770	0.16	1.26	**2.15**	0.16	-1.44	**-3.03**	gigantea protein (GI)	FB, GIGANTEA, T22J18.6
	At5g55240	0.35	-2.90	**-9.51**	0.35	-1.85	**-4.57**	caleosin-related family protein	MCO15.19
	At4g26740	0.07	-3.05	**-8.72**	0.07	-1.29	**-2.57**	embryo-specific protein 1 (ATS1)	CALEOSIN1, CLO1, F10M23.80
	At2g02120	0.43	-2.11	**-5.82**	0.43	-0.63	**-2.09**	plant defensin-fusion protein (PDF2.1)	F5O4.11, LCR70
	At4g28520	0.23	-2.61	**-7.19**	0.23	-1.04	**-2.42**	12S seed storage protein	CRC, CRU3, F20O9.210
	At2g43530	-0.60	-2.25	**-3.14**	-0.60	0.94	**2.90**	trypsin inhibitor 2 precursor (MTI-2)	T1O24.27
enzyme activity *	At1g09500	0.14	-0.98	**-2.17**	0.14	-1.10	**-2.37**	cinnamyl-alcohol dehydrogenase CPRD14	F14J9.16
	At5g65165	-0.07	-4.78	**-26.27**	-0.07	-2.78	**-6.57**	succinate dehydrogenase SDH2-3	
	At5g24420	-0.37	-1.45	**-2.11**	-0.37	1.55	**3.80**	galactosamine-6-phosphate isomerase 6PGL	K16H17.13, PGL5
	At1g07645	0.31	-2.92	**-9.34**	0.31	-2.44	**-6.73**	dessication-induced 1VOC superfamily protein	ATDSI-1VOC
	At5g51760	0.19	-3.15	**-10.13**	0.19	-2.30	**-5.62**	protein phosphatase 2C PP2C	AHG1, MIO24.11
	At3g05260	0.53	-3.36	**-14.87**	0.53	-2.60	**-8.77**	short-chain dehydrogenase/reductase (SDR)	T12H1.23
	At2g31980	0.85	-2.53	**-10.41**	0.85	-0.81	**-3.15**	cysteine proteinase inhibitor	F22D22.27
	At1g17010	1.38	-1.66	**-8.20**	1.38	-1.03	**-5.33**	oxidoreductase, 2OG-Fe(II) oxygenase	F20D23.29
	At5g65550	0.30	-3.66	**-15.67**	0.30	-2.33	**-6.21**	UDP-glucoronosyl/UDP-glucosyl transferase	K21L13.6
	At3g54940	0.00	-4.48	**-22.28**	0.00	-2.96	**-7.77**	cysteine proteinase	F28P10.80
	At5g22470	-0.29	-3.87	**-12.03**	-0.29	-2.37	**-4.24**	poly (ADP-ribose) polymerase family protein	MQJ16.1
	At2g24210	0.84	-0.38	**-2.33**	0.84	-0.41	**-2.39**	myrcene/ocimene synthase (TPS10)	F27D4.12
unknown	At1g77910	1.35	0.16	**-2.28**	1.35	-0.92	**-4.84**	hypothetical protein	F28K19.12
	At3g42410	0.98	-0.83	**-3.50**	0.98	-0.32	**-2.46**	replication protein-related	T14K23.120
	At3g53550	0.70	-0.71	**-2.66**	0.70	-1.75	**-5.48**	hypothetical protein	F4P12.250
	At1g52690	0.61	-4.58	**-36.53**	0.61	-2.19	**-7.00**	putative / LEA protein	F6D8.9
	At1g23660	0.97	-0.45	**-2.69**	0.97	-0.18	**-2.22**	expressed protein	F28C11.23
	At1g27990	0.39	-4.59	**-31.55**	0.39	-2.54	**-7.61**	expressed protein	F13K9.9
	At3g14500	1.41	-0.18	**-3.01**	1.41	-0.43	**-3.58**	hypothetical protein	MOA2.10
	At5g13220	0.73	-0.32	**-2.08**	0.73	-0.31	**-2.06**	expressed protein	JAS1, JAZ10, T31B5.40, TIFY9
	At1g50160	1.30	-0.45	**-3.37**	1.30	-0.71	**-4.03**	hypothetical protein	F14I3.22
	At3g47230	0.83	-1.36	**-4.54**	0.83	-1.01	**-3.58**	expressed protein	F13I12.280
	At3g33073	0.31	-1.07	**-2.61**	0.31	-1.82	**-4.39**	hypothetical protein	T25F15.5
	At2g36640	0.49	-4.08	**-23.81**	0.49	-2.80	**-9.81**	nearly identical to to LEA protein in group 3	ATECP63, F13K3.4
	At5g51795	0.85	-0.73	**-2.99**	0.85	-1.13	**-3.95**	Kin17 DNA-binding protein-related	
	At4g31350	2.36	-0.62	**-7.93**	2.36	-0.15	**-5.69**	expressed protein	F8F16.170
	At5g26805	0.69	-0.91	**-3.03**	0.69	-1.15	**-3.6**	expressed protein	
	At3g48185	0.89	-0.16	**-2.07**	0.89	-0.28	**-2.24**	expressed protein	
	At1g80090	1.42	-4.35	**-54.44**	1.42	-2.23	**-12.5**	CBS domain-containing protein	F18B13.17

* genes encoding for proteins with enzyme activities unless annotation details allowed more precise functional classification

functional category	At No.	normalized intensity values: control 0° 2h 1*g*	normalized intensity values: exp. 0° 62x 2*g*	FC: exp. vs. control	normalized intensity values: control 0° 2h 1*g*	normalized intensity values: exp. 0° 2h flight	FC: exp. vs. control	description	other names
unknown	At5g50270	0.38	-0.82	**-2.30**	0.38	-2.16	**-5.81**	F-box family protein	K6A12.13
	At1g32560	0.78	-3.68	**-21.96**	0.78	-2.56	**-10.1**	late embryogenesis abundant group 1 protein	T9G5.2
	At5g22670	1.33	0.12	**-2.31**	1.33	-1.07	**-5.27**	F-box family protein	MDJ22.9
	At1g03810	0.82	-0.79	**-3.07**	0.82	-0.68	**-2.84**	DNA-binding protein-related	F21M11.28
	At5g09980	0.53	-1.40	**-3.82**	0.53	-0.57	**-2.15**	expressed protein	MYH9.20, PROPEP4
	At3g46260	1.96	-0.30	**-4.78**	1.96	-0.17	**-4.36**	protein kinase-related	F12M12.230
	At1g54860	1.11	-4.00	**-34.51**	1.11	-2.51	**-12.3**	expressed protein	F14C21.37
	At3g28060	1.22	-0.90	**-4.36**	1.22	-0.34	**-2.95**	similar to MtN21	MMG15.10
	At1g66770	0.51	-1.94	**-5.48**	0.51	-1.79	**-4.91**	MtN3/saliva family protein	F4N21.10
	At4g27530	-0.62	-5.07	**-21.97**	-0.62	-2.79	**-4.51**	expressed protein	T29A15.20
	At5g55135	-0.40	-3.40	**-8.01**	-0.40	-2.44	**-4.11**	hypothetical protein	
	At5g07330	-0.18	-4.64	**-21.97**	-0.18	-3.12	**-7.64**	expressed protein	T2I1.40
	At1g62670	-1.06	0.60	**-8.01**	-1.06	0.21	**2.413**	pentatricopeptide (PPR) protein	F23N19.4
	At3g60700	0.56	-1.50	**-4.19**	0.56	-0.63	**-2.29**	expressed protein	T4C21.110
	At2g35300	0.48	-3.67	**-17.82**	0.48	-2.16	**-6.26**	late embryogenesis abundant group 1 protein	T4C15.3
	At5g10040	-0.56	-2.11	**-2.91**	-0.56	1.37	**3.84**	expressed protein	T31P16.30
	At5g45690	-0.06	-3.52	**-10.98**	-0.06	-2.79	**-6.64**	expressed protein	MRA19.8
	At1g05510	0.11	-3.12	**-9.40**	0.11	-2.59	**-6.48**	expressed protein	T25N20.16
	At3g51750	-0.11	-2.54	**-5.41**	-0.11	-1.40	**-2.45**	expressed protein	T18N14.130
	At2g42560	0.29	-4.68	**-31.15**	0.29	-3.12	**-10.6**	late embryogenesis abundant protein	F14N22.17
	At3g12960	-0.72	-4.17	**-10.96**	-0.72	-2.79	**-4.21**	expressed protein	MGH6.8
	At5g42290	-0.45	-3.82	**-10.30**	-0.45	-2.57	**-4.33**	transcription activator-related	K18I23.2
	At5g05220	-0.65	-3.58	**-7.58**	-0.65	-2.44	**-3.45**	expressed protein	T20D16.13
	At2g23240	0.35	-4.56	**-30.02**	0.35	-3.55	**-14.9**	plant EC metallothionein-like family 15 protein	T20D16.13
	At3g22490	0.25	-4.19	**-21.76**	0.25	-3.03	**-9.69**	putative / LEA protein	F16J14.21
	At1g72080	0.79	-0.38	**-2.24**	0.79	-1.66	**-5.48**	hypothetical protein	F28P5.14
	At5g01300	-0.09	-3.9	**-14.13**	-0.09	-2.93	**-7.16**	phosphatidylethanolamine-binding protein	T10O8.10

8.4 µ*g*-related genes – annotations and normalized values

Table VII (pp 101 - 104). Normalized intensity values of the 142 µ*g*-related genes for flight and in-flight controls of a two-hour flight, as well as for vertically and horizontally positioned flight samples during a one-hour flight. The fold change (FC) denotes the ratio of intensity value of the respective treatement to vertical control at 1*g* (0° 2h 1*g*). Annotation details (description and other names) sourced by TAIR.

		normalized intensity values		FC	normalized intensity values		FC		
functional category	At No.	in-flight control 0° (1*g*, 2*g*)	flight 0° (µ*g*, 1*g*, 2*g*)	flight vs. in-flight control	flight 0° (µ*g*, 1*g*, 2*g*)	flight 90° (µ*g*, 1*g*, 2*g*)	flight 90° vs. flight 0°	description	other names
lipid metabolism	At5g59310	3.19	-0.24	**-10.76**	0.50	0.43	**-1.05**	lipid transfer protein 4 (LTP4)	MNC17.4
	At5g59320	2.24	0.09	**-4.44**	0.64	0.51	**-1.10**	lipid transfer protein 3 (LTP3)	MNC17.10
	At3g01570	-0.24	-2.23	**-3.97**	0.38	0.31	**-1.04**	oleosin	F4P13.12
	At4g25140	-0.18	-2.31	**-4.36**	-0.17	0.04	**1.16**	oleosin	F24A6.9. OLE1. OLEO1. OLEOSIN 1
	At5g51210	-0.56	-2.07	**-2.85**	0.46	0.23	**-1.18**	oleosin	MWD22.16. OLEO3. OLEOSIN3
	At3g18570	-0.72	-2.63	**-3.76**	0.70	0.36	**-1.27**	oleosin	K24M9.6
	At1g48990	-0.67	-2.40	**-3.31**	0.18	0.05	**-1.09**	oleosin	F27J15.22
	At5g40420	-0.26	-1.86	**-3.04**	0.26	0.25	**-1.01**	oleosin	OLE2. OLEO2. OLEOSIN 2
	At2g25890	-1.05	-2.70	**-3.13**	0.32	0.00	**-1.25**	oleosin	F17H15.8
	At4g33550	0.28	-0.99	**-2.42**	0.69	0.45	**-1.18**	lipid transfer protein (LTP)	T16L1.40
	At4g21020	-0.09	-1.56	**-2.77**	1.50	2.02	**1.44**	LEA domain-containing protein	T13K14.180
	At5g38180	-0.48	-1.70	**-2.33**	-1.82	-1.88	**-1.05**	lipid transfer protein (LTP)	MXA21.16
	At2g37870	0.46	-1.06	**-2.86**	0.03	-0.08	**-1.08**	lipid transfer protein (LTP)	T8P21.22
	At4g27140	1.82	-0.28	**-4.28**	0.91	1.17	**1.20**	NWMU1-2S albumin 1	T24A18.90
	At5g54740	-0.50	-2.17	**-3.18**	0.43	0.57	**1.10**	lipid transfer protein (LTP)	K5F14.10
	At1g72100	-0.61	-2.53	**-3.79**	0.43	0.22	**-1.15**	LEA domain-containing protein	F28P5.13
	At4g27150	1.77	0.09	**-3.21**	-0.69	-0.25	**1.35**	NWMU2-2S albumin 2	T24A18.100
	At4g27160	0.74	-0.96	**-3.25**	-0.63	-0.55	**1.05**	NWMU2-2S albumin 3	AT2S3. T24A18.110
	At1g71250	-0.15	-1.20	**-2.07**	-0.53	-0.51	**1.02**	family II lipase EXL3	F3I17.10
DNA metabolism	At5g37080	-1.57	0.75	**5.01**	-1.21	-1.52	**-1.24**	hypothetical protein	MJG14.6
	At5g55770	-0.95	0.47	**2.68**	0.75	0.35	**-1.32**	DC1 domain-containing protein	MDF20.21
	At4g21440	0.54	-0.98	**-2.87**	-0.25	-0.34	**-1.07**	myb family transcription factor (MYB102)	ATM4. ATMYB102. F18E5.60
	At5g21960	-1.55	-0.23	**2.49**	-1.70	-1.44	**1.20**	similar to TINY	MSJ3.9
	At3g30460	-0.24	-1.31	**-2.10**	0.69	0.47	**-1.16**	C3HC4-type RING finger protein	
	At2g33870	2.56	-1.51	**-16.78**	-1.62	-1.39	**1.17**	Ras-related GTP-binding protein	ARRABA1H. T1B8.16
	At3g24650	-0.26	-1.27	**-2.01**	0.38	0.58	**1.15**	abscisic acid-insensitive protein 3 (ABI3)	ABI3. MSD24.3. SIS10
	At3g10040	-0.69	0.56	**2.38**	0.63	1.42	**1.73**	expressed protein	T22K18.13
	At3g18650	-2.06	-0.01	**4.13**	-0.66	-1.75	**-2.13**	MADS-box family protein	AGL103. MVE11.1
	At5g07210	-1.51	0.29	**3.48**	-1.68	-1.22	**1.38**	two-component responsive regulator protein	ARR21. T28J14.150
	At2g43140	-0.35	0.68	**2.04**	0.93	1.34	**1.33**	basic helix-loop-helix protein (bHLH)	F14B2.8
	At5g63900	-1.65	-0.07	**2.99**	-2.05	-0.74	**2.48**	PHD finger family protein	MGI19.10
	At5g40590	-1.16	0.41	**2.98**	-0.39	0.02	**1.33**	DC1 domain-containing protein	MNF13.11
	At3g31950	-1.44	0.43	**3.64**	-1.88	-1.30	**1.50**	hypothetical protein	F8N14.12
transporter acitivity	At1g69260	0.32	-0.69	**-2.01**	0.17	0.13	**-1.03**	expressed protein	AFP1. F4N2.22
	At4g02690	-0.63	-1.82	**-2.29**	0.01	-0.28	**-1.22**	N-methyl-D-aspartate receptor-associated	T10P11.23
	At1g73190	-0.19	-2.03	**-3.60**	-0.04	0.04	**1.05**	tonoplast intrinsic protein. alpha-TIP (TIP3.1)	ALPHA-TIP. T18K17.14
	At3g61940	-1.03	0.02	**2.06**	0.53	0.21	**-1.25**	putative similar to zinc transporter ZAT	ATMTPA1. F21F14.110. MTPA1
	At4g16160	-1.19	-2.83	**-3.12**	0.55	0.40	**-1.11**	translocase subunit Tim17/Tim22/Tim23	ATOEP16-2. DL4120W. FCAALL.207

functional category	At No.	normalized intensity values: in-flight control 0° (1g, 2g)	normalized intensity values: flight 0° (µg, 1g, 2g)	FC: flight vs. in-flight control	normalized intensity values: flight 0° (µg, 1g, 2g)	normalized intensity values: flight 90° (µg, 1g, 2g)	FC: flight 90° vs. flight 0°	description	other names
transporter acitivity	At3g11050	-1.26	-2.75	**-2.80**	-0.16	-0.20	**-1.03**	putative similar to ferritin subunit cowpea2	ATFER2. F11B9.26. FERRITIN 2
	At4g15680	1.06	-1.30	**-5.11**	1.02	-0.05	**-2.10**	glutaredoxin family protein	DL3880W. FCAALL.384
	At5g64210	-0.06	-1.46	**-2.64**	0.53	0.64	**1.08**	alternative oxidase 2. mitochondrial (AOX2)	AOX2. MSJ1.5
stress / defense response	At4g33870	0.74	-0.64	**-2.61**	-0.04	0.70	**1.67**	peroxidase. putative similar to peroxidase	F17I5.60
	At5g45220	-0.91	0.20	**2.16**	-0.09	-0.01	**1.06**	Toll-Interleukin-Resistance (TIR) protein	K18C1.10
	At4g13810	-1.65	-0.22	**2.69**	0.53	0.76	**1.18**	disease resistance family protein	ATRLP47. F18A5.200
	At2g34315	-0.13	-1.37	**-2.36**	-0.50	-0.55	**-1.04**	disease resistance protein-related	
	At2g38905	-0.60	-2.22	**-3.08**	0.49	0.06	**-1.35**	low temperature / salt responsive protein LTI6A	
	At3g15280	-2.02	-3.28	**-2.39**	0.31	-0.06	**-1.29**	low similarity to cold regulated gene REP14	K7L4.8
	At5g66400	0.05	-2.30	**-5.12**	-0.22	-0.38	**-1.12**	dehydrin (RAB18)	ATDI8. K1F13.5. RAB18
	At3g50980	-0.71	-2.45	**-3.34**	0.28	-0.08	**-1.29**	putative similar to dehydrin Xero 1	F24M12.20. XERO1
signaling	At5g10120	0.28	-0.82	**-2.15**	-0.68	-0.31	**1.29**	ethylene insensitive 3 family protein	T31P16.110
	At5g59220	0.25	-1.38	**-3.08**	-1.46	-1.59	**-1.10**	putative ABA induced protein phosphatase 2C	HAI1. MNC17.13
	At3g05310	0.62	-1.75	**-5.14**	0.63	-1.72	**-5.11**	GTP-binding protein. similarity to rac 1 protein	MIRO3. T12H1.28
	At5g44300	0.59	-0.93	**-2.86**	-0.95	-1.15	**-1.16**	auxin associated family protein	K9L2.6
	At5g62490	-0.97	-2.57	**-3.03**	0.32	0.12	**-1.15**	ABA-responsive protein (HVA22b)	ATHVA22B. HVA22B. K19B1.10
protein metabolism	At5g15500	2.44	0.33	**-4.31**	0.51	0.55	**1.03**	ankyrin repeat family protein	T20K14.110
	At1g65120	-1.21	0.29	**2.84**	-1.19	-0.43	**1.70**	ubiquitin carboxyl-terminal hydrolase (DUF629)	T23K8.3
	At3g21380	0.48	-1.07	**-2.93**	0.31	0.66	**1.27**	jacalin lectin family protein	MHC9.6
	At5g57550	0.12	-1.01	**-2.20**	-0.82	-0.84	**-1.01**	xyloglucan endotransglycosylase (XTR3)	MUA2.12. XTR3
	At4g24000	0.61	-1.30	**-3.76**	0.90	1.12	**1.16**	cellulose synthase family protein	ATCSLG2. CSLG2. T32A16.170
cell wall modification	At3g13784	1.62	-0.40	**-4.07**	1.66	1.94	**1.21**	beta-fructosidase / cell wall invertase	ATCWINV5. MMM17.25
	At2g27380	0.45	-0.85	**-2.46**	-0.18	-0.14	**1.03**	proline-rich family protein	ATEPR1. F12K2.4
	At5g59170	0.68	-0.43	**-2.17**	-0.25	-0.17	**1.06**	proline-rich family protein	MNC17.8
	At5g55360	-0.05	-2.27	**-4.68**	-1.73	-1.48	**1.19**	wax synthase family protein	MTE17.7
enzyme activity *	At2g04440	-1.47	-0.13	**2.53**	-1.14	-0.65	**1.40**	NUDIX/mutT hydrolase family protein	T1O3.15
	At2g29380	-0.15	-2.31	**-4.44**	0.09	0.07	**-1.01**	protein phosphatase 2C	F16P2.24. HAI3
	At1g48470	0.12	-1.07	**-2.28**	1.29	1.38	**1.06**	glutamine synthetase	GLN1 5. T1N15.8
	At2g28420	-0.22	-2.00	**-3.43**	0.87	0.33	**-1.46**	lactoylglutathione lyase family protein	T1B3.6
	At4g01970	-0.17	-1.26	**-2.13**	0.26	0.15	**-1.08**	galactinol-raffinose galactosyltransferase	ATSTS. T7B11.23
	At3g26140	1.30	-1.23	**-5.79**	-1.63	-0.87	**1.69**	glycosyl hydrolase family 5 protein	MTC11.4
	At5g35960	-1.22	0.05	**2.42**	0.07	0.25	**1.14**	protein kinase	MEE13.6
	At2g17170	-1.79	0.16	**3.86**	-1.52	-0.01	**2.85**	protein kinase family protein	T23A1.3
	At5g50600	-0.30	-1.84	**-2.89**	-0.11	-0.30	**-1.14**	short-chain dehydrogenase/reductase (SDR)	ATHSD1. HSD1. MFB16.22
	At3g56350	-0.53	-2.09	**-2.95**	0.04	0.18	**1.10**	manganese superoxide dismutase	T5P19.1
	At2g44990	-1.34	0.20	**2.91**	-0.69	0.28	**1.95**	similarity to carotenoid cleavage dioxygenase 1	ATCCD7. CCD7. MAX3. T14P1.21
	At1g48130	-0.70	-2.15	**-2.72**	-0.14	0.00	**1.10**	peroxiredoxin (PER1) / rehydrin	ATPER1. F21D18.15
	At5g28510	1.76	0.18	**-2.99**	-0.17	-0.12	**1.03**	glycosyl hydrolase family 1 protein	BGLU24. T26D3.6
	At1g07430	0.66	-0.95	**-3.05**	0.11	0.23	**1.09**	protein phosphatase 2C	F22G5.22. HAI2
	At5g50770	0.26	-1.24	**-2.82**	-0.20	-0.16	**1.03**	short-chain dehydrogenase/reductase (SDR)	ATHSD6. MFB16.17
	At4g29250	-1.22	-0.11	**2.16**	-1.00	-0.39	**1.53**	transferase family protein low similarity to CER2	F17A13.70
	At1g09350	1.65	2.96	**2.48**	2.47	1.91	**-1.47**	galactinol synthase	ATGOLS3. F14J9.1
	At2g01900	-0.46	0.65	**2.15**	0.88	1.17	**1.22**	similar to inositol polyphosphate 5-phosphatase	T23K3.9

* genes encoding for proteins with enzyme activities unless annotation details allowed more precise functional classification

functional category	At No.	normalized intensity values: in-flight control 0° (1g, 2g)	normalized intensity values: flight 0° (µg, 1g, 2g)	FC: flight vs. in-flight control	normalized intensity values: flight 0° (µg, 1g, 2g)	normalized intensity values: flight 90° (µg, 1g, 2g)	FC: flight 90° vs. flight 0°	description	other names
enzyme activity *	At5g42600	0.18	-0.94	**-2.17**	-1.70	-1.51	**1.14**	pentacyclic triterpene synthase	MFO20.1. MRN1
	At3g24230	-0.34	1.00	**2.53**	1.65	1.76	**1.08**	pectate lyase family protein	MUJ8.14
	At5g58780	-1.64	-0.39	**2.39**	0.63	0.29	**-1.26**	dehydrodolichyl diphosphate synthase	MZN1.33
	At5g62360	0.42	2.19	**3.41**	1.61	1.56	**-1.04**	invertase/pectin methylesterase inhibitor	MMI9.1
other	At1g03120	-0.72	-2.23	**-2.84**	0.24	0.02	**-1.16**	seed maturation family protein	ATRAB28. F10O3.5
	At5g44120	1.52	-0.12	**-3.12**	1.12	1.52	**1.32**	12S seed storage protein (CRA1)	ATCRA1.CRU1. MLN1.4
	At2g18540	-0.83	-2.18	**-2.56**	1.01	0.73	**-1.21**	cupin family protein	F24H14.11
	At1g03880	1.60	-0.57	**-4.51**	1.16	1.73	**1.48**	12S seed storage protein (CRB)	CRU2. CRUCIFERIN B. F21M11.19
	At3g01830	0.48	-1.14	**-3.07**	1.55	-1.17	**-6.55**	regulator of gene silencing. calmodulin-related	F28J7.16
unknown	At1g16850	0.26	-0.95	**-2.32**	-0.00	-0.23	**-1.17**	expressed protein	F17F16.17. F6I1.15
	At1g29680	-1.07	-2.80	**-3.32**	0.15	0.16	**1.01**	expressed protein	F15D2.23
	At5g55750	0.06	-2.02	**-4.23**	-0.01	-0.39	**-1.30**	hydroxyproline-rich glycoprotein family protein	MDF20.19
	At1g11690	-1.75	-0.46	**2.44**	0.79	1.08	**1.22**	hypothetical protein	F25C20.16
	At5g63350	0.49	-1.04	**-2.88**	0.47	0.29	**-1.13**	expressed protein	K9H21.8
	At1g48405	-1.12	-0.06	**2.09**	-0.46	0.64	**2.14**	hypothetical protein	
	At4g01985	2.03	0.38	**-3.13**	-0.41	-0.68	**-1.21**	expressed protein	
	At5g45630	0.53	-0.65	**-2.27**	-0.34	-0.25	**1.07**	expressed protein	
	At4g18650	0.17	-2.33	**-5.67**	3.15	2.44	**-1.63**	TGACG-sequence specific DNA-binding protein	TGA2.1. MRA19.3
	At2g04190	-0.07	-1.64	**-2.96**	0.21	0.41	**1.15**	meprin and TRAF homology protein	T16B23.4
	At5g27170	-1.82	0.46	**4.83**	-1.02	-1.51	**-1.40**	hypothetical protein	T21B4.80
	At1g04560	-1.00	-3.03	**-4.08**	0.42	0.06	**-1.28**	AWPM-19-like membrane family protein	T1G11.19
	At5g50360	0.18	-1.34	**-2.87**	0.48	0.41	**-1.05**	expressed protein	
	At1g61090	-1.36	0.68	**4.11**	-0.55	-1.90	**-2.56**	hypothetical protein	T7P1.22
	At2g47770	-0.21	-2.07	**-3.64**	0.22	-0.09	**-1.24**	peripheral-type benzodiazepine receptor (PBR)	PKBS
	At1g23070	-1.00	-2.12	**-2.17**	0.89	0.81	**-1.06**	hypothetical protein	ATTSPO. F17A22.16
	At5g04010	-0.63	-2.69	**-4.17**	-0.13	-0.45	**-1.25**	expressed protein	T26J12.15
	At2g42640	-1.37	0.02	**2.62**	-1.52	-0.05	**2.77**	expressed protein weak similarity to EDR1	F14N22.9
	At1g07985	-0.01	-1.17	**-2.24**	0.11	-0.07	**-1.13**	expressed protein	
	At1g47980	-0.49	-1.69	**-2.29**	0.23	0.08	**-1.11**	expressed protein	T2J15.11
	At5g16460	-0.14	-1.31	**-2.26**	0.53	0.64	**1.07**	hypothetical protein	MQK4.19
	At2g41260	-0.56	-2.13	**-2.97**	-0.81	-0.42	**1.31**	late embryogenesis abundant protein (M17)	ATM17. F13H10.19. M17
	At3g62990	1.46	-1.59	**-8.25**	0.03	-0.33	**-1.29**	expressed protein	T20O10.90
	At2g10602	-1.54	-0.12	**2.69**	-1.95	-0.74	**2.32**	hypothetical protein	
	At2g38890	-1.29	0.17	**2.75**	-0.47	0.19	**1.58**	expressed protein	T7F6.6
	At5g05965	0.95	-0.18	**-2.18**	-2.06	-1.94	**1.08**	hypothetical protein	
	At5g38386	-0.62	-1.86	**-2.37**	-1.97	-2.00	**-1.02**	F-box family protein	
	At3g19600	0.52	-1.98	**-5.66**	-1.29	-2.32	**-2.04**	NLI interacting factor (NIF) family protein	
	At1g22600	-0.72	-2.16	**-2.72**	0.46	0.14	**-1.25**	hypothetical protein	MMB12.7
	At3g49040	0.58	-1.34	**-3.79**	-0.06	-1.72	**-3.16**	F-box family protein	T2J13.120
	At1g35180	0.43	-0.73	**-2.24**	-0.25	-0.03	**1.17**	expressed protein	T32G9.28
	At3g21660	0.79	-1.02	**-3.51**	-1.15	-0.44	**1.63**	UBX domain-containing protein	MIL23.23
	At4g14810	-0.01	-1.25	**-2.36**	-0.30	-0.16	**1.11**	hypothetical protein	DL3445W. FCAALL.327
	At3g19920	-1.03	-2.46	**-2.69**	0.44	0.24	**-1.14**	expressed protein	MPN9.17
	At3g44790	-1.46	-0.17	**2.45**	-1.56	-0.93	**1.55**	meprin and TRAF homology protein	T32N15.4
	At5g46200	0.48	-1.11	**-3.01**	-1.39	-1.12	**1.21**	similarity to carboxyl-terminal proteinase	MDE13.2

* genes encoding for proteins with enzyme activities unless annotation details allowed more precise functional classification

functional category	At No.	normalized intensity values: in-flight control 0° (1g, 2g)	normalized intensity values: flight 0° (µg, 1g, 2g)	FC: flight vs. in-flight control	normalized intensity values: flight 0° (µg, 1g, 2g)	normalized intensity values: flight 90° (µg, 1g, 2g)	FC: flight 90° vs. flight 0°	description	other names
	At5g03210	0.17	-1.23	**-2.63**	-0.32	-0.75	**-1.35**	expressed protein	F15A17.240
	At3g44450	-0.58	0.46	**2.06**	2.02	1.82	**-1.15**	expressed protein	F14L2.1
	At5g42760	0.43	1.51	**2.11**	2.81	2.81	**1.01**	O-methyltransferase N-terminus protein	MJB21.14
	At5g53710	0.76	-0.51	**-2.42**	-0.11	-0.29	**-1.13**	expressed protein	MGN6.6
	At1g02700	-0.79	-2.65	**-3.63**	0.23	0.06	**-1.12**	expressed protein	T14P4.2
unknown	At2g34870	0.79	-2.76	**-11.79**	0.56	0.52	**-1.03**	hydroxyproline-rich glycoprotein family protein	F19I3.10. MEE26
	At4g02360	0.94	-0.10	**-2.06**	-0.05	-0.24	**-1.15**	expressed protein DUF538	T14P8.17
	At2g35070	0.79	-0.57	**-2.56**	-0.84	-0.55	**1.22**	expressed protein	T4C15.27
	At3g24220	0.70	-1.30	**-3.99**	0.26	-0.57	**-1.78**	9-cis-epoxycarotenoid dioxygenase	ATNCED6. MUJ8.12. NCED6
	At4g36600	-1.19	-2.52	**-2.53**	0.86	0.96	**1.07**	LEA domain-containing protein	AP22.17
	At1g16730	-0.20	-1.35	**-2.22**	0.44	0.21	**-1.18**	expressed protein	F19K19.18. UP6
	At4g30380	-1.02	0.14	**2.23**	0.08	-0.02	**-1.07**	expansin-related. blight-associated protein p12	
	At1g52240	-1.89	-0.28	**3.07**	0.40	0.21	**-1.15**	expressed protein	F17I23.280
	At4g18920	-0.12	-1.57	**-2.73**	0.37	0.00	**-1.29**	expressed protein	ATROPGEF11. F9I5.12. ROPGEF11
	At5g53905	-1.76	-0.43	**2.52**	-1.33	-1.40	**-1.05**	expressed protein	
	At3g14880	-0.24	-1.71	**-2.76**	0.47	0.33	**-1.10**	DNA-binding protein	K15M2.2

PUBLICATIONS

VAGT, N., HAUSLAGE, J., HORN, A., NZIENGUI-IKAPI, J.H., PALME, K. & BRAUN, M. (2010): High gravisensitivity and great efficiency on cellular and molecular level ensures most beneficial gravitropic response of plants. (in preparation)

VAGT, N., HAUSLAGE, J., LIMBACH, C. & BRAUN, M. (2010): How to activate gravireceptors in higher plants. Early mechanisms of gravity sensing in Arabidopsis roots during parabolic flights. (submitted)

GREUEL, N., HAUSLAGE, J. & BRAUN, M. (2007): Early mechanisms of gravity sensing in plants. Proceedings of the 18th ESA Symposium on European Rocket and Balloon Programmes and Related Research, Visby, Sweden, ESA SP-647, 469-472.

TALKS AT INTERNATIONAL SYMPOSIA

GREUEL, N. & BRAUN, M. (September 2009): Gene expression studies under parabolic flight conditions – a new differentiated looks on the molecular basis of gravity-related processes in plants. European Low Gravity Research Association (ELGRA), In the footsteps of Columbus, Bonn, Germany.

GREUEL, N. & Braun, M. (August 2009): Molecular analyses of gravitropism related signaling pathways in unicellular and multicellular plant model systems. SpaceLife Summer School "Living with a Star: Basics in Space Life Sciences", Bad Honnef, Germany.

GREUEL, N. & Braun, M. (August 2009): Gravity-sensors and gravi-orientation of plants. SpaceLife Summer School "Living with a Star: Basics in Space Life Sciences", Bad Honnef, Germany.

GREUEL, N. & Braun, M. (June 2009): Gravity-sensing processes and gravity-dependent gene expression in plants studied under hyper- and microgravity conditions. 19th ESA Symposium on European Rocket and Balloon Programmes and Related Research, Bad Reichenhall, Germany.

GREUEL, N. & Braun, M. (2008): Mechanisms of gravitropism in single-celled systems. Committee On Space Research (COSPAR), Montreal, Canada.

GREUEL, N. & Braun, M. (2007): Early mechanisms of gravity sensing in plants. 18th ESA Symposium on European Rocket and Balloon Programmes and Related Research, Visby, Sweden.

ERKLÄRUNG

Ich versichere hiermit, dass ich die vorliegende Arbeit in allen Teilen selbst und ohne jede unerlaubte Hilfe angefertigt habe. Diese oder eine ähnliche Arbeit ist noch keiner anderen Stelle als Dissertation eingereicht worden.

Ich habe früher noch keinen Promotionsversuch unternommen.

Bonn, den 07.06.2010